

**RESERVOIR DIAGNOSIS AND RESERVE ESTIMATION FOR
BAKHRABAD GAS FIELD USING PRODUCTION DATA**

A Thesis

Submitted to the Department of Petroleum & Mineral Resources Engineering
in partial fulfillment of the requirements for the degree of Master of
Science in Petroleum Engineering

By

Mohammad Shahedul Hossain



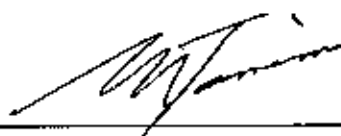
**DEPARTMENT OF PETROLEUM & MINERAL RESOURCES ENGINEERING
BANGLADESH UNIVERSITY OF ENGINEERING & TECHNOLOGY
DHAKA
BANGLADESH**

MAY, 2009

RECOMMENDATION OF THE BOARD OF EXAMINERS

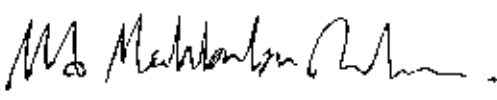
The undersigned certify that they have read and recommended to the Department of Petroleum and Mineral Resources Engineering, for acceptance, a thesis entitled "RESERVOIR DIAGNOSIS AND RESERVE ESTIMATION FOR BAKHRABAD GAS FIELD USING PRODUCTION DATA" submitted by MOHAMMAD SHAHEDUL HOSSAIN in partial fulfillment of the requirements for the degree of MASTER OF SCIENCE IN PETROLEUM ENGINEERING on 30th May, 2009.

Chairman (Supervisor) :



Dr. Mohammad Tamim
Professor
Department of PMRE, BUET, Dhaka

Member :



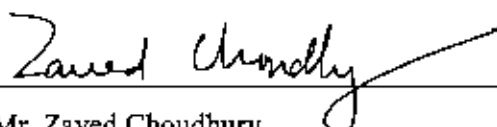
Dr. Mahbubur Rahman
Head and Assistant Professor
Department of PMRE, BUET, Dhaka

Member :



Mr. Sohrab Hossain
Lecturer
Department of PMRE, BUET, Dhaka

Member (External) :



Mr. Zaved Choudhury
Manager, Reservoir & Data
Management Department, Petrobangla,
Petrocenter, 3-Kawranbazar C/A, Dhaka

DECLARATION

It is hereby declared that this thesis or any part of it has not been submitted elsewhere for the award of any degree or diploma.



(Mohammad Shahedul Hossain)

To Abba and Amma who set me free with their love and trust

ABSTRACT

The Bakhrabad gas field is an old and matured gas field in Bangladesh, which is producing since 1984. This thesis presents a systematic diagnosis of reservoir behavior of this gas field with respect to different flow regimes, reservoir connectivity or compartmentalization, reservoir drive mechanism, estimation of reserve, and nature of production decline. Production data such as flowing wellhead pressure and production rate are used in different simple diagnostic tools like pressure vs. rate, decline and approximated wellhead material balance. The same data is also analyzed with different type curve methods including Fetkovich, Blasingame, Agarwal-Gardner, and Normalized Pressure Integral (NPI) type curves. Commercial production analysis (PA) software is used for this purpose.

Pressure vs. rate diagnosis reveals reservoir flow behavior with approximate duration of flow regimes for the wells of respective sands of Bakhrabad gas field. It is found that Pseudo-Steady State (PSS) flow regime is currently dominating in all producing sands. No compartmentalization is detected in any of the producing sands. Decline diagnosis shows exponential type of production decline in all major sands. Approximate wellhead material balance diagnosis indicates volumetric depletion as the drive mechanism for this field. Type curve analysis show good agreement between production data and the assumed radial reservoir model for this field. The Gas Initially in Place (GIIP) estimated by different methods range from 916 to 1263 BCF, with the most likely value being 1200 BCF. These values compare well with the previously reported values based on volumetric method, which ranges from 1281 to 1392 BCF. Assuming abandonment at 600 psia, the estimated recovery factors range from 53% to 73%.

ACKNOWLEDGEMENTS

The author wishes to express sincere gratitude and appreciation to Dr. M. Tamim, Professor of the department of Petroleum and Mineral Resources Engineering, for his encouragement, support and guidance throughout this research. His patience, generosity and trust made this work successful.

The author is grateful to Dr. Mahbubur Rahman, Assistant Professor of Petroleum and Mineral Resources Engineering for his valuable advice, help and supervision in different stage of this research.

The author wishes to thank Mr. Sohrab Hossain, Assistant Professor of Petroleum and Mineral Resources Engineering Department for his valuable suggestions and help during running the commercial package of F.A.S.T. RTA.

Special thanks is extended to the author's parents, wife, Suborna and to his daughter Samiha, whose birth brought much joy and happiness.

The author wishes to express appreciation to all faculty and staff members of Petroleum and Mineral Resources Engineering Department for extending their hands of co-operation in different phases of this work.

Last but not the least; the author gratefully thanks Petrobangla authority for supporting this research with providing the requisite data of Bakhrabad gas field.

TABLE OF CONTENTS

	Page
ABSTRACT.....	i
ACKNOWLEDGEMENTS.....	ii
TABLE OF CONTENTS.....	iii
LIST OF FIGURES.....	vi
LIST OF TABLES.....	x
NOMENCLATURE.....	xii
CHAPTER 1 INTRODUCTION.....	1
CHAPTER 2 LITERATURE REVIEW.....	7
2.1 Material Balance Methods.....	9
2.2 Decline Curve Analysis.....	11
CHAPTER 3 PRESSURE VS. RATE DIAGNOSIS.....	17
3.0 Sand-wise pressure vs. rate diagnosis.....	17
3.1 J Sand.....	18
3.2 DL Sand.....	21
3.3 DU Sand.....	23
3.4 B Sand.....	23
3.5 G Sand.....	24
CHAPTER 4 DECLINE DIAGNOSIS.....	27
4.0 Sand-wise decline diagnosis.....	29
4.1 J Sand.....	29
4.2 G Sand.....	32
4.3 DL Sand.....	34
4.4 DU Sand.....	36
4.5 B Sand.....	36
CHAPTER 5 AWMB DIAGNOSIS.....	38
5.0 Sand-wise AWMB diagnosis.....	38
5.1 J Sand.....	39
5.2 G Sand.....	41
5.3 DL Sand.....	42
5.4 DU Sand.....	44
5.5 B Sand.....	45
CHAPTER 6 TYPECURVE ANALYSIS.....	47
6.0 Computer based production data analysis.....	47
6.1 Fetkovich Typecurve Analysis.....	48
6.1.1 J Sand.....	51
6.1.2 G Sand.....	54

6.1.3 DL Sand.....	55
6.1.4 DU Sand.....	56
6.1.5 B Sand.....	57
6.2 Blasingame Typecurve Analysis.....	59
6.2.1 J Sand.....	61
6.2.2 G Sand.....	63
6.2.3 DL Sand.....	65
6.2.4 DU Sand.....	66
6.2.5 B Sand.....	67
6.3 Agarwal-Gardner Typecurve Analysis.....	69
6.3.1 J Sand.....	71
6.3.2 G Sand.....	73
6.3.3 DL Sand.....	75
6.3.4 DU Sand.....	76
6.3.5 B Sand.....	77
6.4 NPI (Normalized Pressure Integral) Typecurve Analysis.....	79
6.4.1 J Sand.....	80
6.4.2 G Sand.....	83
6.4.3 DL Sand.....	84
6.4.4 DU Sand.....	86
6.4.5 B Sand.....	87
6.5 Transient Typecurve Analysis.....	88
6.5.1 J Sand.....	90
6.5.2 G Sand.....	92
6.5.3 DL Sand.....	94
6.5.4 DU Sand.....	95
6.5.5 B Sand.....	96
CHAPTER 7 NON - TYPECURVE ANALYSIS.....	98
7.1 Arps (Traditional) Decline Analysis.....	98
7.1.1 J Sand.....	99
7.1.2 G Sand.....	102
7.1.3 DL Sand.....	103
7.1.4 DU Sand.....	105
7.1.5 B Sand.....	106
7.2 Flowing Material Balance.....	106
7.2.1 J Sand.....	107
7.2.2 G Sand.....	110

7.2.3 DL Sand.....	111
7.2.4 DU Sand.....	113
7.2.5 B Sand.....	114
CHAPTER 8 CONCLUSION AND RECOMMENDATION.....	116
8.1 Conclusion	116
8.2 Recommendation.....	117
REFERENCES	118
APPENDIX A — Derivation of p-q Slope for different Flow Regime.....	123
APPENDIX B — Decline Curves of Individual Wells of Bakhrabad Gas Field.....	130
APPENDIX C — Input parameters for computer based PDA.....	136

LIST OF FIGURES

FIGURE	Page
1 Bakhrabad Seismic Culminations A, B and C	2
2 Different Major Development Sands of Bakhrabad Gas Field.....	3
2.1 Diagnostic $P_{wf}-q$ graph for a closed system.	8
3.1 $p_{wh}-q-t$ diagnostic plot of BK1 at J Sand.....	18
3.2 $p_{wh}-q-t$ diagnostic plot of BK6 at J Sand	18
3.3 $p_{wh}-q-t$ diagnostic plot of BK7 at J Sand.....	19
3.4 $p_{wh}-q-t$ diagnostic plot of BK8 at J Sand.....	19
3.5 $p_{wh}-q$ diagnostic plot of all wells at J Sand.....	20
3.6 $p_{wh}-q-t$ diagnostic plot of BK2 at DL Sand.....	21
3.7 $p_{wh}-q-t$ diagnostic plot of BK5 at DL Sand.....	22
3.8 $p_{wh}-q$ diagnostic plot of all wells at DL Sand.....	22
3.9 $p_{wh}-q-t$ diagnostic plot of BK4 at DU Sand.....	23
3.10 $p_{wh}-q-t$ diagnostic plot of BK5 at B Sand.....	24
3.11 $p_{wh}-q-t$ diagnostic plot of BK3 at G Sand.....	24
3.12 $p_{wh}-q-t$ diagnostic plot of BK4 at G Sand.....	25
3.13 $p_{wh}-q$ diagnostic plot of all wells at G Sand.....	25
4.1 Decline curve shapes for a Cartesian plot of rate vs. time.....	27
4.2 Decline-curve shapes for a semilog plot of rate vs. time.....	28
4.3 Decline curve shapes for a Cartesian plot of rate vs. cumulative production	28
4.4 Decline-curve shapes for a semilog plot of rate vs. cumulative production.....	28
4.5 Cartesian plot of Rate vs. Time of all wells in J Sand.....	30
4.6 Semilog plot of Rate vs. Time of all wells in J Sand.	30
4.7 Cartesian plot of Rate vs. cumulative production of all wells in J Sand.....	31
4.8 Semilog plot of Rate vs. cumulative production of all wells in J Sand.....	31
4.9 Cartesian plot of Rate vs. Time of all wells in G Sand.....	32
4.10 Semilog plot of Rate vs. Time of all wells in G Sand.....	32
4.11 Cartesian plot of Rate vs. cumulative production of all wells in G Sand.....	33
4.12 Semilog plot of Rate vs. cumulative production of all wells in G Sand.....	33
4.13 Cartesian plot of Rate vs. Time of all wells in DL Sand.....	34
4.14 Semilog plot of Rate vs. Time of all wells in DL Sand.....	34
4.15 Cartesian plot of Rate vs. cumulative production of all wells in DL Sand.....	35
4.16 Semilog plot of Rate vs. cumulative production of all wells in DL Sand.....	35
4.17 Cartesian plot of Rate vs. cumulative production of BK4 in DU Sand.....	36
4.18 Cartesian plot of Rate vs. cumulative production of BK5 in B Sand.....	36

FIGURE	Page
5.1 Shapes of p/z plots for various drive mechanisms.....	38
5.2 AWMB plot of BK1 of J Sand.....	39
5.3 AWMB plot of BK6 of J Sand.....	39
5.4 AWMB plot of BK7 of J Sand.....	40
5.5 AWMB plot of BK8 of J Sand.....	40
5.6 AWMB plot of BK3 of G Sand.....	41
5.7 AWMB plot of BK4 of G Sand.....	42
5.8 AWMB plot of BK2 of DL Sand.....	43
5.9 AWMB plot of BK5 of DL Sand.....	43
5.10 AWMB plot of BK4 of DU Sand.....	44
5.11 AWMB plot of BK5 of B Sand.....	45
6.1 Fetkovich Typecurve Analysis of BK1 at J Sand.....	51
6.2 Fetkovich Typecurve Analysis of BK6 at J Sand.....	52
6.3 Fetkovich Typecurve Analysis of BK7 at J Sand.....	52
6.4 Fetkovich Typecurve Analysis of BK8 at J Sand.....	53
6.5 Fetkovich Typecurve Analysis of BK3 at G Sand.....	54
6.6 Fetkovich Typecurve Analysis of BK4 at G Sand.....	54
6.7 Fetkovich Typecurve Analysis of BK2 at DL Sand.....	55
6.8 Fetkovich Typecurve Analysis of BK5 at DL Sand.....	56
6.9 Fetkovich Typecurve Analysis of BK4 at DU Sand.....	57
6.10 Fetkovich Typecurve Analysis of BK5 at B Sand.....	58
6.11 Blasingame Typecurve Analysis of BK1 at J Sand.....	61
6.12 Blasingame Typecurve Analysis of BK6 at J Sand.....	62
6.13 Blasingame Typecurve Analysis of BK7 at J Sand.....	62
6.14 Blasingame Typecurve Analysis of BK8 at J Sand.....	63
6.15 Blasingame Typecurve Analysis of BK3 at G Sand.....	64
6.16 Blasingame Typecurve Analysis of BK4 at G Sand.....	64
6.17 Blasingame Typecurve Analysis of BK2 at DL Sand.....	65
6.18 Blasingame Typecurve Analysis of BK5 at DL Sand.....	66
6.19 Blasingame Typecurve Analysis of BK4 at DU Sand.....	67
6.20 Blasingame Typecurve Analysis of BK5 at B Sand.....	68
6.21 Agarwal-Gardner Typecurve Analysis of BK1 at J Sand.....	71
6.22 Agarwal-Gardner Typecurve Analysis of BK6 at J Sand.....	72
6.23 Agarwal-Gardner Typecurve Analysis of BK7 at J Sand.....	72
6.24 Agarwal-Gardner Typecurve Analysis of BK8 at J Sand.....	73
6.25 Agarwal-Gardner Typecurve Analysis of BK3 at G Sand.....	74

FIGURE	Page
6.26 Agarwal-Gardner Typecurve Analysis of BK4 at G Sand.....	74
6.27 Agarwal-Gardner Typecurve Analysis of BK2 at DL Sand.....	75
6.28 Agarwal-Gardner Typecurve Analysis of BK5 at DL Sand.....	76
6.29 Agarwal-Gardner Typecurve Analysis of BK4 at DU Sand.....	77
6.30 Agarwal-Gardner Typecurve Analysis of BK5 at B Sand.....	78
6.31 NPI Typecurve Analysis of BK1 at J Sand.....	81
6.32 NPI Typecurve Analysis of BK6 at J Sand.....	81
6.33 NPI Typecurve Analysis of BK7 at J Sand.....	82
6.34 NPI Typecurve Analysis of BK8 at J Sand.....	82
6.35 NPI Typecurve Analysis of BK3 at G Sand.....	83
6.36 NPI Typecurve Analysis of BK4 at G Sand.....	84
6.37 NPI Typecurve Analysis of BK2 at DL Sand.....	85
6.38 NPI Typecurve Analysis of BK5 at DL Sand.....	85
6.39 NPI Typecurve Analysis of BK4 at DU Sand.....	86
6.40 NPI Typecurve Analysis of BK5 at B Sand.....	87
6.41 Transient Typecurve Analysis of BK1 at J Sand.....	90
6.42 Transient Typecurve Analysis of BK6 at J Sand.....	91
6.43 Transient Typecurve Analysis of BK7 at J Sand.....	91
6.44 Transient Typecurve Analysis of BK8 at J Sand.....	92
6.45 Transient Typecurve Analysis of BK3 at G Sand.....	93
6.46 Transient Typecurve Analysis of BK4 at G Sand.....	93
6.47 Transient Typecurve Analysis of BK2 at DL Sand.....	94
6.48 Transient Typecurve Analysis of BK5 at DL Sand.....	95
6.49 Transient Typecurve Analysis of BK4 at DU Sand.....	96
6.50 Transient Typecurve Analysis of BK5 at B Sand.....	97
7.1 Arps Decline Analysis of BK1 at J Sand.....	100
7.2 Arps Decline Analysis of BK6 at J Sand.....	100
7.3 Arps Decline Analysis of BK7 at J Sand.....	101
7.4 Arps Decline Analysis of BK8 at J Sand.....	101
7.5 Arps Decline Analysis of BK3 at G Sand.....	102
7.6 Arps Decline Analysis of BK4 at G Sand.....	103
7.7 Arps Decline Analysis of BK2 at DL Sand.....	104
7.8 Arps Decline Analysis of BK5 at DL Sand.....	104
7.9 Arps Decline Analysis of BK4 at DU Sand.....	105
7.10 Arps Decline Analysis of BK5 at B Sand.....	106
7.11 FMD Analysis of BK1 at J Sand.....	108



FIGURE	Page
7.12 FMB Analysis of BK6 at J Sand.....	108
7.13 FMB Analysis of BK7 at J Sand.....	109
7.14 FMB Analysis of BK8 at J Sand.....	109
7.15 FMB Analysis of BK3 at G Sand.....	110
7.16 FMB Analysis of BK4 at G Sand.....	111
7.17 FMB Analysis of BK2 at DL Sand.....	112
7.18 FMB Analysis of BK5 at DL Sand.....	112
7.19 FMB Analysis of BK4 at DU Sand.....	113
7.20 FMB Analysis of BK5 at B Sand.....	114

LIST OF TABLES

TABLE	Page
2.1 Summary of the "Arps Analysis".....	12
3.1 Present Status of all wells in different sands of Bakhrabad gas field.....	17
4.1 Summary of results of Decline diagnosis for all wells of Bakhrabad gas field.....	37
5.1 Summary of results of AWMB method for all wells of J Sand.....	41
5.2 Summary of results of AWMB method for all wells of G Sand.....	42
5.3 Summary of results of AWMB method for all wells of DL Sand.....	44
5.4 Summary of results of AWMB method for all wells of DU Sand.....	44
5.5 Summary of results of AWMB method for all wells of B Sand.....	45
5.6 Comparison of the GIP (bcf) estimates of Bakhrabad Gas Field in different studies.....	46
6.1 Summary of results of Fetkovich analysis for all wells of J Sand.....	53
6.2 Summary of results of Fetkovich analysis for all wells of G Sand.....	55
6.3 Summary of results of Fetkovich analysis for all wells of DL Sand.....	56
6.4 Summary of results of Fetkovich analysis for well BK4 of DU Sand.....	57
6.5 Summary of results of Fetkovich analysis for well BK5 of B Sand.....	58
6.6 Summary of results of Blasingame analysis for all wells of J Sand.....	63
6.7 Summary of results of Blasingame analysis for all wells of G Sand.....	65
6.8 Summary of results of Blasingame analysis for all wells of DL Sand.....	66
6.9 Summary of results of Blasingame analysis for well BK4 of DU Sand.....	67
6.10 Summary of results of Blasingame analysis for well BK5 of B Sand.....	68
6.11 Summary of results of Agarwal-Gardner analysis for all wells of J Sand.....	73
6.12 Summary of results of Agarwal-Gardner analysis for all wells of G Sand.....	75
6.13 Summary of results of Agarwal-Gardner analysis for all wells of DL Sand.....	76
6.14 Summary of results of Agarwal-Gardner analysis for well BK4 of DU Sand.....	77
6.15 Summary of results of Agarwal-Gardner analysis for well BK5 of B Sand.....	78
6.16 Summary of results of NPI analysis for all wells of J Sand.....	83
6.17 Summary of results of NPI analysis for all wells of G Sand.....	84
6.18 Summary of results of NPI analysis for all wells of DL Sand.....	86
6.19 Summary of results of NPI analysis for well BK4 of DU Sand.....	86
6.20 Summary of results of NPI analysis for well BK5 of B Sand.....	87
6.21 Summary of results of Transient analysis for all wells of J Sand.....	92
6.22 Summary of results of Transient analysis for all wells of G Sand.....	94
6.23 Summary of results of Transient analysis for all wells of DL Sand.....	95
6.24 Summary of results of Transient analysis for well BK4 of DU Sand.....	96
6.25 Summary of results of Transient analysis for well BK5 of B Sand.....	97
7.1 Summary of results of Arps analysis for all wells of J Sand.....	102

TABLE	Page
7.2 Summary of results of Arps analysis for all wells of G Sand	103
7.3 Summary of results of Arps analysis for all wells of DL Sand.....	105
7.4 Summary of results of Arps analysis for well BK4 of DU Sand.....	105
7.5 Summary of results of Arps analysis for well BK5 of B Sand.....	106
7.6 Summary of results of FMB analysis for all wells of J Sand.	110
7.7 Summary of results of FMB analysis for all wells of G Sand.	111
7.8 Summary of results of FMB analysis for all wells of DL Sand.....	113
7.9 Summary of results of FMB analysis for well BK4 of DU Sand.....	113
7.10 Summary of results of FMB analysis for well BK5 of B Sand.....	114
7.11 Comparison of gas in place (bcf) of different sands of Bakhrabad Gas Field using typecurve, non-typecurve and AWMB methods.....	115

NOMENCLATURE

A	Reservoir drainage area, ft ²
B	Formation volume factor, reservoir bbl/stock tank bbl
b	hyperbolic exponent
b_{jwo}	y-intercept of normalized PSS equation for oil, psi/bbl
C_A	Dietz shape factor for drainage area, dim-less
c_f	Formation (rock) compressibility, psi ⁻¹
c_g	Gas compressibility, psi ⁻¹
c_t	Total system compressibility, psi ⁻¹
c_w	Water compressibility, psi ⁻¹
DER	Pressure derivative
D_{Arps}	Arps decline rate constant, Day ⁻¹
D_i	Decline rate constant (Exponential), Day ⁻¹
d_i	Nominal decline rate, per cent
G	Original-gas-in-place, MSCF or BSCF
G_p	Cumulative gas production, MSCF
h	Reservoir (net pay) thickness, ft
k	Formation permeability, md
L	Tubing length, ft
m	semilog slope (=162.6 <i>Bμ/kh</i>), psi/log-cycle
$m(p)$	Real gas pseudopressure, psia ² /cp
n_w	number of wells
N	Original-oil-in-place (OOIP), STB
N_p	Cumulative oil production, STB
\bar{p}	Average reservoir pressure, psia
p_{ab}	Bottomhole abandonment pressure, psia
p_D	Dimensionless, pressure, dim-less
p_{Di}	Dimensionless pressure-Integral
p_{Dnd}	Dimensionless pressure-Integral-Derivative
p_i	Initial reservoir pressure, psia
p_I	Normalized Pressure-Integral, psi/bbl
p_{Id}	Normalized Pressure-Integral-Derivative
p_{wf}	Flowing bottomhole pressure, psia
p_{wh}	Flowing wellhead pressure, psig
q	Production rate, MMscfd or bbl/d
q_I	Normalized Rate-Integral, bbl/psi

q_{id}	Normalized Rate-Integral Derivative, bbl/psi
q_D	Dimensionless production rate
q_{Dfd}	Fetkovich dimensionless production rate
q_{Dit}	Dimensionless Rate-Integral
q_{Ditd}	Dimensionless Rate-Integral-Derivative
q_g	Gas flowrate, MSCF/D
Q	Cumulative production, MMscf or bbl
Q_n	Normalized cumulative production
r_{eD}	Dimensionless reservoir radius, dim-less
r_e	Reservoir drainage radius, ft
R_s	Solution gas-oil ratio, scf/scf
r_w	Wellbore radius, ft
r_{we}	Apparent wellbore radius (including formation damage, etc.),
s	Skin factor
s_{avg}	Average skin factor
S_g	Gas saturation, fraction
S_w	Residual water saturation, fraction
t	Time, hr
t_c	Material-balance-time, days
t_{co}	Material-balance-pseudo-time, days
t_D	Dimensionless time
t_{DA}	Dimensionless time based on area
t_{DM}	Fetkovich dimensionless time
T_R	Reservoir temperature, deg R (T is also given in deg F, but deg R is used in calculations)
t_w	Dimensionless "decline" time
z	Gas compressibility factor

Subscripts:

avg	Average
$base$	Base (reference) conditions
D	Dimensionless
g	Gas
o	Oil
i	Initial condition
i	well number index
j	time-step index
k	well position index

n	nth flow period
p	Pseudopressure
w_f	Wellbore flowing conditions
θ	initial condition
$1,2,3$	indices of flow period

Greek Symbols:

ϕ	Porosity, fraction
γ	0.577216, Euler's constant
μ	Fluid viscosity, cp



INTRODUCTION

Reservoir characterization, reservoir flow behavior identification and reserve estimation are very important topics for investigation of any reservoir. Such investigation provides deeper understanding of the nature of the reservoir and help in proper development of the field. Different techniques have been developed to conduct these investigations, involving a variety of data and parameters. Most of these methods involve analysis and interpretation of production data which are routinely collected and available from industry databases.

The Bakhrabad gas field is an old and matured gas field in Bangladesh, which is producing since 1984. Geologically Bakhrabad Gas Field falls within the eastern folded region in the Meghna basin of Bangladesh, some 25 miles east of Dhaka and located at north-west part of the city of Comilla. The Bakhrabad structure is interpreted from seismic data (Figure 1) as a relatively gentle, symmetrical fold, developed as an elongate anticline with a NNW-SSE trend. On the basis of single fold seismic data, Welldrill (1990) mapped three culminations, C to the north (Narshingdi gas field), B in the middle (Marichakandi/Meghna gas field) and A to the south (Bakhrabad gas field). The age of the sediments penetrated in the Bakhrabad wells is Neogene, but more precise dating is uncertain in the context of Bengal Basin stratigraphy as a whole. The sediments may be placed in the Surma and Tipam Groups, tentatively assigned to the Miocene and Mio-Pliocene age respectively (Choudhury 1999).

The Bakhrabad gas field has 5 major producing sand layers namely B, DU, DL, G and J. (Figure 2). There are 8 wells, of which 4 are producing from these sands and the rest are suspended from production due to excessive sand and water production. The presence of potential gas-bearing structure at Bakhrabad was first recognized from a gravity survey in 1953 (Choudhury 1999). First exploratory well, BK-1 was drilled vertically to a depth of 2827 m in the year 1968-69 and proved the presence of reservoir succession as A, B, C, D, F, G, J, K and L Sands. Under the first phase development project four more development wells were drilled from the same pad including work-over of BKB-1 in 1981-82. Additional 3 development wells were

drilled in the most potential "J" sand in the period of 1988-89 implementing second stage development in view of rapidly increasing gas demand in Bangladesh.

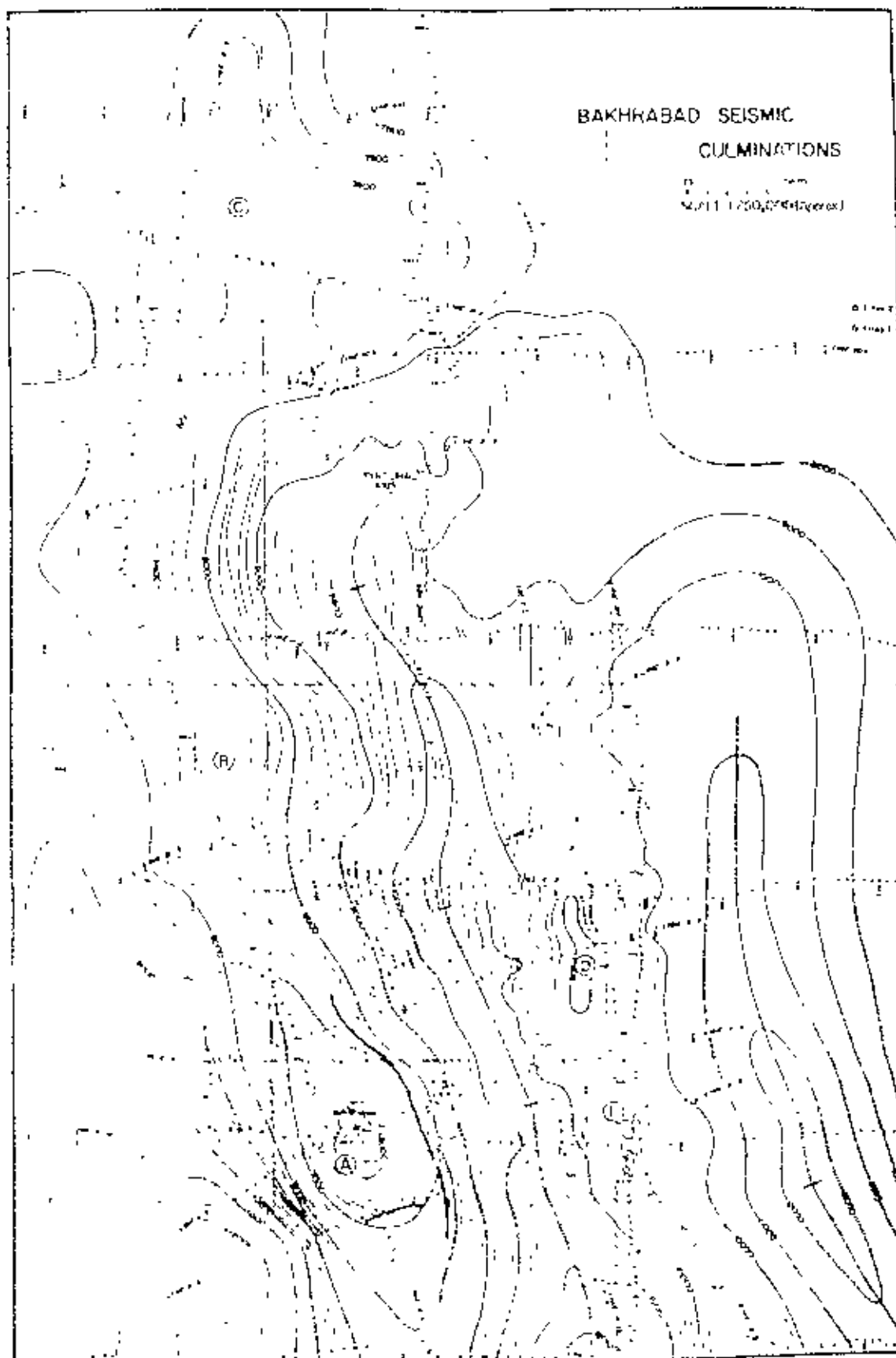


Figure 1 - Bakhrabad Seismic Culminations A, B and C.

Gas production rate from this field reached slightly above 200 MMSCFD from 8 (eight) producing wells in 1992 to meet the country's demand. During this time, the wellhead pressure started to decline with sand and excessive water production. Following excessive water production and subsequent decline in wellhead pressure well no. BK 4 and KB 5 were closed and gas production rate was reduced to 95 MMSCFD gradually over the period of 1992-97. To overcome the production problem, some well have been re-perforated and re-completed; no considerable improvement was observed afterwards. Two more wells (BK 6 in August, 1998 and BK 2 in June, 1999) were closed due to excessive water production with subsequent pressure decline. At present 4 wells (Well no Bk. 1, Bk. 3, Bk. 7 & Bk. 8) are flowing and production from this field is near about 35 MMSCFD since July 1999. Present rate of water production is about 4.6 BBL/MMSCF and condensate production is 0.80-1.00 BBL/MMSCF (Choudhury 1999).

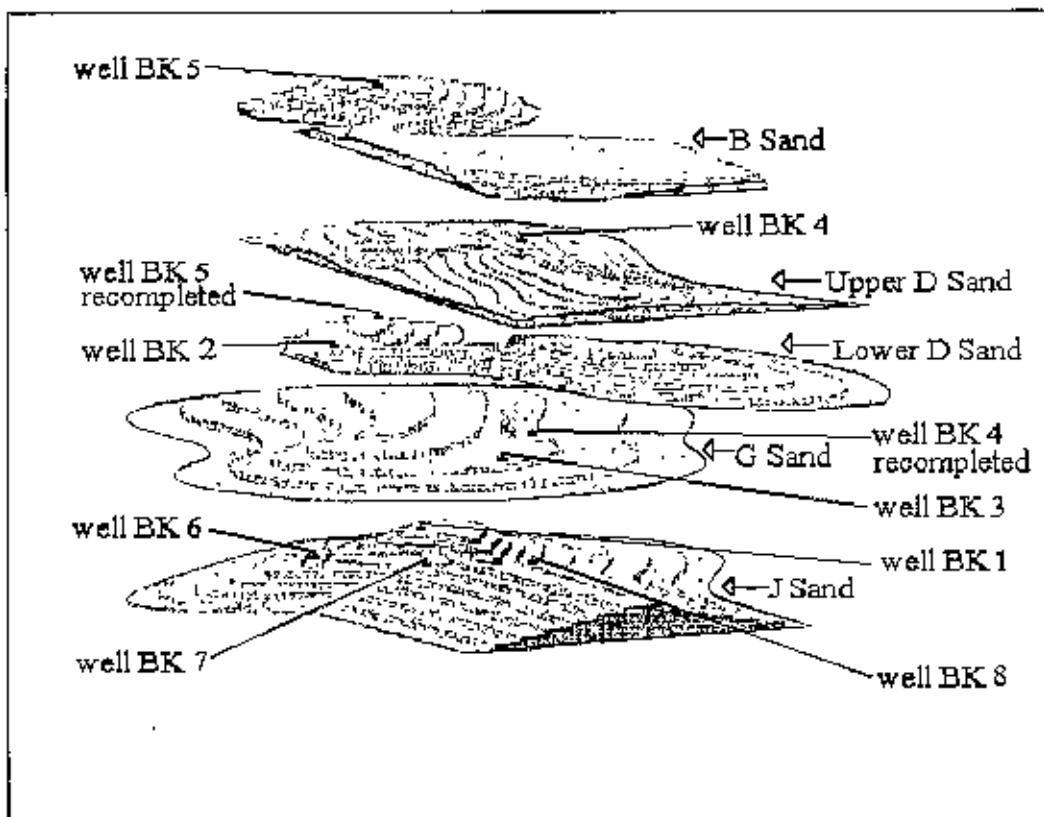


Figure 2 - Different Major Development Sands of Bakhrabad Gas Field

The advancements in production data analysis enable more sophisticated analyses accompanied by more reliable results. The value of these analyses, however, is strongly dependent upon the quality of real production data and importantly, the

analyst's ability to filter out the noisy data and retain the true reservoir signal. The blind application of these analysis methods, without consideration of data quality issues, can lead to misinterpretation and erroneous results. In this respect, practical diagnostic procedures of production data enable engineers to more effectively apply advanced analysis techniques to real data at the operational level, by limiting the possibility of misinterpreting the data.

Practical diagnostic procedures that can be applied to production data are either general – based on simple production data charts, or specific – using advanced typecurves. Like well test analysis, modern production data techniques employ the use of typecurves, which enable the quantitative and qualitative evaluation of a system through identifying and matching trends in the data that are similar to the shape of the underlying typecurve model. These typecurves are mostly production decline typecurves where a clear distinction can be made between transient and boundary dominated flow periods. Transient rate and pressure data are used to determine reservoir permeability, near wellbore condition (damage or improvement) and fracture length. Boundary dominated data are required to estimate the fluid-in-place and reserves.

Kabir and Izgec (2006) presented a simple diagnostic tool from which flow regimes can be identified from raw production data such as wellhead flowing pressure and rate. Here data diagnosis imposes graphing pressure with rate and discerning trends. Positive slope signifies the pseudo-steady state (PSS) flow period, which is boundary dominated. Negative slope implies infinite-acting (IA) or transient flow, when boundary effects are not felt. These plots also reveal compartmentalization and communication of wells in reservoirs especially those wells that are produced from volumetric reservoirs. The duration of different flow regimes can also be identified approximately from this diagnosis procedure, which is an outcome of this study.

According to Lee and Wattenbarger (1996), simple Cartesian and semi log plots of production data (mainly rate, cumulative production and time) show characteristic shapes for a volumetric reservoir which can be used as a diagnostic tool to determine the type of decline before any calculations are made. Similarly, Cartesian plot of

flowing pressure and cumulative production can reassure the drive mechanism of the reservoir and identify any additional drive, as it is done in the material balance plot.

Various analysis techniques exist to analyze production rate data for estimating in-place fluid volume and remaining reserves. These methods entail from traditional decline curve analysis, such as those offered by Arps (1945) and Fetkovich (1980) to more sophisticated techniques (Agarwal, Gardner, Kleinsteiber and Fussell 1999; Blasingame, McCray and Lee 1991; Blasingame, Johnston and Lee 1989; Mattar and McNeil 1997) involving both flowing bottomhole pressure and rate. Most of these methods apply to single wells in volumetric reservoirs producing single-phase fluids from a fixed drainage boundary. Mattar and Anderson (2003) provide a comprehensive treatment of the pertinent methods.

Changes in well performance may often be attributed to condensate banking or liquid loading, reservoir subsidence or layered characteristics of reserve, fines migration precipitating changing skin, and a host of completion and/or wellbore-lift issues, besides depletion.

Objective of the Study

In this study identification of flow regimes with time intervals, overall decline type and drive mechanism of Bakhrabad gas field are determined using simple diagnosis procedures. After diagnosis and analysis of all the wells in the Bakhrabad field in a systematic approach, both the gas-in-place and expected ultimate recoverable reserves will be determined using some advanced methods mentioned above. A commercial software package (F.A.S. I. RTA) will be used for this purpose.

The objective of the study has been subdivided as follows:

1. Diagnosis of reservoir characteristics from measured production (pressure/rate) data:
 - a) Flow regime identification (i.e., PSS, Transient etc.) with time intervals
 - b) Determination of reservoir connectivity and compartmentalization
 - c) Determination of overall decline type of reserve
 - d) Determination of drive mechanism

2. To estimate remaining reserve with Estimated Ultimate Recovery (EUR) and Recovery Factor (RF), and compare outcomes from different methods using production data

Methodology

To achieve the above objectives the following methods are to be adopted:

1. To collect all the available production, reservoir and field data for Bakhrabad and screen the reservoir signal from the production data set (which may contain a lot of unanalyzable data).
2. To use simple tools (graphical representations) to diagnose long-term well performance, especially those that are influenced by outer boundaries, in particular, whether wells belong to the same or different compartments using spreadsheet programs.
3. To analyze production data with traditional (Arps) decline analysis, and different type curve analysis methods including Fetkovich, Blasingame, Agarwal-Gardner, Normalized Pressure Integral (NPI) and Transient typecurve analysis to estimate the remaining gas reserves and recovery factor.
4. To further analyze the data using Flowing Material Balance (FMB) and Approximated Wellhead Material Balance (AWMB) methods.
5. A commercial production analysis software (F.A.S.T. RTA by Fekete Associates Inc.) will be used to carryout the above.

Chapter 2

LITERATURE REVIEW

There are several practical diagnostic procedures, some general and others specific, that can be applied to production data, both on simple production charts and on advanced typecurves. Using currently accepted methods for analysis of production data, the estimation of original gas-in-place may require several iterations and/or secondary calculations, as well as other reservoir or well parameters. However, the characteristic behavior of pseudosteady-state or boundary-dominated flow, must be exhibited prior to any material balance calculations. When production is initiated in a well, various flow regimes are encountered as transition from infinite-action (IA) to pseudosteady-state (PSS). A systematic discussion on production data diagnosis with a normal Cartesian plot was performed by Kabir and Izgec (2006). According to their paper, data diagnosis imposes graphing pressure with rate and discerning trends: positive and negative. The slope of the infinite acting (IA) flow period during variable-rate production in a liquid system is given by:

$$\frac{dp_{wf}}{dq_n} = \frac{-m \left\{ \sum_{j=1}^n \frac{q_j - q_{j-1}}{t_n - t_{j-1}} \right\} - m \frac{dq_n}{dt_n} \left\{ \log \left(\frac{k}{\phi \mu c_v r_w^2} \right) - 3.23 + 0.869s \right\}}{\frac{dq_n}{dt_n}} \quad \dots \quad (2.1)$$

In the above equation, the numerator remains negative, suggesting negative slope for the p_{wf} vs. q graph during the IA flow period. For the constant-rate case, $dq_n/dt_n = 0$, thus leading dp_{wf}/dq_n to infinity i.e. vertical line in graph. When a well is produced at a constant p_{wf} , the slope attains a zero value. The diagnostic tool, p_{wf} vs. q graph, is very simple as it requires no calculations and leads to understanding of reservoir compartmentalization.

For variable-rate production during PSS (closed outer boundaries) flow in a liquid system the slope is given by:

$$\frac{dp_{wf}}{dq_n} = \frac{-\frac{0.2339B}{\phi hc_v A} q_n}{-\frac{dq_n}{dt_n}} \quad \dots \quad (2.2)$$

The above equation shows that the slope is positive and is dominated by reciprocal of connected pore volume (CPV), $\phi h \Lambda$. Rate declines exponentially with time in a volumetric system. This fact implies that the dq_n/dt_n term in the denominator directly influences the slope on the p_{wf} vs. q graph, because the numerator is a linear term. It can be also noted that the slope retains the same value so long the drainage volume remains contiguous. Thus during PSS flow, wells belonging to the same container will exhibit the same slope. Differences in slope are an indication of lateral or vertical compartmentalization of the reservoir.

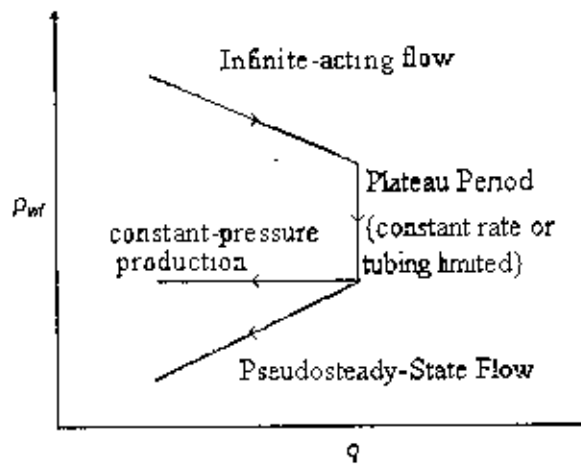


Fig. 2.1: Diagnostic P_{wf} - q graph for a closed system.

From Figure 2.1, it is clear that positive slope indicates the pseudosteady-state (PSS) flow period, whereas the negative slope implies infinite-acting (IA) flow. Constant-rate production exhibits infinite slope whereas constant-pressure production shows zero slope.

Wellhead pressure data can be used for diagnosis in pressure vs. rate graph, as they are readily available and are representative of bottomhole conditions. Moreover flowing bottom hole pressure, p_{wf} has one-to-one correlation with flowing wellhead pressure, p_{wh} (Kabir and Hasan 2006) and do not interfere with diagnosis. It is also possible to identify approximate duration of different flow regimes if production rate vs. time is plotted in the same pressure vs. rate graph (where time is plotted in the secondary y-axis and rate is the common x-axis). In this procedure time scale can be adjusted so that rate vs. time curve overlay upon the pressure vs. rate curve. Thus from the combined curves, i.e. p_{wh} - q - t , approximate duration of different flow regimes can be easily identified and used conveniently to other diagnostic procedures.

Different Reserve Estimation Methods

The reserve estimation methods discussed in this section are primarily those methods typically applied to volumetric dry-gas reservoirs. In such cases gas expansion is the only drive mechanism — no external source(s) of energy are considered in the calculations. All of these methods presume that the entire reservoir is being characterized by performance from a single well.

2.1 Material Balance Methods

The material balance method was developed after the volumetric method (i.e., estimates base on porosity, thickness, areal extent) and material balance has evolved to become the most popular mechanism for estimating reserves. Schilthius (1941) presented a general form of material balance equation derived using a volumetric balance on a hydrocarbon system. Material balances typically assume that the reservoir pore volume remains unchanged or it changes in a consistent manner with respect to reservoir pressure. The data required for material balance calculations include: fluid production data, reservoir temperature, reservoir pressure data, reservoir fluid properties, and core data. The material balance equation for a volumetric dry gas reservoir system presented by Schilthius neglecting water drive and interstitial water production is given as:

$$GB_{gi} = (G - G_p) B_g \quad \dots \quad \dots \quad (2.3)$$

Where GB_{gi} is the reservoir volume occupied by gas at the initial reservoir pressure, p_i , and, on the right hand side, $(G - G_p) B_g$ is the reservoir volume occupied by gas after gas production at any pressure below the initial pressure. Schilthius used the principle of conservation of mass to calculate remaining gas-in place. In volumetric terms, the statement of the material balance equation is that remaining reserves are the initial reserves less the produced reserves. In this case, the simplest form of the material balance equation for a volumetric dry-gas reservoir is

$$\text{Initial Volume} = \text{Volume Remaining} + \text{Volume Removed} \quad \dots \quad \dots \quad (2.4)$$

The material balance equation was simplified by Havlena and Odch (1963) and represented graphically and, in particular, a plot of \bar{p}/\bar{z} versus G_p yields a straight-line trend requiring only

an extrapolation of the \bar{p}/\bar{z} trend to the G_p -axis to get the estimated ultimate gas produced, or the gas reserves. This relation is given by:

$$\frac{P}{z} = \frac{P_i}{z_i} \left[1 - \frac{G_p}{G} \right] = \frac{P_i}{z_i} - \frac{P_i}{z_i G} G_p \quad \dots \quad \dots \quad (2.5)$$

The material balance method can be applied for production at constant rate or constant bottomhole flowing pressure — or any variable-rate/variable-pressure condition. An advantage of the \bar{p}/\bar{z} versus G_p plot is that it can be applied at any period of reservoir development. Most importantly, the material balance method gives a good estimate of recoverable gas-in-place as it reports on only the volumes, which are in pressure communication. It is noted that material balance methods are developed in terms of cumulative fluid production and changes in reservoir pressure, and therefore require accurate measurements of both quantities.

The material balance plot (i.e., the \bar{p}/\bar{z} versus G_p plot) has historically been used to provide an indication of the reservoir drive mechanism from the shape of the \bar{p}/\bar{z} trend. A consistent deviation of data from the straight-line trend can indicate external source(s) of energy or a secondary drive mechanism. It is noted that, this fact can be used as a diagnostic tool to identify external source(s) of energy and cases other than the case of a volumetric dry gas reservoir system can easily be addressed.

It is important to note that material balance methods require a sufficient duration of the production history in order to yield accurate results — typically 10 percent of the estimated reserves must be produced to provide a reliable estimate of gas reserves. Due to the sensitivity of the material balance methods to both data quantity and quality, one may rely on the volumetric method for reserve estimation in the early stages of production, and then use the material balance methods to refine the reserves estimation when sufficient data are available. (F.A.S.T.)

The complexity associated with the material balance method for reserve estimation is linked to the availability of average and initial reservoir pressure data. The pressure dependent parameters in the material balance equation are evaluated at the average reservoir pressure. The average

reservoir pressure remains the reference point for all parameters throughout the producing life of the reservoir; and therefore it is important in the material balance method. In obtaining the average reservoir pressure estimates, most operators use a pressure build-up test, which is costly, particularly for tight (or low permeability) gas reservoirs. Pressure build-up tests for gas wells require long-shut-in periods for the reservoir pressure profile to stabilize. This practice is simply uneconomical for many low permeability reservoirs.

Mattar and McNeil (1997) introduced the "Flowing" Gas Material Balance (FMB) for which shut-in reservoir pressures are not required. Instead p/z plot of the "flowing" pressure versus cumulative production is used. In this method, a straight line drawn through the flowing pressure data and then, a parallel line drawn through the initial reservoir pressure gives the original gas-in-place (OGIP). As wellhead pressure measurements are representative of bottomhole conditions (no fluid influx into the wellbore), a procedure similar to FMB, but ignoring compressibility factor z , is used to generate a reasonable wellhead material balance calculation, which they defined as Approximate Wellhead Material Balance (AWMB). This method is a very practical and simple tool for the early quantification of reserves.

2.2 Decline Curve Analysis

The analysis of production decline curve data can provide estimates of original gas-in-place, gas reserves, drainage area, future expected production rate and the remaining productive life of the well. As with other methods, the decline curve technique is dependent on the quantity and quality of data, and this method is applicable only when the reserve is in natural decline. The basis for the decline curve methods varies from empirical relations (e.g., the exponential and hyperbolic relations) to semi-analytical relations derived using material balance and pseudosteady-state flow relations. The calculated reserves are considered to be the hydrocarbons in communication with a particular producing well.

The use of production data as a forecasting tool dates back to 1918 when Lewis and Beal (1918) presented the consistent shape of the production decline curve as a mathematical tool, which may be used to forecast future production. Lewis and Beal (1918) observed that the production decline on a Cartesian plot of rate against time has a "power law" behavior actually a straight-

line trend on a log-log plot, and using the model trend or the calculated coefficients, a forecast of future production can be projected.

Production data analysis became a popular reserve forecasting tool in the 1940's when Arps (1945) presented his harmonic, exponential, and hyperbolic decline relations each of which were empirically based. This technique, developed by Arps, although well received in the industry, was used only for prediction and interpretation of production rate decline — not for the estimation of in-place fluid reserves or formation properties.

Arps later expanded the use of decline curve analysis to provide the prediction of primary reserves. This approach involved the extrapolation of rate-time data using hyperbolic and exponential decline data models. For reference, the Arps relations for flowrate and cumulative production are given in Table 2.1.

Table 2.1 Summary of the “Arps Analysis”:

Arps Flow rate Relations:

Case	Rate Relations			
Exponential: (b = 0)	$q(t) = q_i \exp(-D_i t)$	(2.6)
Hyperbolic: (0 < b < 1)	$q(t) = \frac{q_i}{[1 + bD_i t]^b}$	(2.7)
Harmonic: (b = 1)	$q(t) = \frac{q_i}{[1 + bD_i t]}$	(2.8)

Arps Cumulative Production Relations:

Case	Rate Relations			
Exponential: (b = 0)	$N_p(t) = \frac{q_i}{D_i} [1 - \exp(-D_i t)]$	(2.9)
Hyperbolic: (0 < b < 1)	$N_p(t) = \frac{q_i}{(1-b)D_i} [1 - (1 + bD_i t)^{-(1/b)}]$	(2.10)
Harmonic: (b = 1)	$N_p(t) = \frac{q_i}{D_i} \ln(1 + D_i t)$	(2.11)

Arps' observations regarding the decline curve exponent, b , for solution gas drive reservoir systems are given below:

$b = 0$ — Reservoir is highly undersaturated.

$b = 0$ — Dominant producing mechanism is due to gravity drainage and no free surface.

$b = 0.5$ — Gravity drainage with free surface.

$b = 0.667$ — Solution gas-drive reservoir, when average reservoir pressure, p versus cumulative oil, N_p is linear.

$b = 0.333$ — Solution gas-drive reservoir, when average reservoir pressure squared, $2p$ versus cumulative oil, N_p is linear.

Fetkovich (1980) proposed a substantial improvement in decline curve analysis by suggesting the matching production data onto specialized "type curves" (analogous to the analysis of well test data). Fetkovich presented the "unified" exponential decline type curve (which is the analytical solution for the case of a single well in a bounded symmetric reservoir) and coupled this data with the Arps hyperbolic rate relations (given in terms of specialized dimensionless rate and time function) to create what has become known as the "Fetkovich Decline Type Curve" (or simply the "Fetkovich Type Curve"). The Fetkovich type curve is the most familiar and widely accepted type curve for the analysis of production data.

Regarding the hyperbolic "stems" on the Fetkovich type curve, these trends are thought to account for "non-ideal" reservoir behavior such as: changes in mobility, reservoir heterogeneity and layering. It is also noted that the "early time" portion of the Fetkovich decline type curve is utilized much the same as type curve analysis for well test data. The analysis of early time production data using the Fetkovich (1980) decline type curve is often problematic — the quantity and quality of these data may prevent a unique analysis from being achieved.

Fetkovich and coworkers combined the appropriate material balance and pseudosteady-state flowrate equations to develop explicit rate-time decline equations for single-phase flow behavior in both oil and gas reservoir systems. This work was seen as a theoretical attempt to justify the Arps empirical equations, which Fetkovich had used as the foundation to develop the unified type-curves. Fetkovich advised that reservoir volume and volume-related flow characteristics

should not be estimated using decline type curve analyses prior to the full development of boundary dominated flow behavior. The reported use of decline curve analyses on several field cases in Fetkovich's paper illustrates the versatility and utility of the decline type curve analysis concept.

Al-Hussainy, et al. (1966) presented a new mechanism for addressing the effects of pressure-dependent gas properties. The new concept was that of a "pseudopressure" as a variable that could be used to partially linearize the gas diffusivity equation. The definition of pseudopressure as given by the authors is:

$$m(p) = 2 \int_{p_{\text{DNR}}}^p \frac{p}{\mu_g(p)z(p)} dp \quad \dots \quad \dots \quad (2.12)$$

The first comprehensive attempt to linearize the entire gas flow equation was by Agarwal (1979). Agarwal presented a pseudotime function for a real gas that incorporates changes in gas viscosity and total compressibility as a function of time. The pseudotime function as proposed by Agarwal is given as:

$$t_a(t) = \int_0^t \frac{1}{\mu_g(p)c_t(p)} dt \quad \dots \quad \dots \quad (2.13)$$

Another type curve solution for analysis of gas flow systems was presented by Carter (1985), who correlated the case of a gas well produced at a constant bottomhole pressure using specialized dimensionless variables. This type curve clearly exhibits the influence of the pressure drawdown (i.e., $p_i - p_{wf}$) on the gas flowrate behavior. In theory, the "Carter type curve" addresses the issue of the compressibility-viscosity product (as a function of the average reservoir pressure), however, it is noted that the controlling factor on the Carter formulation is the assumption of the constant bottomhole pressure condition.

Carter used the λ -variable to reflect the magnitude of pressure drawdown and the influence of pressure drawdown on the compressibility-gas viscosity product. For example, the $\lambda=1$ case corresponds to the exponential decline curve exponent (i.e., $b=0$) — that is, the equivalent liquid case. Large pressure drawdown cases yield λ -values as low as 0.75 (or lower). As noted, the Carter type curve was developed as a solution to boundary dominated radial gas flow equations

for production at constant bottomhole pressure — where these conditions make the Carter type curve the appropriate choice for the estimation of gas well reserves (for the case of gas flowrate-time analysis). The Carter λ -variable is given as:

$$\lambda = \frac{\mu_g c_h}{\mu_r c_i} \dots \dots (2.14)$$

The Fetkovich decline type curve with all its innovation in the improvement of production data analyses has its limitations. Doublet, Pande, McCollum and Blasingame (1994) reported the limitations of Fetkovich decline type curve analysis are largely due to non-compatibility with field operations and reservoir inconsistencies that distort the production data (in particular, the variable rate/pressure histories common in practice as well as the analysis of gas reservoir systems). These issues are significant and often render the original “Fetkovich” analysis approach untenable.

Another issue associated with the Fetkovich decline type curve approach is the oversimplification of the gas flow solution. The liquid solution presented by Fetkovich is only applicable for gas flow cases during transient flow and for very small pressure drawdowns. These small drawdowns assume gas properties remain constant or change only slightly with changing pressures. For large drawdown cases the liquid case can not be used to represent the gas flow case.

The pseudopressure and pseudotime functions are shown to linearize (Lee, et al. 1996) the gas diffusivity equation and thus, permit us to use liquid flow solutions as a basis (e.g., the Fetkovich type curve) for the analyses of gas production data — provided that the pseudopressure and pseudotime functions are appropriately defined and computed for the case of boundary-dominated gas flow behavior.

Fraim and Wattenbarger (1987) modified the Agarwal definition of the pseudotime function to yield a “normalized” formulation and proposed to use this form to account for the non-linear product of total compressibility and gas viscosity using the average reservoir pressure as the reference pressure in the pseudotime integral. The normalized pseudopressure and pseudotime functions are shown to linearize (Fraim and Wattenbarger, 1987) the gas diffusivity equation

(i.e., create an "equivalent liquid" response) — and, as such, allows for the use of liquid flow solutions for the analyses of gas production data. The Fraim and Wattenbarger pseudopressure and pseudotime formulations can be directly incorporated into decline type curve analysis. This approach provides a direct mechanism to address the variation in pressure dependent properties for the gas flow case — however, this approach does not address the variable-rate/pressure-drop case.

Blasingame and Lee (1986) introduced a new concept for addressing the issue of variable-rate and variable pressure production data — in particular, how to analyze such data to provide estimates of drainage area and reservoir shape. This work was applied to type curve matching.

Palacio and Blasingame (1993) proposed a rigorous approach for the analysis of variable-rate and variable bottomhole pressure data using a modified pseudotime function (where this result was a combination of the Fraim and Wattenbarger pseudotime relation (for gas) and the Blasingame and Lee variable-rate/variable pressure drop relation. The approach was both straightforward and stable, and was a significant improvement over work presented by McCray, et al.(1991) — where the objective was to establish a constant pressure production analog. As such, Palacio and Blasingame proposed a constant rate analog where $q_g/\Delta p_p$ data were plotted against a pseudotime function, and the data trend was matched onto the Arps harmonic stem ($b=1$) on the Fetkovich decline type curve.

Callard and Scheneweck(1995) presented a simplified approach for well performance using a "combined type curve" analysis. They provided a method for the pressure normalization of cumulative production in decline curve analysis. Variations in the bottomhole flowing pressures were addressed by dividing the cumulative production by the pressure difference between initial and bottomhole pressures.

In 1998 Agarwal, et al. presented a combined package of decline type curve analysis using the work of Palacio and Blasingame (1993), Carter (1985), and Callard and Scheneweck (1995). Agarwal, et al. also presented a "Rate-Cumulative Production Decline Type Curve" which is a plot of normalized gas flowrate as a function of cumulative production.

Chapter 3

PRESSURE VS. RATE DIAGNOSIS

Diagnosis means the process of identifying or determining the nature of reservoir through evaluation of production history, examination and review of production or performance data. Thus a prior assessment of the quality and completeness of the production data is a must. The available production data of Bakhrabad Gas Field from BGFCL are monthly flowing wellhead pressures and monthly average gas flow rates of different wells (8 wells). Data frequency is a non-issue for diagnosis. Kabir and Izgec (2006) stated in their paper that data frequency ranging from high (minutes) to low (months) has no bearing on the ability to establish trends, provided sufficient number of data points are available. Flowing pressure averaged over any period have little significance, unless operating conditions are stable and reasonably constant. In diagnosis the key ingredient is data synergy.

In this chapter pressure vs. rate diagnostic tool is used to identify reservoir flow behavior and approximate duration of different flow regimes from a Cartesian pressure/rate graph. In the next two chapters decline diagnosis and approximate well head material balance (AWMB) analysis are presented respectively with the production data of Bakhrabad gas field.

3.0 Sand-wise pressure vs. rate diagnosis

Since the inception in May 1984, number of production wells in Bakhrabad Gas Field is eight and they were producing from B, DU, DL, G and J sands. Their present status is given in the following table:

Table 3.1 Present Status of all wells in different sands of Bakhrabad gas field:

Sand	Well	Start of Production	Current Status	Remarks
J	BK1	Aug. '85	Producing	
	BK6	Dec. '89	Suspended	
	BK7	Dec. '89	Producing	
	BK8	Dec. '89	Producing	
G	BK3	Oct. '86	Producing	
	BK4	Oct. '94	Suspended	Recompleted well
DL	BK2	May. '84	Suspended	
	BK5	Dec. '94	Suspended	Recompleted well
DU	BK4	Oct. '86	Suspended	
B	BK5	Oct. '84	Suspended	

3.1 J Sand

J Sand is one of the major reservoirs of Bakhrabad Gas Field. This sand was penetrated by all eight wells and was tested in wells BK1, BK2, BK6, BK7 and BK8. At Well BK2, lower part of J Sand was found to be tight. Thus there are four wells that produced from J Sand, i.e., BK1, BK6, BK7 and BK8.

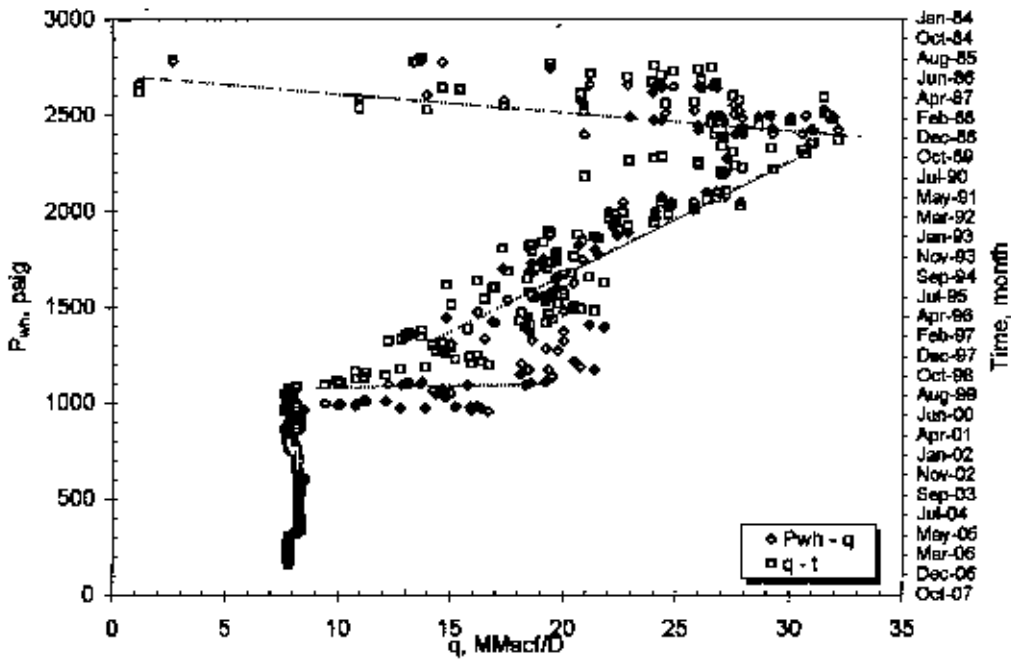


Fig 3.1 $p_{wh}-q-t$ diagnostic plot of BK1 at J Sand

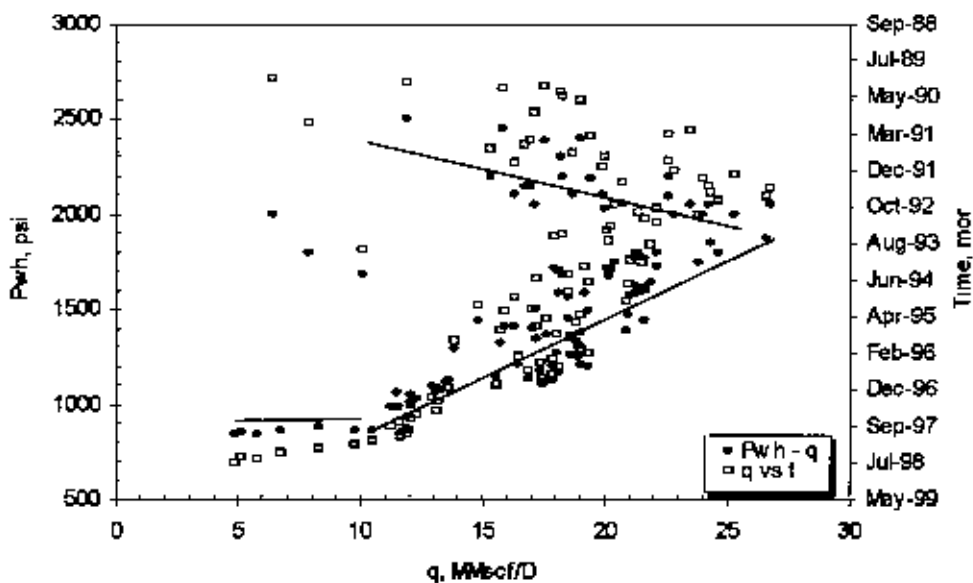


Fig 3.2 $p_{wh}-q-t$ diagnostic plot of BK6 at J Sand

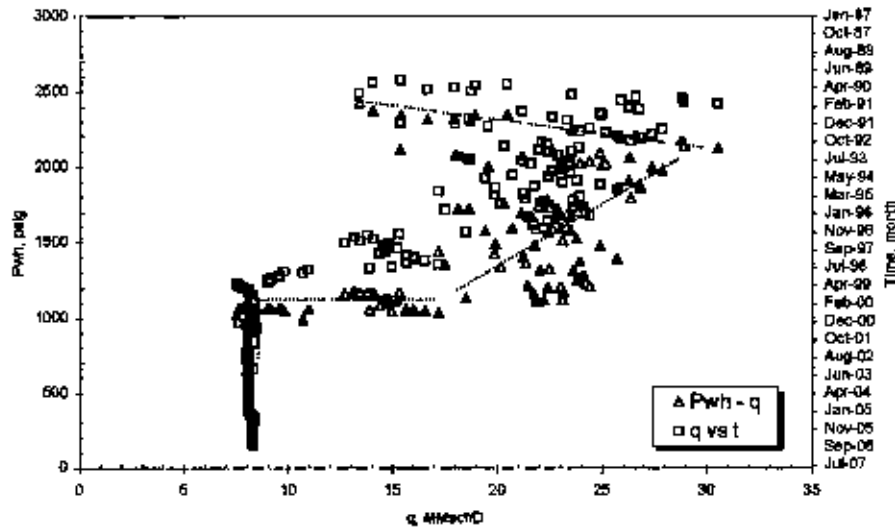


Fig 3.3 p_{wh} - q - t diagnostic plot of BK7 at J Sand

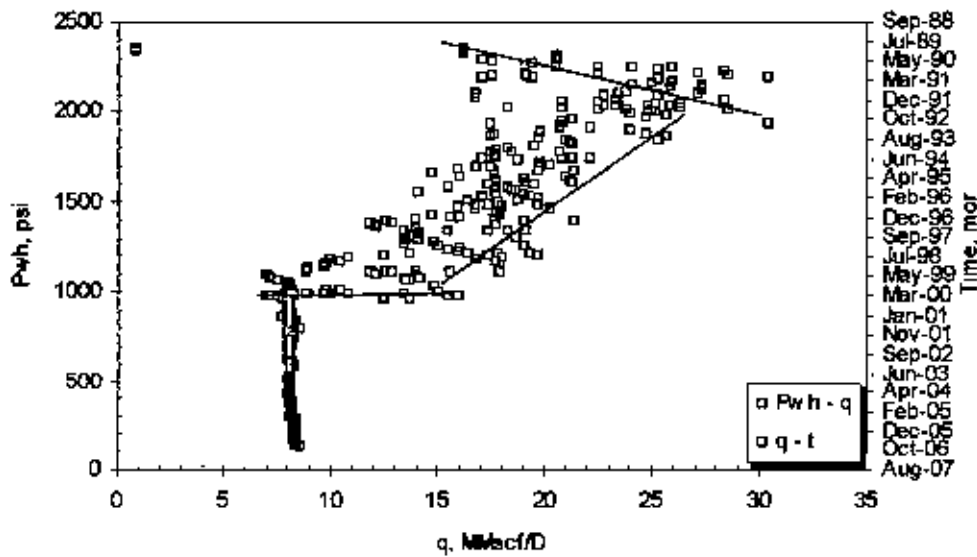


Fig 3.4 p_{wh} - q - t diagnostic plot of BK8 at J Sand

From Figures 3.1 to 3.4, it is clearly visible that all wells of J Sand have gone through IA, PSS, constant rate and constant pressure flow periods. In August 1985, BK 1 was put on production and it showed IA period from start of the production to February 1988. Then it followed long PSS flow duration, exhibiting positive slope line up to May 1998. Then it followed constant pressure production up to May 1999 and since then rate restriction was imposed, i.e. constant rate production at about 8 MMscf/D was followed (Fig 3.1).

BK 6 was put on production in December 1989 and showed IA flow period up to June 1992. Then from August 1992 to February 1998, BK 6 followed PSS flow and from February 1998 to August 1998, it followed constant pressure flow period. No constant rate production period was found as this well had suspended for excessive water production long before the imposed rate restriction (Fig 3.2).

BK 7 was also put on production in December 1989 and showed IA flow period up to January 1991. Then from March 1992 to February 1998, it followed PSS flow and from February 1998 to August 1998, it followed constant pressure flow period. From October 1999, it started to produce at an imposed constant rate of about 8 MMscf/D (Fig 3.3).

Similarly BK 8 was also put on production in December 1989 and showed IA flow period up to January 1991. Then from March 1992 to March 1998, it followed PSS flow and from March 1998 to April 1999, it followed constant pressure flow period. From October 1999, it started to produce at an imposed constant rate of about 8 MMscf/D (Fig 3.4).

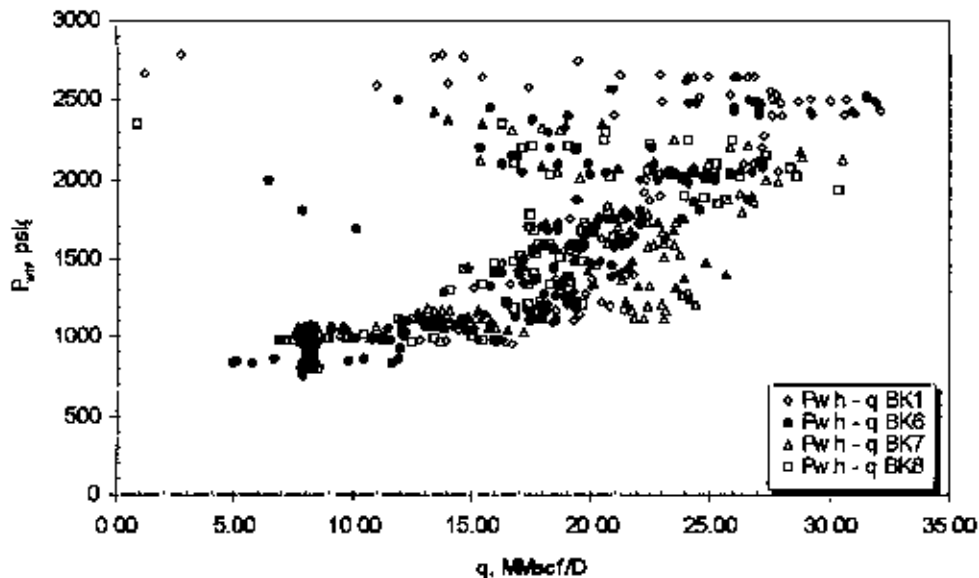


Fig 3.5 p_{wh} - q diagnostic plot of all wells at J Sand

Figure 3.5 shows that wells are from same area, essentially replicate the PSS flow behavior amid scatter. Thus from p_{wh} - q graph, well performance can reveal connectivity. In the above figure, with unequal p_{wf} , p - q graph indicates separation. But with about same slope, the graph represents the wells are in same reserve. The changing p_{wf} may due to heterogeneity or changing kh .

3.2 DL Sand

DL Sand was produced by two wells, BK2 and BK5. Well BK5 was watered out in May 1997. Well BK2 in the DL Sand was perforated in two intervals: 1) 7390 – 7475 ft and 2) 7480 – 7500 ft. Thus BK2 was produced by commingled system.

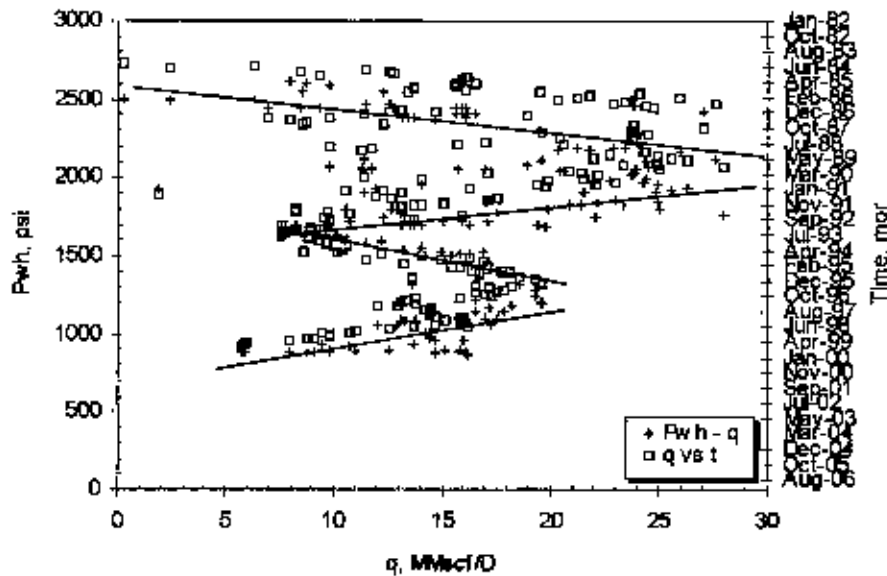


Fig 3.6 p_{wh} - q - t diagnostic plot of BK2 at DL Sand

BK 2 was put on production in May 1984. From Fig 3.6, it is found that unlike other wells BK2 have two separate phase of production. Each phase have their individual IA and PSS flow periods. From May 1984 to December 1985, BK 2 followed IA flow and then following a long plateau period it showed PSS flow period from January 1989 to October 1992 (Fig 3.6). If this phase of production is named as phase 1 production for BK 2, then after going through a two month workover period (November and December 1992) the final phase of production may named as phase 2 production. In the workover period, a sand trap was installed before the processing plant to reduce sand production, which didn't work properly later. Thus in phase 2 production, well BK2 showed IA flow period from January 1993 to October 1995 and following a plateau period it again showed PSS flow period from January 1998 to June 1999 (Fig 3.6). This well had also been suspended for excessive water production after June 1999.

After recompletion in DL sand BK5 was put on production on December 1994. BK5 showed very small IA flow period in the recompleted zone. From Fig 3.7, it is seen that BK5

followed PSS flow from December 1994 to May 1997. It followed two near constant flow periods – at the start of production from February 1995 to February 1996 and at the end of production from January 1997 to May 1997.

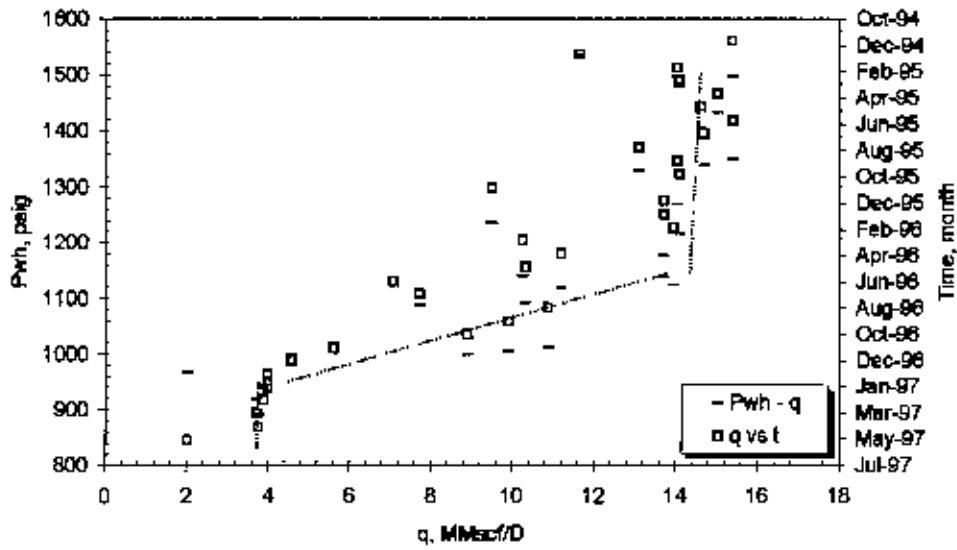


Fig 3.7 p_{wh} - q - t diagnostic plot of BK5 at DL Sand

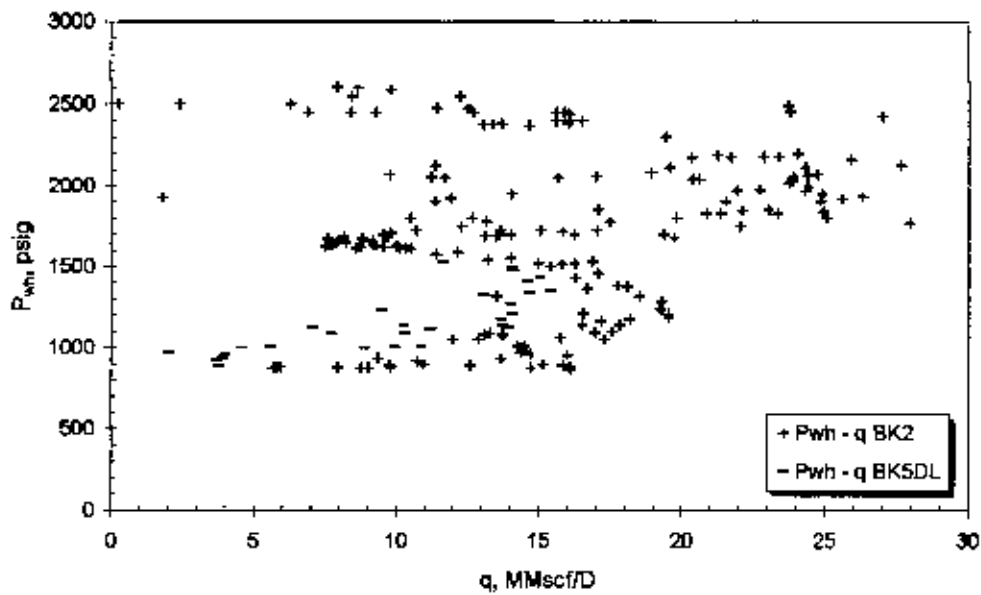


Fig 3.8 p_{wh} - q diagnostic plot of all wells at DL Sand

Figure 3.8 shows that wells are replicating the PSS flow behavior. Thus from p_{wh} - q diagnostic plot, it reveals connectivity. In the above figure, with unequal p_{wh} , p - q graph indicates separation, but with same slope, the graph represents the wells are in same reserve.

3.3 DU Sand

DU Sand was produced by well BK4 only. Well BK4 started its production in October 1986 and was out of production due to excessive water production in November 1992. Well BK4 in the DU Sand was perforated in the interval 7110 – 7145 ft.

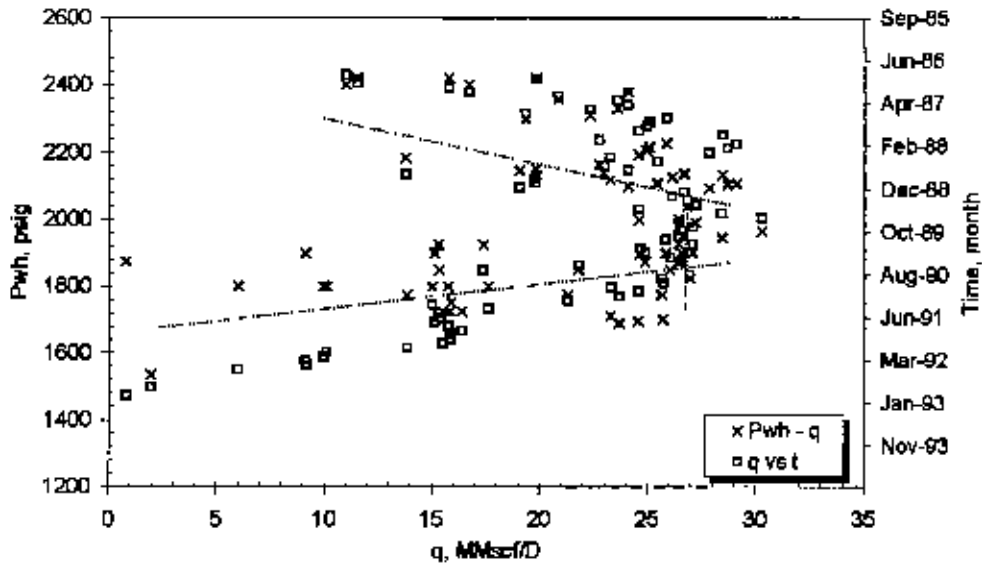


Fig 3.9 p_{wh} - q - t diagnostic plot of BK4 at DU Sand

BK4 showed IA flow period up to February 1988. Then from July 1989 to November 1992, BK4 followed PSS flow and from February 1988 to July 1989, it followed plateau period (Fig 3.9).

3.4 B Sand

B Sand was produced by well BK5 only. Well BK5 started production in October 1986 and was out of production due to excessive water and sand production in October 1994. BK5 showed IA flow period up to January 1987. Then from September 1990 to October 1994, BK5 followed PSS flow and in between January 1987 to September 1990, it followed plateau period (Fig 3.10).

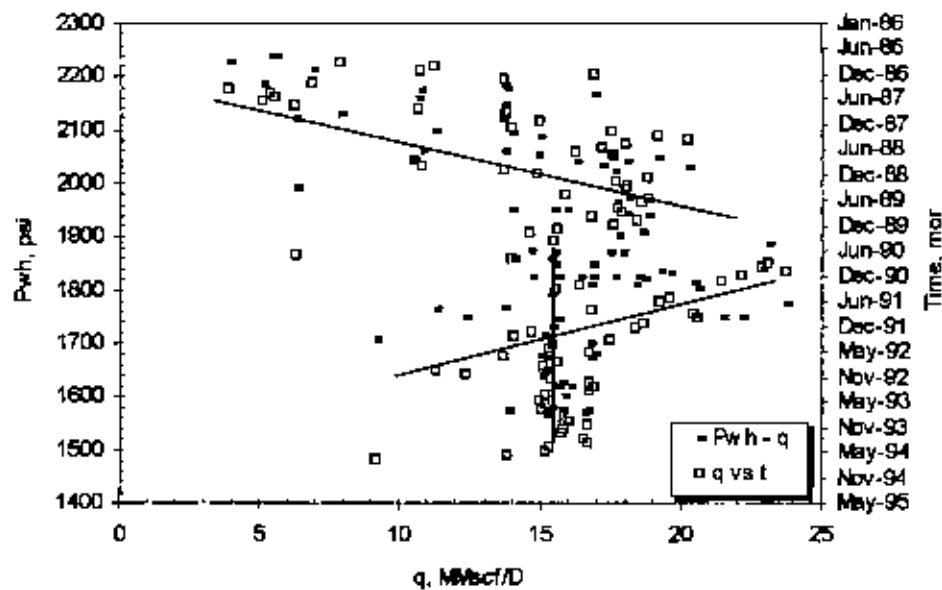


Fig 3.10 p_{wh} - q - t diagnostic plot of BK5 at B Sand

3.5 G Sand

G Sand was produced by wells, BK3 and BK4. Well BK3 is a producing well and BK4 was recompleted in this sand later when its production had been suspended from DU Sand due to excessive amount of water production. BK3 started its production from October 1986 and showed IA flow period up to February 1988 (Fig 3.11).

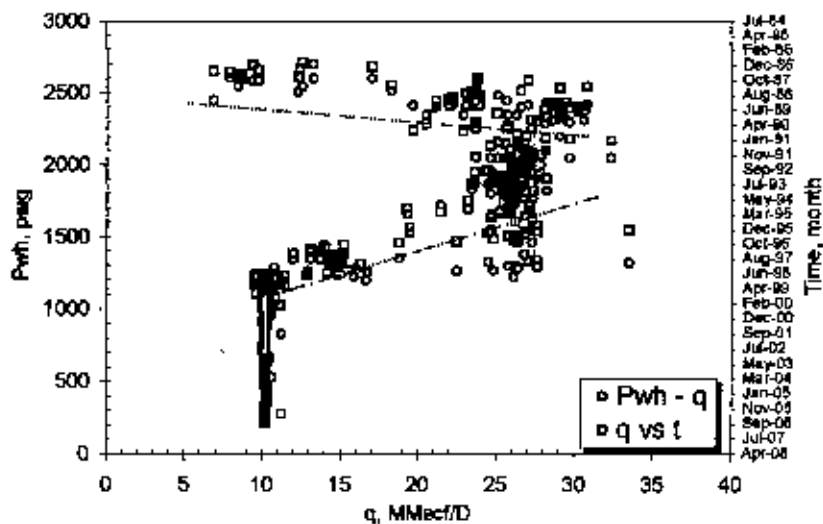


Fig 3.11 p_{wh} - q - t diagnostic plot of BK3 at G Sand

Then from January 1995 to April 1999, it followed PSS flow and from April 1999 it started to produce at an imposed constant rate of about 10 MMscf/D.

After recompletion in G sand BK4 was put on production on October 1994. BK4 showed very short IA flow period in the recompleted zone. From Fig 3.12, it is seen that BK5 followed PSS flow from October 1994 to December 1996. Then it followed a constant flow periods from December 1996 to November 1997.

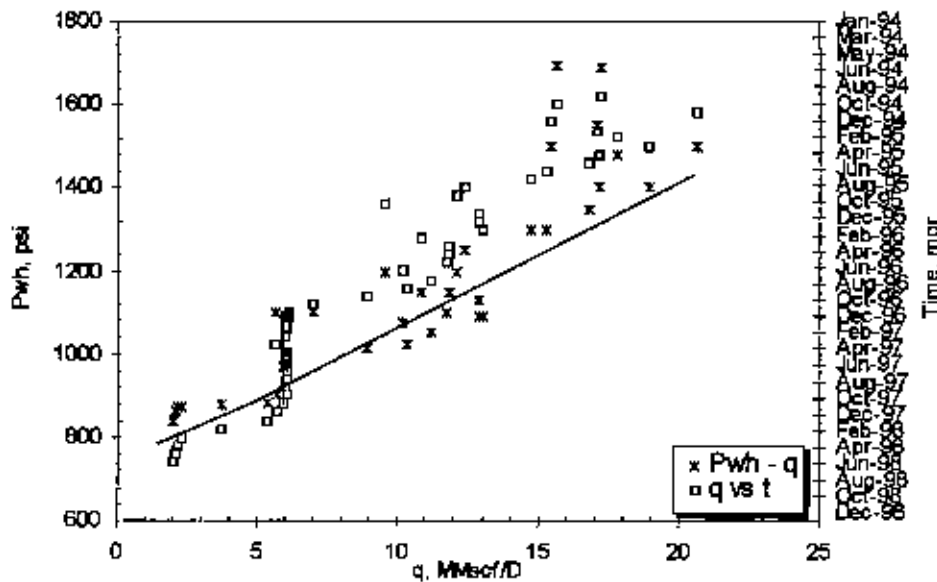


Fig 3.12 p_{wh} - q - t diagnostic plot of BK4 at G Sand

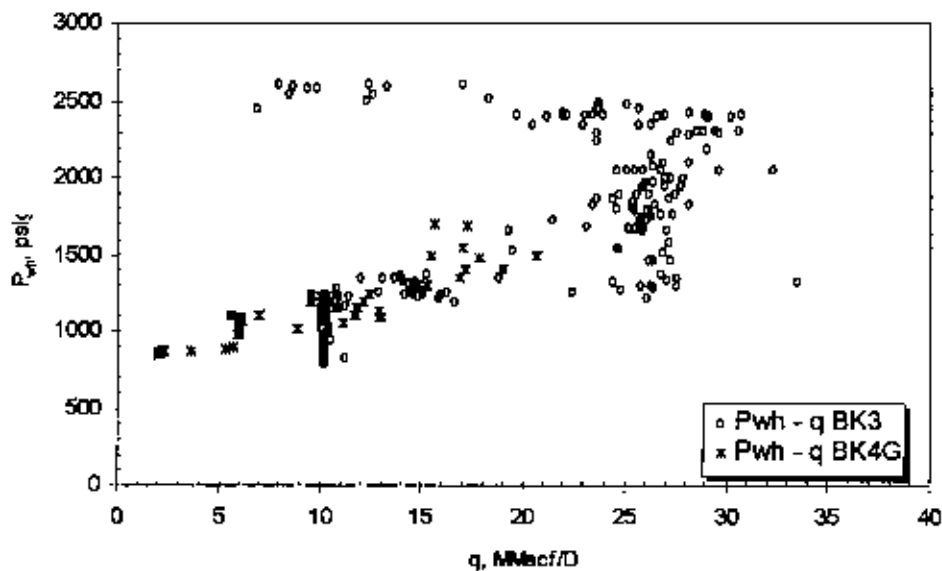


Fig 3.13 p_{wh} - q diagnostic plot of all wells at G Sand

Figure 3 13 shows that wells are replicating the PSS flow behavior. Thus from p_{wh} - q diagnostic plot, it reveals connectivity. In the above figure, with unequal p_{wh} , p - q graph indicates separation, but with same slope, the graph indicates that the wells are in same reserve.

Figure 3.5 shows that in p_{wf} - q graph, wells of J sand are nearly overlapping in PSS regime with scattered data. Thus from p vs. q diagnosis, wells performance reveal connectivity. In that figure, with unequal p_{wf} , p - q graph indicates separation but with about same slope, the graph represents the wells are in same reserve. Figure 3.8 also shows that wells are replicating the PSS flow behavior and reveals connectivity. Thus wells of DU sand are in same reserve. Figure 3.13 shows that wells of G sand are also representing same slope in the PSS flow behavior. Thus with same slope, the diagnosis reveals the wells of G sand are in same reserve. From p vs. q diagnosis it is clear that there is no compartmentalization in any of producing sands of Bakhrabad gas field. Wells of their respective sands are producing from the same reserve or sand. This simple diagnostic tool also showed its use in identifying flow regimes of individual wells with approximate duration of different flow regimes.

Chapter 4

DECLINE DIAGNOSTICS

According to Lee and Wattenbarger (1996), the basis of decline-curve analysis is to match past production performance histories or trends with a “model”. Assuming that future production continues to follow the past trend, these models can be used to estimate original gas in place (OGIP) and to predict ultimate gas reserves at some future reservoir abandonment pressure or economic production rate.

Prior to perform any modern decline curve analysis, conventional analysis of three forms of decline – exponential, harmonic and hyperbolic – reveals different shape on Cartesian and semi log graphs of gas production rate vs. time and gas production rate vs. cumulative gas production. Figs. 4.1 through 4.4 show typical responses for exponential, hyperbolic, and harmonic declines. Because of their characteristic shapes, these plots can be used as a diagnostic tool to determine the type of decline before any calculations are made. Cartesian plot of rate vs. cumulative gas production (Fig. 4.3) can be used to extrapolate to raw recoverable reserves (Mattar and McNeil).

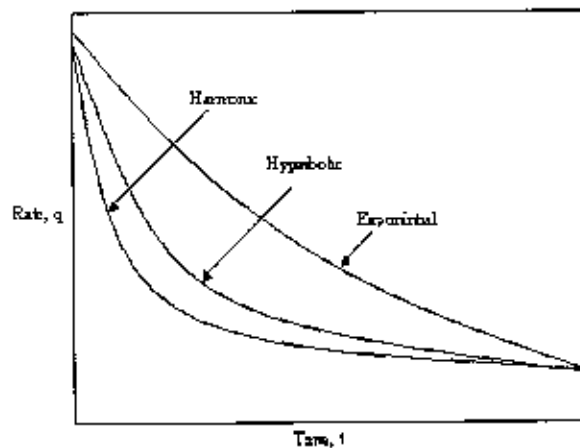


Fig. 4.1 Decline curve shapes for a Cartesian plot of rate vs. time

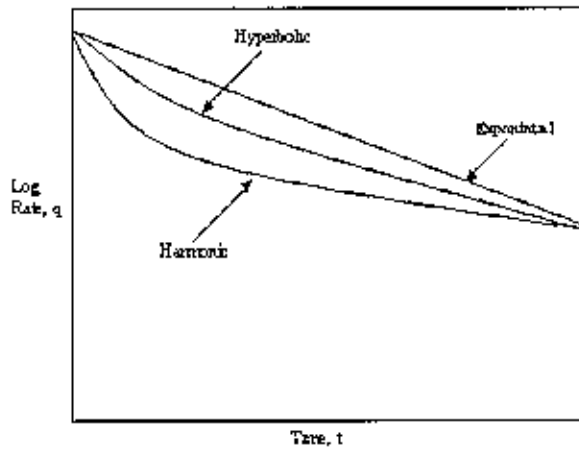


Fig. 4.2 Decline-curve shapes for a semilog plot of rate vs. time.

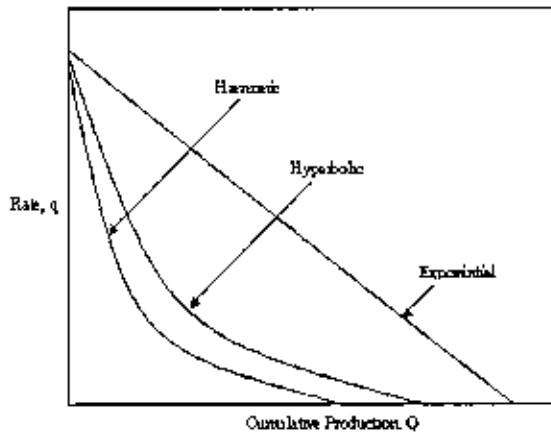


Fig. 4.3 Decline-curve shapes for a Cartesian plot of rate vs. cumulative production.

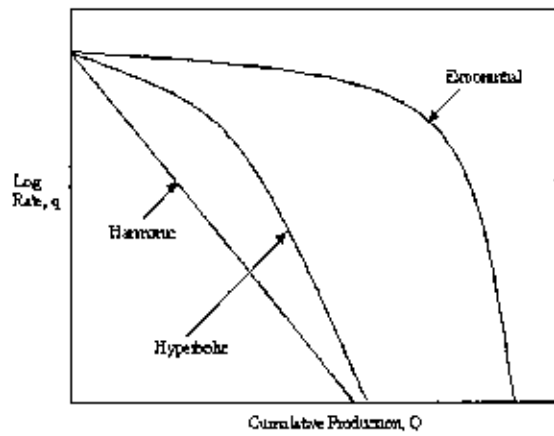


Fig. 4.4 Decline-curve shapes for a semilog plot of rate vs. cumulative production.

According to Ikoku (1992), the factors that directly affect the decline in gas production rate are: (1) reduction in average reservoir pressure and (2) increases in the field water cut in water-drive fields. Certain conditions must prevail before one can analyze a production decline curve with any degree of reliability. The production must have been stable over the period being analyzed; i.e., a flowing well must have been produced with constant choke size or constant wellhead pressure. The production decline observed should truly reflect reservoir productivity and not be the result of external causes, such as a change in production conditions, well damage, production controls, and equipment failure. In this section, type of decline and raw recoverable reserve will be discussed for wells of different sands.

4.0 Sand-wise Decline diagnosis

This section discusses decline-curve methods for estimating ultimate gas recoveries and predicting the type of decline from the analysis of long-term gas-production data from individual wells of different sands.

4.1 J Sand

There are four wells in J Sand: BK1, BK6, BK7 and BK8. Among them BK6 is suspended for production due to excessive water production. Individual well's decline diagnosis plots are presented in appendix B. Here a combined plot is presented for wells in common sand. Cartesian plot of Rate vs. Time of all wells in J Sand is given in the following figure.

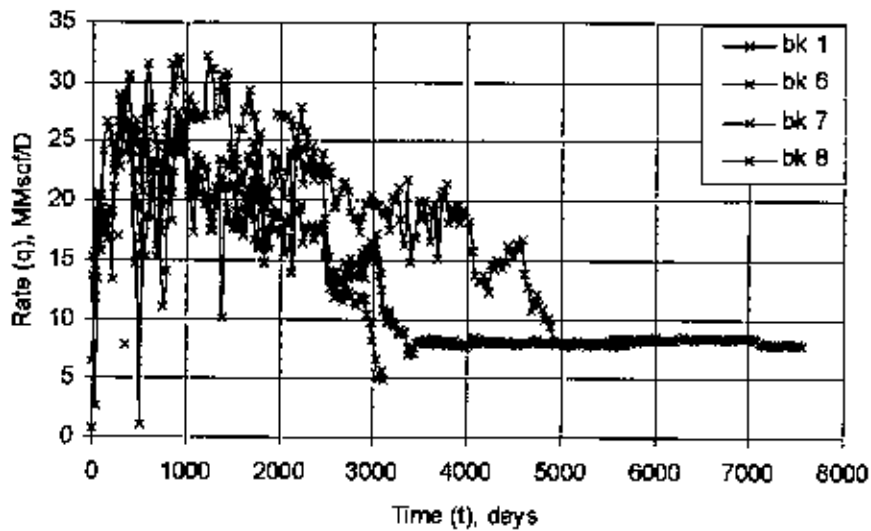


Fig 4.5 Cartesian plot of Rate vs. Time of all wells in J Sand

From this traditional decline plot it is evident that all the wells in J Sand show similar type of decline behavior. BK1 exhibits longer prorated production and declining production than other wells, as it is the oldest well in J Sand (Fig.4.6). For producing wells (BK1, BK7 & BK8) before rate restriction was imposed and for suspended well (BK6) before suspension, a sharp exponential decline is common for all which is an indication of gas wells undergoing liquid loading according to Fetkovich, Fetkovich, and Fetkovich (1994).

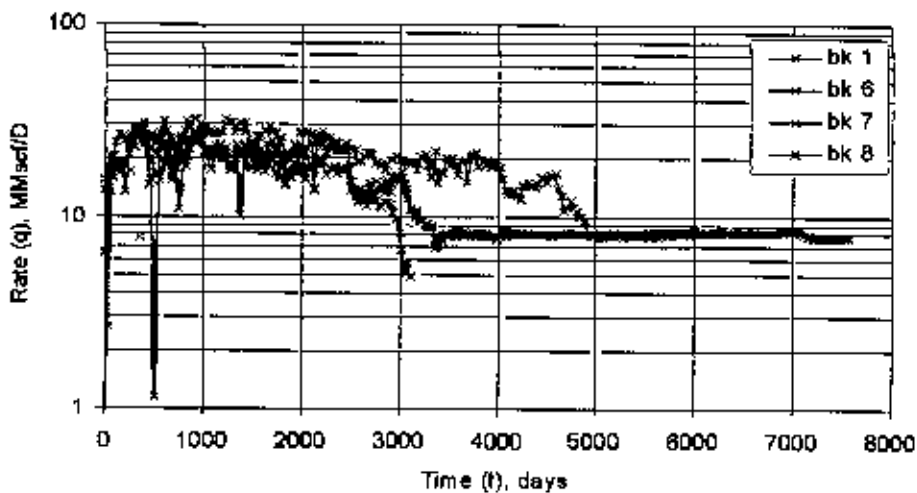


Fig 4.6 Semilog plot of Rate vs. Time of all wells in J Sand

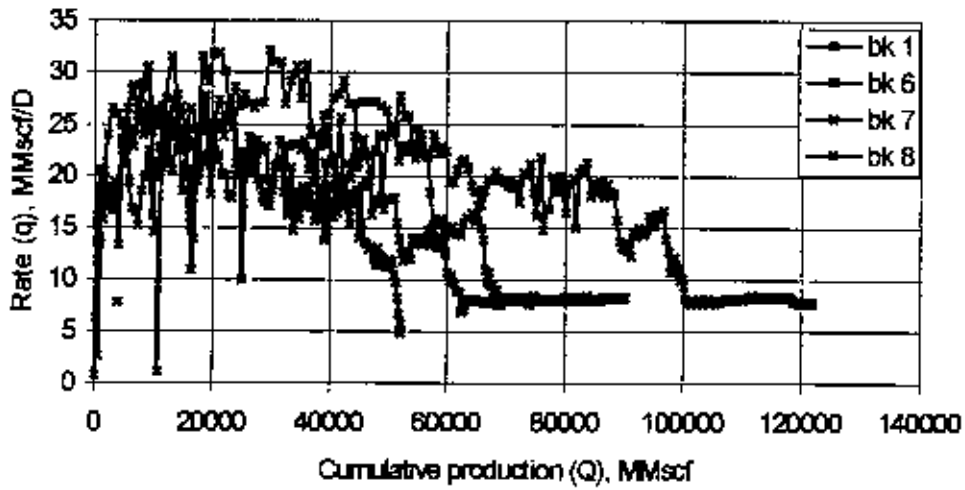


Fig 4.7 Cartesian plot of Rate vs. cumulative production of all wells in J Sand

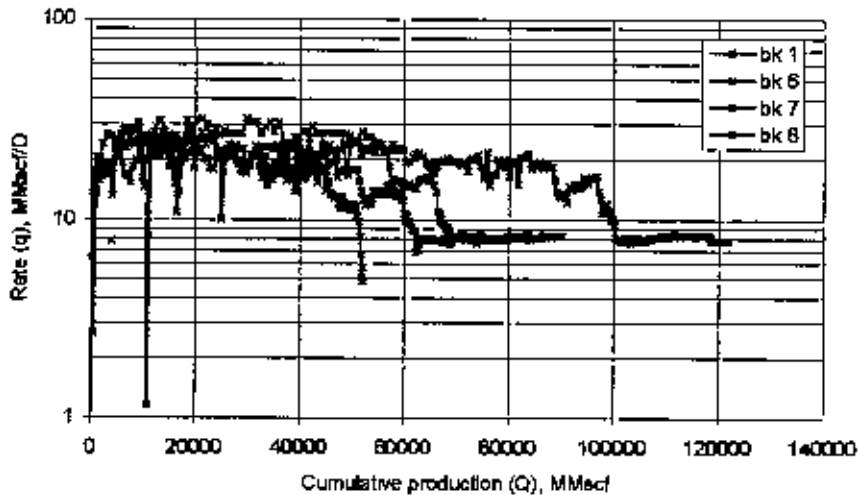


Fig 4.8 Semilog plot of Rate vs. cumulative production of all wells in J Sand

From Cartesian plot of Rate vs. cumulative production of individual wells in appendix B, raw recoverable reserve for BK1 is 139 bcf, for BK6 is 70 bcf, for BK7 is 95 bcf and for BK8 is 100 bcf. And cumulative gas production (G_p) for these wells up to August 2006, are accordingly 121.84, 52.075, 90.2 and 83.63 bcf. Fig 4.7 and fig 4.8 also indicate the identical exponential type decline for all wells in J Sand.

4.2 G Sand

There are two wells in G Sand: BK3 and BK4. Among them BK3 is producing well and BK4 (recompleted in G Sand) is suspended due to excessive water production and pressure decline. Cartesian plot of Rate vs. Time of all wells in G Sand is given in the following figure.

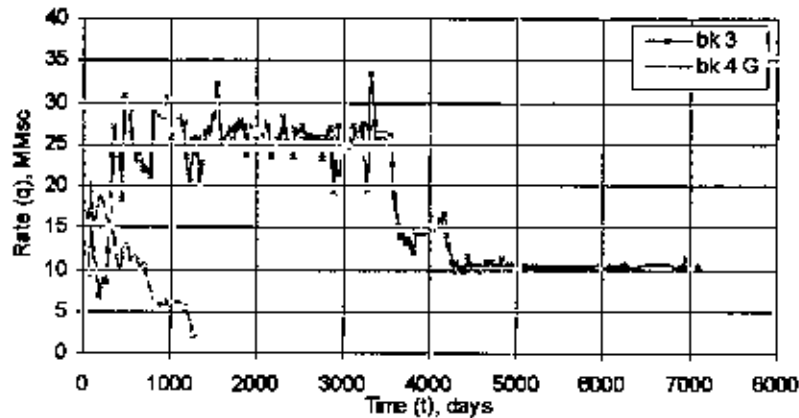


Fig 4.9 Cartesian plot of Rate vs. Time of all wells in G Sand

From this Cartesian plot it is observed that two wells in G Sand show similar type of constant percentage decline behavior. BK3 exhibits long prorated production before declining production, whereas BK4 started declining from the beginning of production in G Sand (Fig.4.10). This sharp exponential decline is an indication of wells undergoing liquid loading.

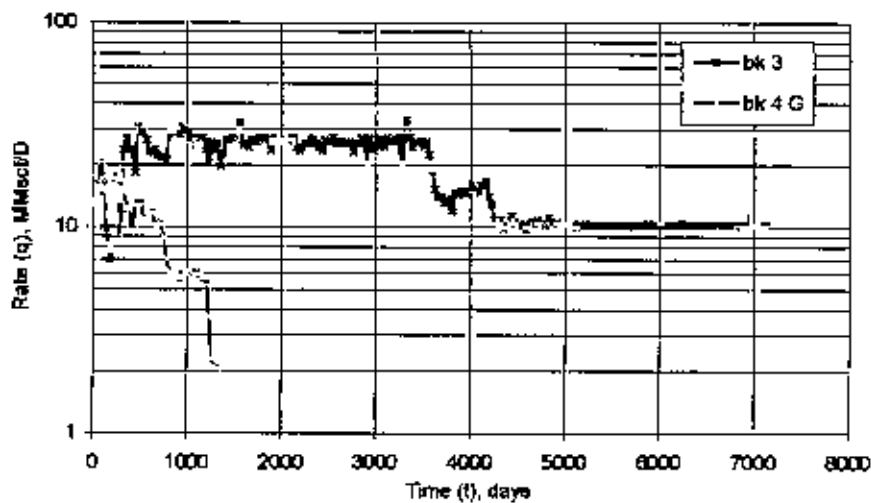


Fig 4.10 Semilog plot of Rate vs. Time of all wells in G Sand

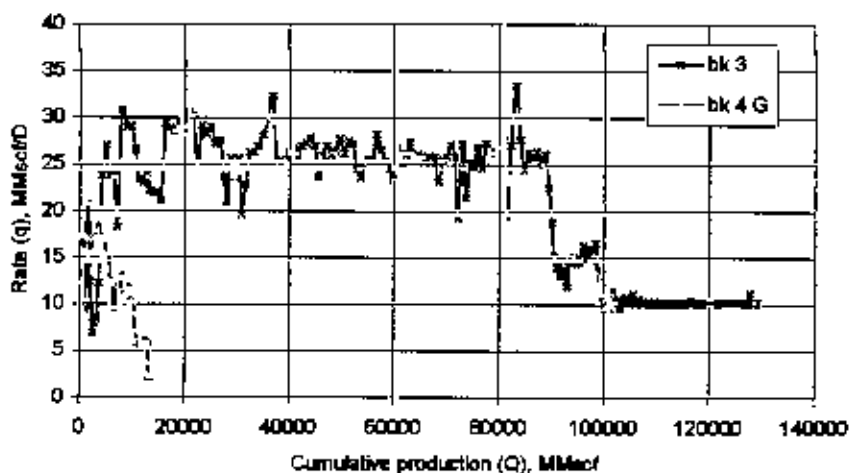


Fig 4.11 Cartesian plot of Rate vs. cumulative production of all wells in G Sand

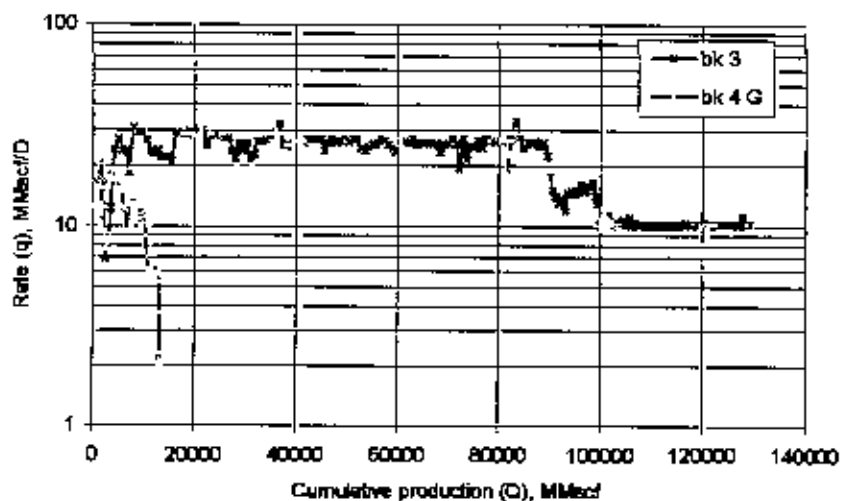


Fig 4.12 Semilog plot of Rate vs. cumulative production of all wells in G Sand

From Cartesian plot of Rate vs. cumulative production of individual wells in appendix B, raw recoverable reserve for BK3 is 135 bcf and for BK4 is 15 bcf and cumulative gas production (G_p) for these wells up to August 2006, are accordingly 129.4 and 13.454 bcf. Fig 4.11 and fig 4.12 also indicate the identical exponential type decline for all wells in G Sand.

4.3 DL Sand

There are two wells in DL Sand: BK2 and BK5 (recompleted in G Sand). Both wells are suspended due to excessive water production and pressure decline. Cartesian plot of Rate vs. Time of all wells in DL Sand is given in the following figure.

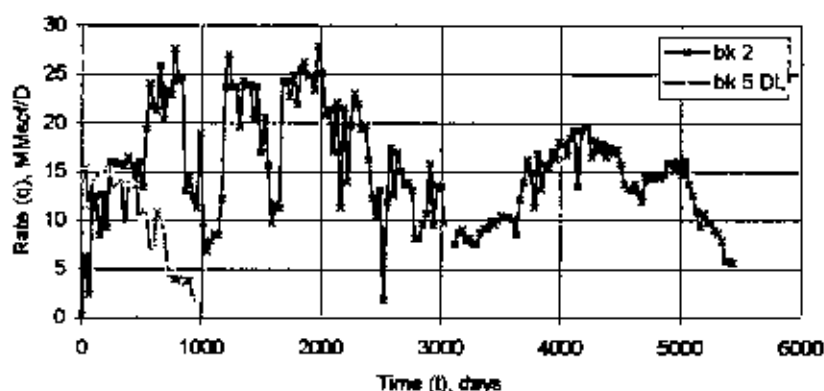


Fig 4.13 Cartesian plot of Rate vs. Time of all wells in DL Sand

From this Cartesian plot it is observed that two wells in DL Sand show similar type of constant percentage decline behavior. BK2 exhibits long prorated production before declining production, whereas BK5 started declining from the beginning of production in DL Sand (Fig 4.14). This sharp exponential decline is an indication of wells undergoing liquid loading.

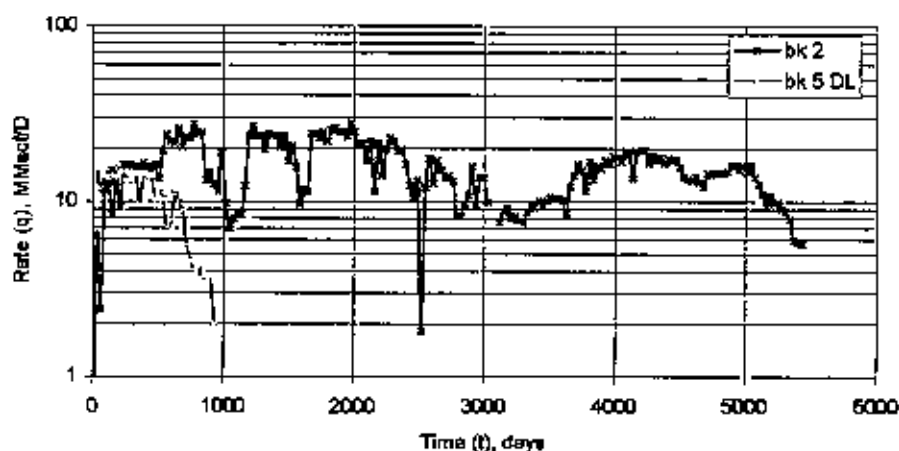


Fig 4.14 Semilog plot of Rate vs. Time of all wells in DL Sand

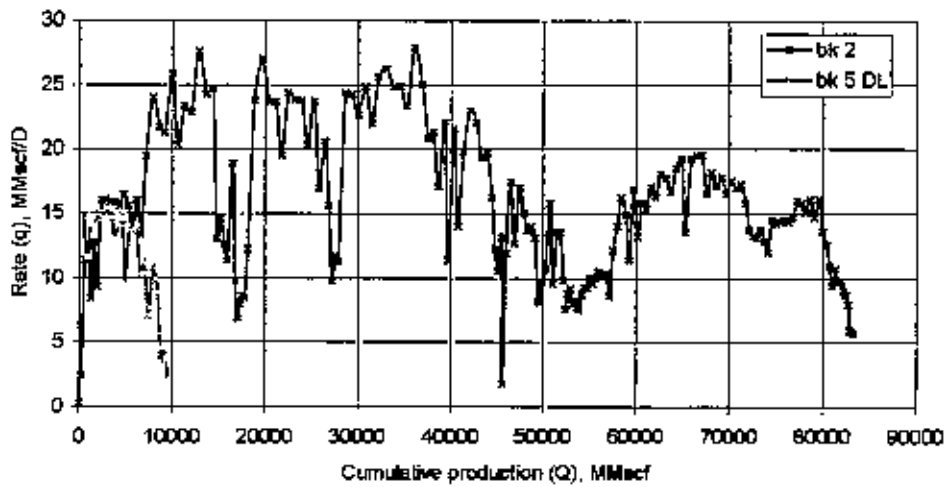


Fig 4.15 Cartesian plot of Rate vs. cumulative production of all wells in DL Sand

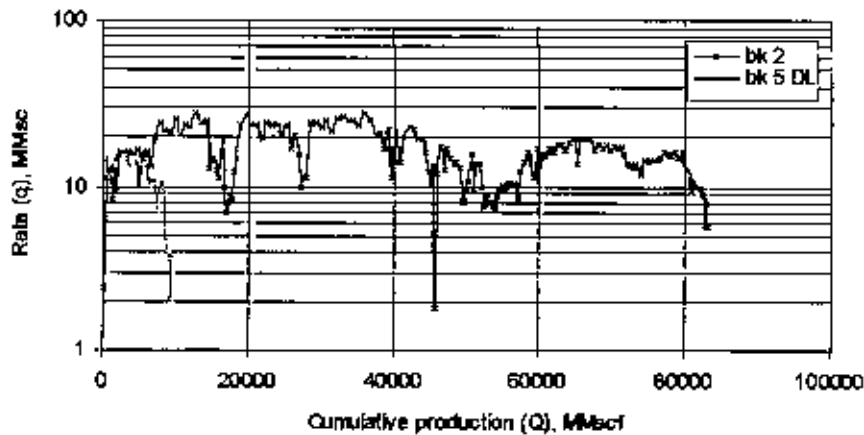


Fig 4.16 Semilog plot of Rate vs. cumulative production of all wells in DL Sand

From Cartesian plot of Rate vs. cumulative production of individual wells in appendix B, raw recoverable reserve for BK2 is 88 bcf and for BK5 is 11 bcf and cumulative gas production (G_p) for these wells up to August 2006, are accordingly 83.29 and 9.446 bcf. Fig 4.15 and Fig 4.16 also indicate the identical exponential type decline for all wells in DL Sand.

4.4 DU Sand

There is only one well in DU Sand BK4, which is suspended due to excessive water production and pressure decline. BK4's decline diagnosis plots are given below:

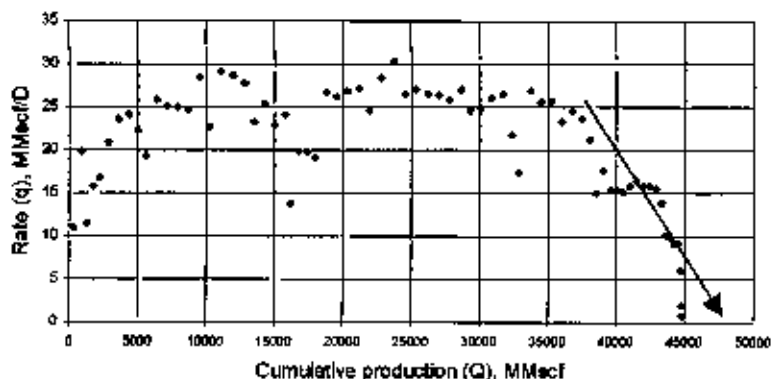


Fig 4.17 Cartesian plot of Rate vs. cumulative production of BK4 in DU Sand

From Cartesian plot of Rate vs. cumulative production of this well in DU Sand (Fig 4.17), raw recoverable reserve is 47 bcf and cumulative gas production (G_p) for this well up to August 2006 is 44.78 bcf. The decline diagnostic curves for this well indicate exponential type decline.

4.5 B Sand

There is only one well in B Sand BK5, which is suspended due to excessive water and sand production. BK5's decline diagnosis plots are given below:

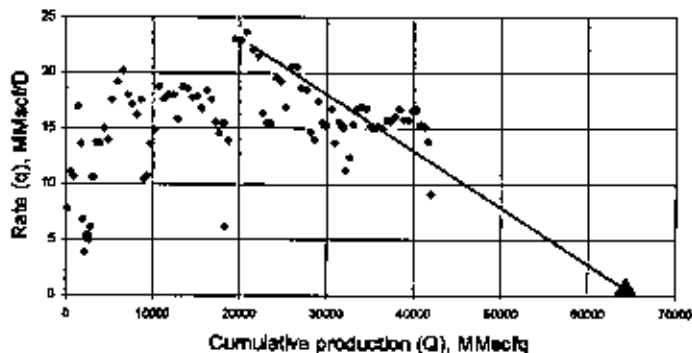


Fig 4.18 Cartesian plot of Rate vs. cumulative production of BK5 in B Sand

From Cartesian plot of Rate vs. cumulative production of this well in B Sand, raw recoverable reserve is 65 bcf and cumulative gas production (G_p) for this well up to August 2006 is 41.96 bcf. The decline diagnostic curves for this well indicate exponential type decline.

In this chapter, from decline diagnosis, the type of decline for all the wells are sought out and from cartesian plot of rate vs. cumulative gas production, raw recoverable reserves and OGIP of all the wells are determined. They are summarized in the following table.

Table 4.1 Summary of results of Decline diagnosis for all wells of Bakhrabad gas field:

Sand	Well	Raw Rccov. Reserve bcf	G_p (Aug'06) bcf	Decline type
J	BK1	139	121.84	Exponential
	BK6	70	52.08	Exponential
	BK7	95	90.2	Exponential
	BK8	100	83.63	Exponential
G	BK3	135	129.4	Exponential
	BK4	15	13.45	Exponential
DL	BK2	88	83.29	Exponential
	BK5	11	9.45	Exponential
DU	BK4	47	44.78	Exponential
B	BK5	65	41.96	Exponential

Chapter 5

AWMB DIAGNOSIS

According to Mattar and McNeil (1997), if compressibility factor z is ignored, a material balance calculation can give a very reasonable approximation of the OGIP. As wellhead pressure measurements are representative of bottomhole conditions (no fluid influx into the wellbore), a procedure similar to flowing material balance (FMB), but ignoring z , can be used to generate a reasonable wellhead material balance calculation, which is approximate wellhead material balance (AWMB).

According to Lee and Wattenbarger (1996), if sufficient pressure and production data are available to define the line of p/z vs. G_p plot fully, the dominant drive mechanism can also be determined from the shape of the plot. Although consistent deviations from a straight line suggest other sources of reservoir energy, errors in pressure and production measurements also can cause departures from a straight line. Thus a similar plot of p/z vs. G_p , the AWMB plot can be used to determine the dominant drive mechanism of this gas reserve. Fig 5.1 shows typical shapes of p/z plots for selected gas reservoir drive mechanisms.

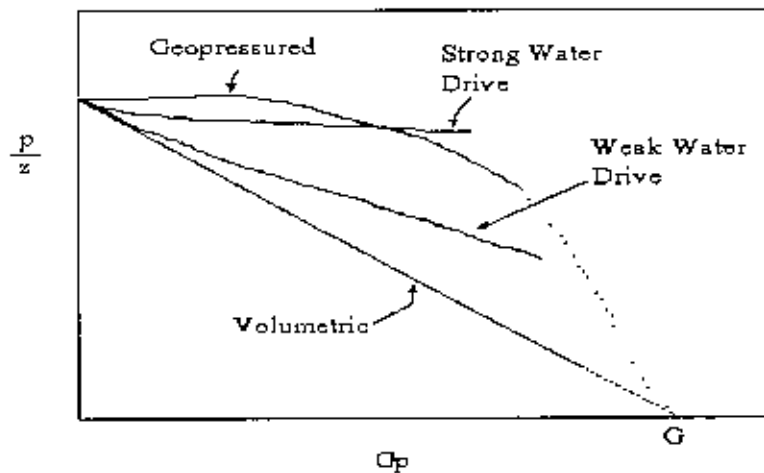


Fig 5.1 Shapes of p/z plots for various drive mechanisms

5.0 Sand-wise Approximate Wellhead Material Balance (AWMB) Analysis

This section discusses material balance method for estimating original gas in place (OGIP) and predicting the drive mechanism of sands from the analysis of long-term gas-production data (mainly pressure and cumulative production data) from individual wells of different sands.

5.1 J Sand

There are four wells in J Sand: BK1, BK6, BK7 and BK8. A simplified material balance analysis has been conducted at each of these wells using AWMB method.

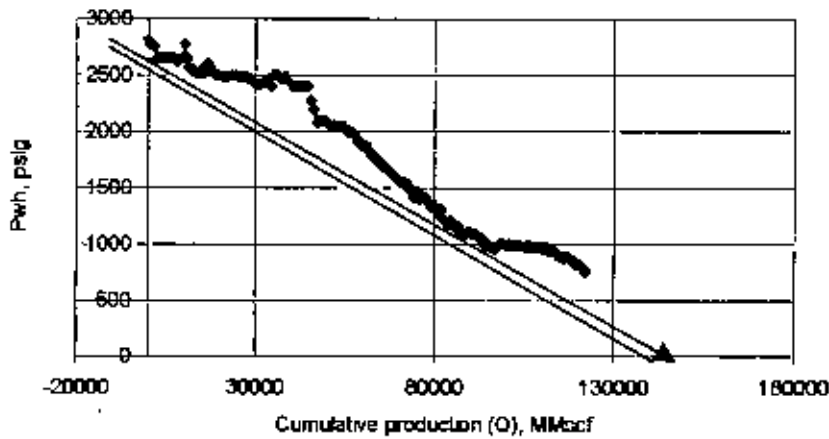


Fig 5.2 AWMB plot of BK1 of J Sand

From the above figure of flowing wellhead pressure vs. cumulative production of BK1, it is seen, the up trend of initial pressure points, a straight declining middle portion and final deviated portion from straight pressure points. Cause of the initial up trend of flowing pressure points is the absence of other three wells in the J Sand during the years 1984 to 1989. Thus pressure declined at a much slower rate initially. When other wells (BK6, BK7 & BK8) came into production in late 1989, the pressure started to decline at a much faster rate. The deviated portion at the end is probably due to the liquid loading problem in J Sand. Initial Gas In Place (OGIP) value estimated from this plot is 148 bcf.

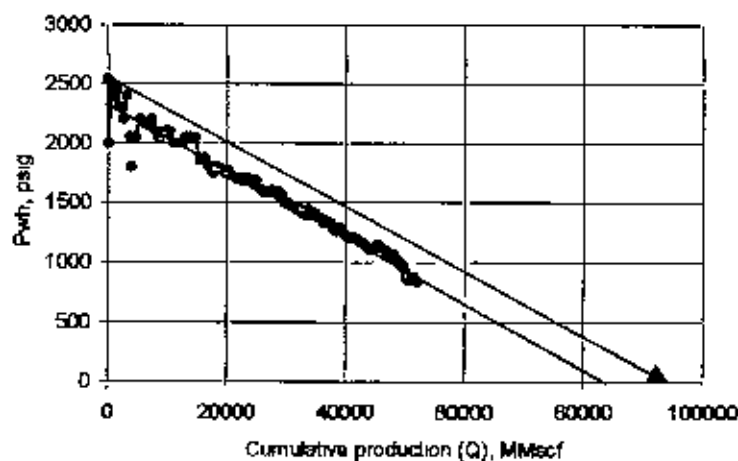


Fig 5.3 AWMB plot of BK6 of J Sand

Figure 5.3 represents plot of flowing wellhead pressure vs. cumulative production of BK6. It is almost a straight declining curve of flowing pressure with cumulative gas production data, except a little deviated portion at the tail end probably due to liquid loading problem. OGIP value estimated from this plot for BK6 is 92 bcf.

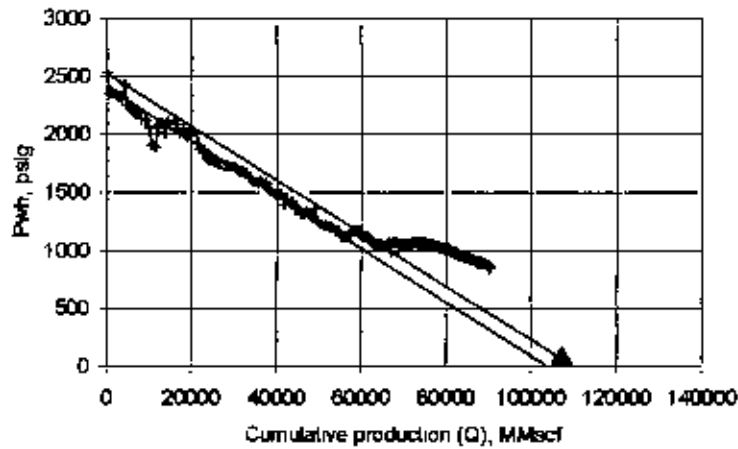


Fig 5.4 AWMB plot of BK7 of J Sand

From Figure 5.4 it is seen that the shape of the curve is straight line but at the end deviated upward from straight portion. The deviated portion at the end is probably due to the liquid loading problem in BK7. OGIP value estimated from this plot is 110 bcf.

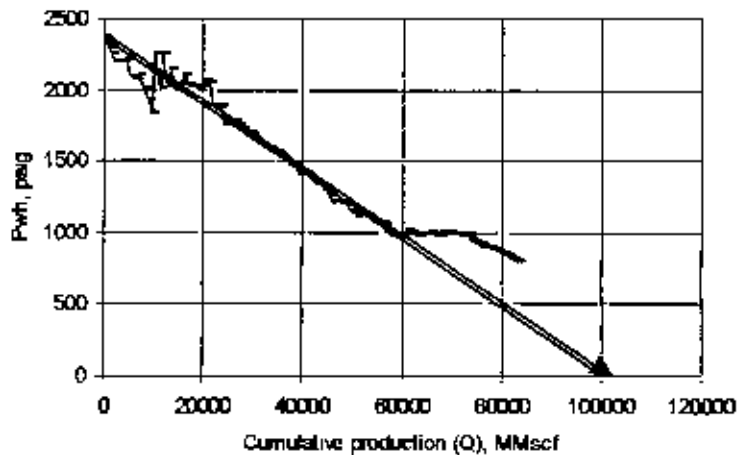


Fig 5.5 AWMB plot of BK8 of J Sand

From Figure 5.5 it is seen that the shape of the curve is straight line but at the end deviated upward from straight portion. The deviated portion at the end is probably due to the liquid loading problem in BK8. OGIP value estimated from this plot is 102 bcf. In the following table summary of results of AWMB method for the wells of J sand is presented:

Table 5.1 Summary of results of AWMB method for all wells of J Sand:

Wells in J Sand	Raw Recov. Reserve bcf	G_p (Aug'06) bcf	OGIP bcf	Remaining Reserve bcf	Recovery Factor %
BK 1	139	121.84	148	17.16	82.324
BK 6	70	52.075	92	17.925	56.603
BK 7	95	90.2	110	4.8	82
BK 8	100	83.63	102	16.37	81.990
Total	404	347.745	452	56.255	76.934

5.2 G Sand

There are two wells in G Sand: BK3 and BK4. A simplified material balance analysis has been conducted at each of these wells using AWMB method.

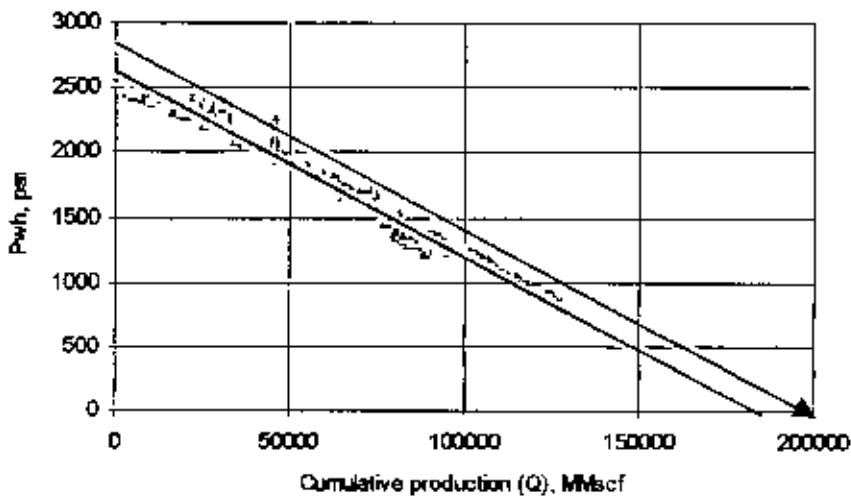


Fig 5.6 AWMB plot of BK3 of G Sand

Figure 5.6 represents plot of flowing wellhead pressure vs. cumulative production of BK3. It is almost a straight declining curve of flowing pressure with cumulative gas production data. OGIP value estimated from this plot for BK3 is 200 bcf.

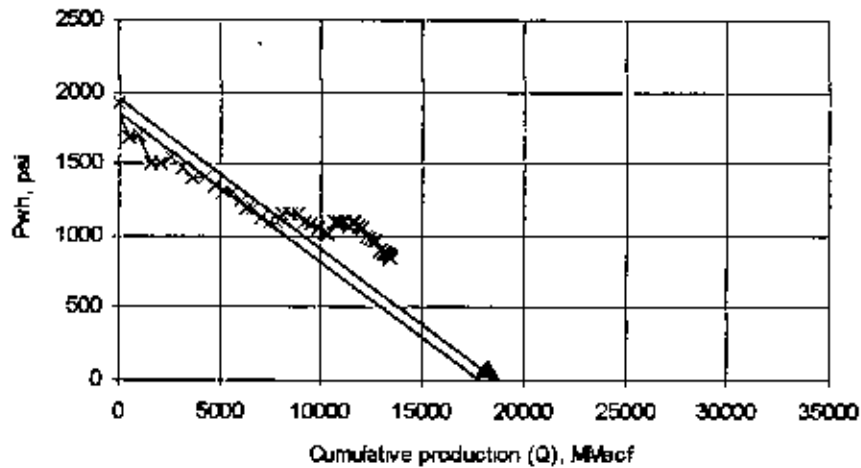


Fig 5.7 AWMB plot of BK4 of G Sand

Figure 5.7 represents plot of flowing wellhead pressure vs. cumulative production of BK4. It is almost a straight declining curve of flowing pressure with cumulative gas production data, except a little deviated portion at the tail end probably due to liquid loading problem. OGIP value estimated from this plot for BK6 is 18 bcf. In the following table summary of results of AWMB method for the wells of G sand is presented:

Table 5.2 Summary of results of AWMB method for all wells of G Sand:

Wells in G Sand	Raw Recov. Reserve bcf	G_p (Aug'06) bcf	OGIP bcf	Remaining Reserve bcf	Recovery Factor %
BK 3	135	129.4	200	5.6	64.7
BK 4	15	13,454	18	1,546	74.744
Total	150	142,854	218	7,146	65.529

5.3 DL Sand

There are two wells in DL Sand: BK2 and BK5. A simplified material balance analysis has been conducted at each of these wells using AWMB method

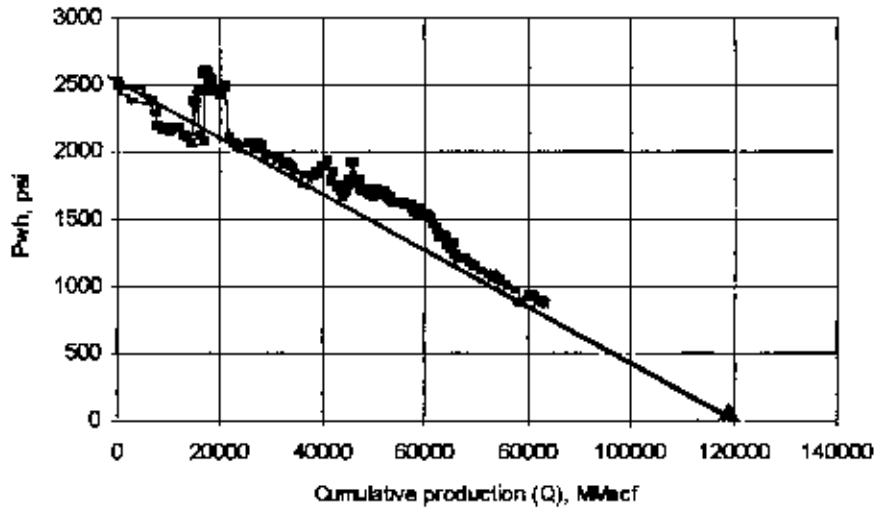


Fig 5.8 AWMB plot of BK2 of DL Sand

Figure 4.40 represents plot of flowing wellhead pressure vs. cumulative production of BK2. It is almost a straight declining curve of flowing pressure with cumulative gas production data, except a little deviated portion at the later portion probably due to liquid loading problem. OGIP value estimated from this plot for BK2 is 121 bcf.

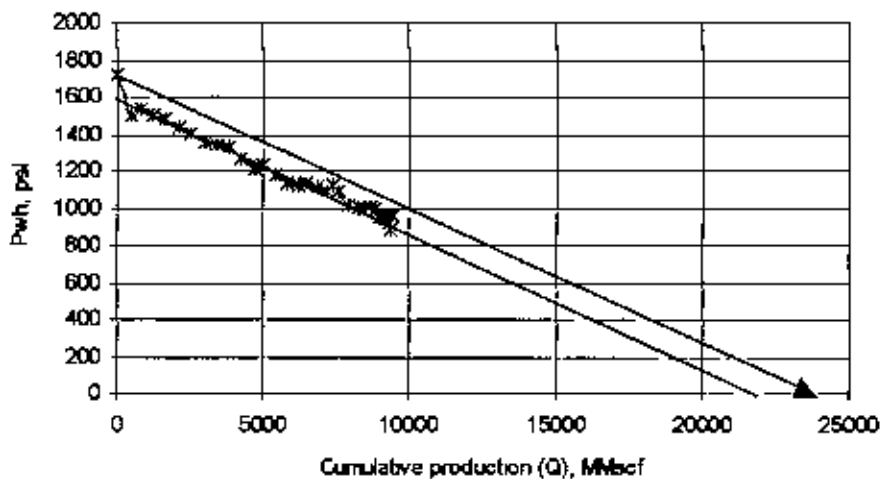


Fig 5.9 AWMB plot of BK5 of DL Sand

Figure 5.9 represents plot of flowing wellhead pressure vs. cumulative production of BK5. It is almost a straight declining curve of flowing pressure with cumulative gas production data. OGIP value estimated from this plot for BK5 is 23.7 bcf. In the following table summary of results of AWMB method for the wells of DL sand is presented:

Table 5.3 Summary of results of AWMB method for all wells of DL Sand:

Wells in DL Sand	Raw Recov. Reserve bcf	G_p (Aug'06) bcf	OGIP bcf	Remaining Reserve bcf	Recovery Factor %
BK 2	88	83.29	121	4.71	68.834
BK 5	11	9.446	23.7	1.554	39.856
Total	99	92.736	144.7	6.264	64.088

5.4 DU Sand

There is one well in DU Sand: BK4. A simplified material balance analysis has been conducted at this well using AWMB method.

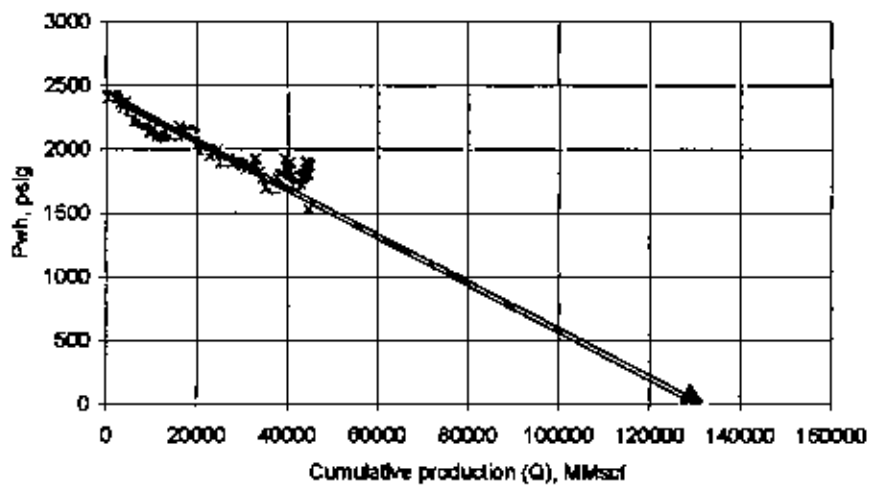


Fig 5.10 AWMB plot of BK4 of DU Sand

Figure 5.10 represents plot of flowing wellhead pressure vs. cumulative production of BK4. It is almost a straight declining curve of flowing pressure with cumulative gas production data, except a little deviated portion at the tail end probably due to liquid loading problem. OGIP value estimated from this plot for BK4 is 130 bcf. In the following table summary of results of AWMB method for the well of DU sand is presented:

Table 5.4 Summary of results of AWMB method for all wells of DU Sand:

Well in DU Sand	Raw Recov. Reserve bcf	G_p (Aug'06) bcf	OGIP bcf	Remaining Reserve bcf	Recovery Factor %
BK 4	47	44.78	130	2.22	34.44

5.5 B Sand

There is one well in B Sand: BK5. A simplified material balance analysis has been conducted at each of these wells using AWMB method.

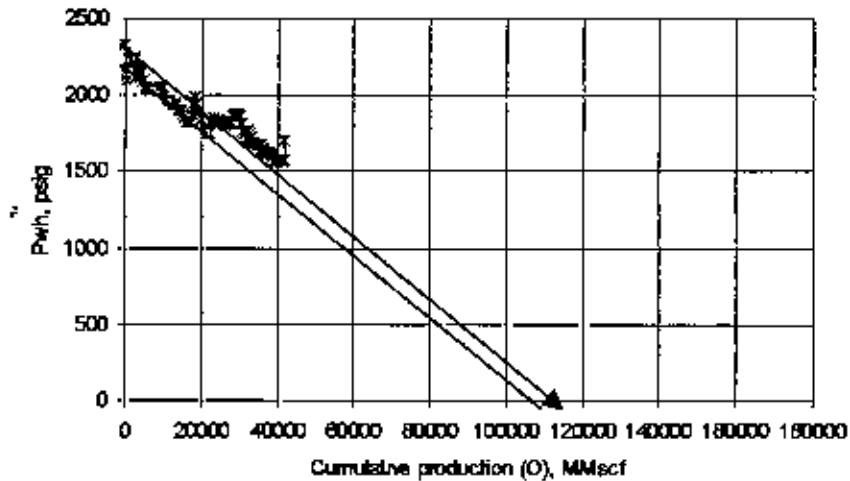


Fig 5.11 AWMB plot of BK5 of B Sand

Figure 5.11 represents plot of flowing wellhead pressure vs cumulative production of BK6. It is almost a straight declining curve of flowing pressure with cumulative gas production data, except a little deviated portion at the tail end probably due to liquid loading problem. OGIP value estimated from this plot for BK5 is 115 bcf. In the following table summary of results of AWMB method for the well of B sand is presented:

Table 5.5 Summary of results of AWMB method for all wells of B Sand:

Well in B Sand	Raw Recov. Reserve bcf	G_p (Aug'06) bcf	OGIP bcf	Remaining Reserve bcf	Recovery Factor %
BK 5	65	41.958	115	23 042	36 485217

Choudhury (1999) presented comparison of the GIP estimates of different studies conducted on Bakhrabad Gas Field using material balance method in his paper. Gas in place estimates of Weidril (1990), IKM (1990), Petrobangla (1993) and Mobil (1997) were close but higher than his study results. Now comparison of GIP estimates of different studies including AWMB method of present study is presented below:

Table 5.6 Comparison of the OGIP (bcf) estimates of Bakhrabad Gas Field from different studies:

Sand	Volumetric			Material Balance						
	Well drill (90)	IKM (90)	Mobil (97)	Well drill (90)	IKM (90)	Petro bangla (93)	Mobil (97)	Chou dhury FBHP (99)	Chou dhury FWHP (99)	AWMB
J	610	554	550	585	597	665	666	460.5	469.5	452
G	300	262	247	370	318	245.5	244	216	221	218
DL	150	151	132	200	148	176	175	144.5	147.5	144.7
DU	187	222	254	167	180	180	187	150	150	130
B	145	143	98	231	145	166.6	167	151	154	115
Total	1392	1332	1281	1553	1388	1433.1	1439	1122	1142	1059.7

From this table it is evident that gas in place values estimated with AWMB method of different sands are very similar to those estimated with flowing bottomhole pressure (FBHP). Flowing wellhead pressure (FWHP) methods of Choudhury and other material balance are also close to volumetric estimation of different studies. Present estimates of gas in place of different sands using AWMB method are the lowest of all other previous studies. AWMB method also reveals volumetric drive mechanism of all wells in different sands and liquid loading problems in some wells. An acceptable method for quantifying OGIP is to provide a minimum and maximum value. The minimum value is easily obtained by using material balance especially FMB methods. A maximum value is found using volumetric determination from geological (or seismic) mapping. Without using diagnostic plots, there is no way of qualifying the level of confidence in production data analysis.

Chapter 6

TYPECURVE ANALYSIS

Only flowing wellhead pressures are available for the wells of Bakhrabad Gas Field for analysis, as down hole electronic pressure measurement systems are not present there. For different analysis procedures, flowing bottom hole pressure is required. In this study flowing bottom hole pressure, p_{wf} is calculated from the monthly representative flowing wellhead pressure, p_{wh} using the software F.A.S.T. RTA. For Dry Gas Wells, F.A.S.T. RTA defaults to a multi-step Cullender Smith procedure as a wellbore correlation option and it is used to calculate p_{wf} . For gas wells with some liquids in flow stream, Beggs & Brill or Gray correlation is used. In this case, Beggs & Brill is the default correlation. In Bakhrabad, produced gas and liquid from all the wells are separated centrally and through a common header, the separated liquid flows further downstream for separation of water and condensate. As a result, it is not possible to determine liquid production from individual wells. Thus liquid production rates with gas production for respective wells cannot be used in the software.

Most of the input parameters used in computer based production data analysis are taken from data supplied from Petrobangla and previous studies conducted by IKM (1990) and Choudhury (1999). The necessary data for these analyses have been derived from geological and geophysical study, core-analysis, well-log analysis and well-test results provided the production data of different wells and sands of Bakhrabad Gas Field. Input parameters for these analyses are given in Appendix C.

6.0 Computer based production data analysis

In this section a systematic approach to production data analysis by typecurve matching is presented with a commercial PA (Production Analysis) tool F.A.S.T. RTA (by Fekete Associates Inc.). It maximizes the benefits of each of the following methods:

- Arps decline analysis
- Fetkovich typecurve analysis
- Blasingame typecurve analysis

- Agarwal-Gardner typecurve analysis
- Normalized Pressure Integral (NPI) typecurves
- Flowing Material Balance (FMB)
- Transient typecurve analysis

These methods are suited for production data of varying quality and completeness. They are utilized to determine both the fluids-in-place and the expected ultimate recoverable reserves (based on current and/or expected future operating conditions) and to verify previous estimations conducted with simple methods. More importantly, they serve to assess the confidence level of the reserves estimate by qualifying the production data as either infinite acting or boundary dominated, as well as volumetric or non-volumetric (aquifer supported, multi-layer, etc) previously determined from production data diagnosis.

Among the above-mentioned methods Fetkovich, Blasingame, Agarwal-Gardner, NPI and Transient are typecurve methods and they will be discussed in this chapter. Arps and FMB are nontypecurve methods and they will be discussed in the next chapter. Each of the typecurve methods yield estimates of EUR (Fetkovich) and/or fluid-in-place (Blasingame, Agarwal-Gardner, NPI and Transient). EUR represents the total amount of gas that can be produced under specified operating conditions (p_{wf} , depth). It is always equal to or less than the OGIP. The primary purpose of typecurve analysis is to determine the dominant flow regime from the production data: infinite acting (radial flow, fracture linear flow, horizontal well flow), transitional (influenced by boundaries and/or heterogeneities) or boundary dominated (depletion or displacement). If the diagnostics indicate that boundary dominated flow has not been reached, there is no way to predict ultimate reserves or fluids-in-place with any confidence.

6.1 Fetkovich Typecurve Analysis

This typecurve is simple to apply and does not require flowing pressure data and does not inherently assume a dominant flow regime (plot does not use superposition time). Empirical nature in depletion analysis (uses Arps theory) makes it versatile. But transient analysis assumes constant flowing pressure. Thus it is useful for production data where flowing

pressures are constant or can be assumed constant. It is also useful for non-volumetric reservoirs with two or more mobile phases.

In this analysis procedure a data curve of flow rate (q) versus time (t) is plotted logarithmically and then matched on q_{Dd} vs. t_{Dd} typecurves. Then transient (t_{eD}) stem is sought out based on closest curve. Similarly depletion (b) stem is selected based on closest cure or the following guidelines:

- $b \approx 0$, Single phase liquid production, high pressure gas (constant flowing pressure)
- $0.1 < b < 0.4$, Solution gas drive oil reservoirs
- $0.4 < b < 0.5$, Most gas wells (excluding tight gas)
- $b = 0.5$, Oil wells under effective edge water drive
- $0.5 < b < 0.9$, Layered, composite, connected reservoirs
- Fetkovich states that b value should never exceed a value of 1 for boundary dominated production.

In detail, type curve analysis is done by selecting a match point, and reading its co-ordinates off the data plot (q and t)_{match}, and off the type curve plot (q_{Dd} and t_{Dd})_{match}. At the same time the stem values (" r_e/r_{wd} " and " b ") of the matching curve are noted. From the right-hand-set of type curves, the Decline Curve Parameters can be obtained:

$$q_i = \frac{q(\text{match})}{q_{Dd}(\text{match})} \quad \dots \quad \dots \quad (6.1)$$

$$D_i = \frac{t_{Dd}(\text{match})}{t(\text{match})} \quad \dots \quad \dots \quad (6.2)$$

b = value of type curve stem (right-hand-set of type curves) (it is noted that for Exponential Decline $D_i = D$ and $b = 0$)

With these, we can now calculate the EUR (Expected Ultimate Recovery). The 'f' subscript denotes conditions at the beginning of the forecast period. Now, we can estimate fluid-in-place and drainage area.

$$EUR = Q_f + \frac{q_f - q_{oh}}{D_f} \quad \dots \quad \dots \quad (6.3)$$

$$q_f = q_i e^{-D_i t_f} \quad \dots \quad \dots \quad (6.4)$$

$$G_i = \frac{EUR \times P_i Z_{wf}}{P_i Z_{wf} - P_{wf} Z_i} \quad (\text{bcf}) \quad \dots \quad \dots \quad (6.5)$$

$$A = \frac{Z_i T P_{sc} G_i}{\phi h s_g P_i T_{sc}} \quad (\text{acres}) \quad \dots \quad \dots \quad (6.6)$$

From left-hand-set of type curves, the 'Reservoir Parameters' can be obtained, if p_i , p_{wf} , μ , h , c_g , ϕ , and r_w are known.

$$\left(\frac{r_e}{r_{wa}} \right)_{match} = \text{value of type curve stem (left-hand-set of type curves)}$$

k is obtained from rearranging the definition of

$$q_{Dd} = q \left(\frac{1.417E6 * T}{kh(p_{pi} - p_{pwf})} \right) \left(\ln \left(\frac{r_e}{r_{wa}} \right)_{match} - \frac{3}{4} \right) \quad \dots \quad \dots \quad (6.7)$$

$$k = \left(\frac{q}{q_{Dd}} \right)_{match} \left(\frac{1.417E6 * T}{h(p_{pi} - p_{pwf})} \right) \left(\ln \left(\frac{r_e}{r_{wa}} \right)_{match} - \frac{3}{4} \right) \quad \dots \quad \dots \quad (6.8)$$

Solving for r_{wa} from the definition of t_{Dd} :

$$t_{Dd} = \frac{0.006328kt}{\frac{1}{2} \phi \mu c_i r_{wa}^2 \left(\left(\frac{r_e}{r_{wa}} \right)_{match}^2 - 1 \right) \left(\ln \left(\frac{r_e}{r_{wa}} \right)_{match} - \frac{3}{4} \right)} \quad \dots \quad \dots \quad (6.9)$$

$$r_{wa} = \sqrt{\left(\frac{t}{t_{Dd}} \right)_{match} \frac{0.006328k}{\phi \mu c_i \frac{1}{2} \left(\left(\frac{r_e}{r_{wa}} \right)_{match}^2 - 1 \right) \left(\ln \left(\frac{r_e}{r_{wa}} \right)_{match} - \frac{3}{4} \right)}} \quad \dots \quad \dots \quad (6.10)$$

$$s = \ln \left(\frac{r_w}{r_{wa}} \right) \quad \dots \quad \dots \quad (6.11)$$

In Fetkovich typecurve analysis, depletion analysis tends to be non-unique (hyperbolic decline curves are very similar in shape) and only EUR, based on historical operating conditions, can be calculated.

Sand-wise Fetkovich typecurve analysis

Number of production wells in Bakhrabad Gas Field is eight and they are producing from B, DU, DL, G and J sands. In this section the results of Fetkovich typecurve analysis of different wells of these sands have been presented.

6.1.1 J Sand

There are 4 wells in J sand: BK1, BK6, BK7 and BK8. In Fetkovich typecurves there are two sets of curves that converge in the center. Matching data on the left side provides information about the transient behavior of the system (k, s) while the right side is meant for boundary dominated data. Fetkovich typecurve analysis of individual wells of J Sand is given below:

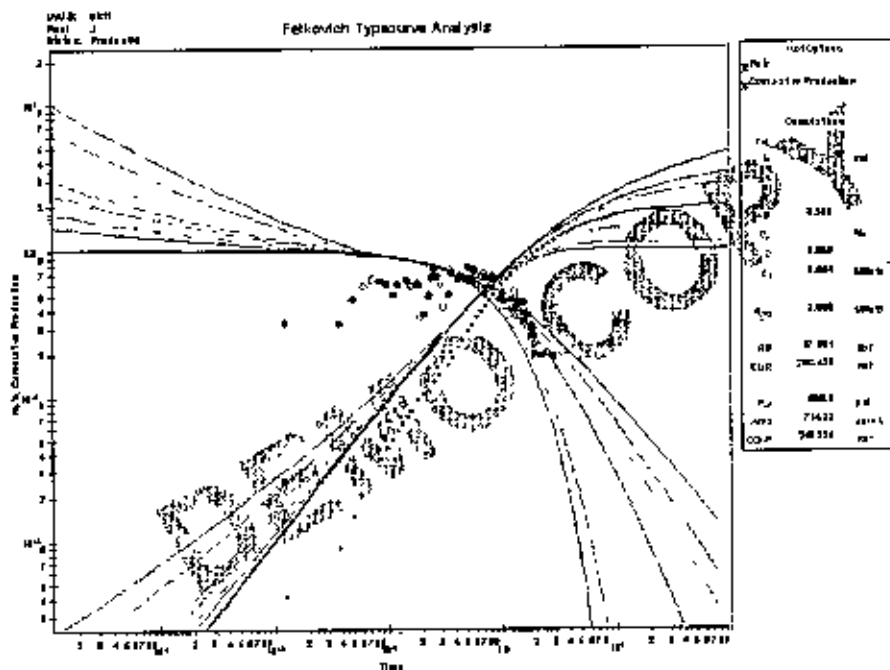


Fig 6.1 Fetkovich Typecurve Analysis of BK1 at J Sand

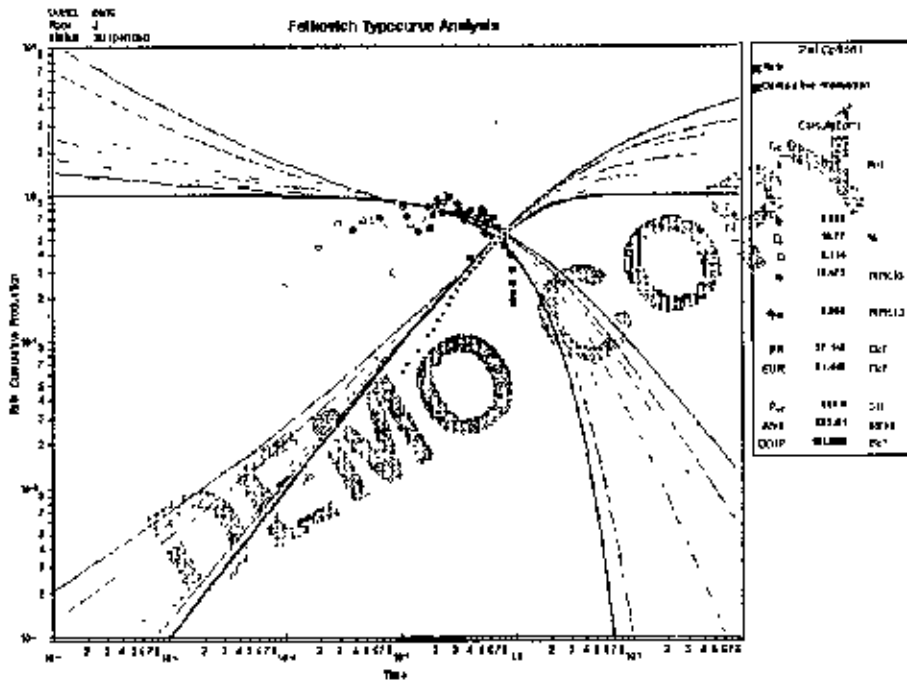


Fig 6.2 Fetkovich Typecurve Analysis of BK6 at J Sand

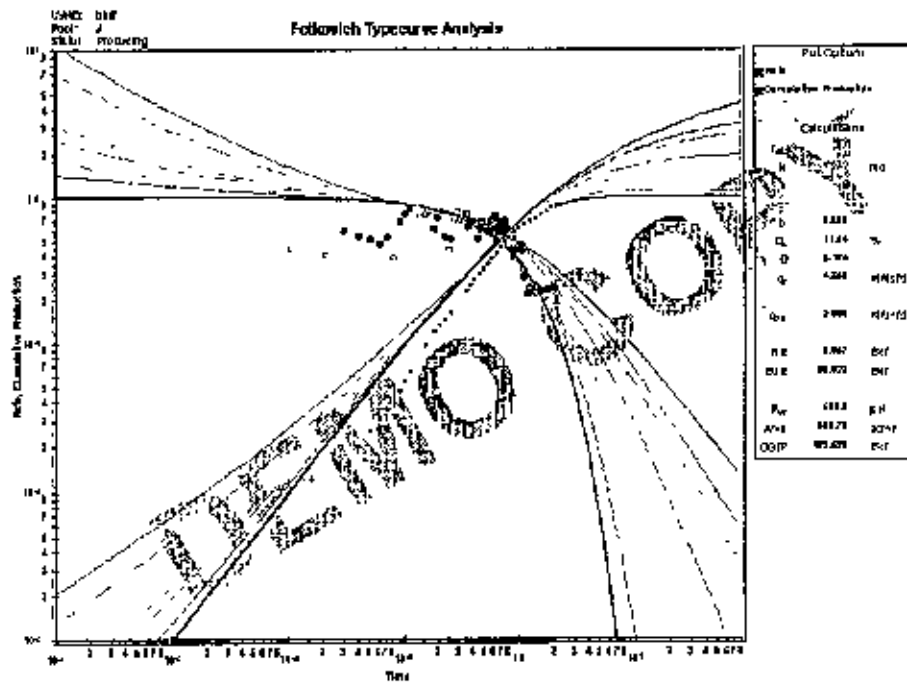


Fig 6.3 Fetkovich Typecurve Analysis of BK7 at J Sand

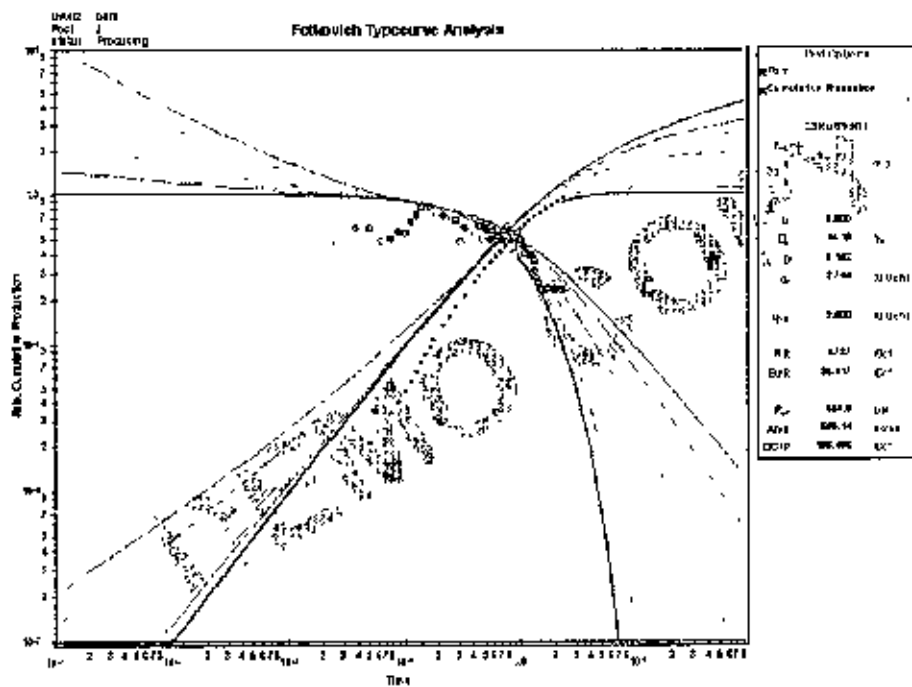


Fig 6.4 Fetkovich Typecurve Analysis of BK8 at J Sand

In these cases, the data do not fit on the Fetkovich curve properly; especially transient data of any well do not fit any type curve, and so cannot be analyzed correctly. The reason for not matching this data set comes from one of the assumptions of the Fetkovich analysis: production occurs under constant bottom hole flowing pressure conditions. Fortunately, most of the other analysis techniques are not limited by constant rate or pressure conditions. The type curve data being very noisy and difficult to interpret, type curve “Data Filter” is used here for better matching. Portion of data fit on the right hand stem type curves probably due to some constant pressure production at the end of production profile of wells BK1, BK7 and BK8. In the following table summary of results of Fetkovich analysis for the wells of J sand is presented:

Table 6.1 Summary of results of Fetkovich analysis for wells of J Sand:

Wells in J Sand	OGIP bcf	Area acre	EUR bcf	D_i	d_i %	b
BK 1	240.385	714.22	200.075	0.058531		0.5
BK 6	101.8	892.61	81.44	0.113937	10.77	0
BK 7	122.529	383.7	97.158	0.123743	11.64	0
BK 8	108.498	360.14	85.417	0.151931	14.1	0

6.1.2 G Sand

There are 2 wells in G sand: BK3 and BK4. Fetkovich typecurve analysis of individual wells of G Sand is given below:

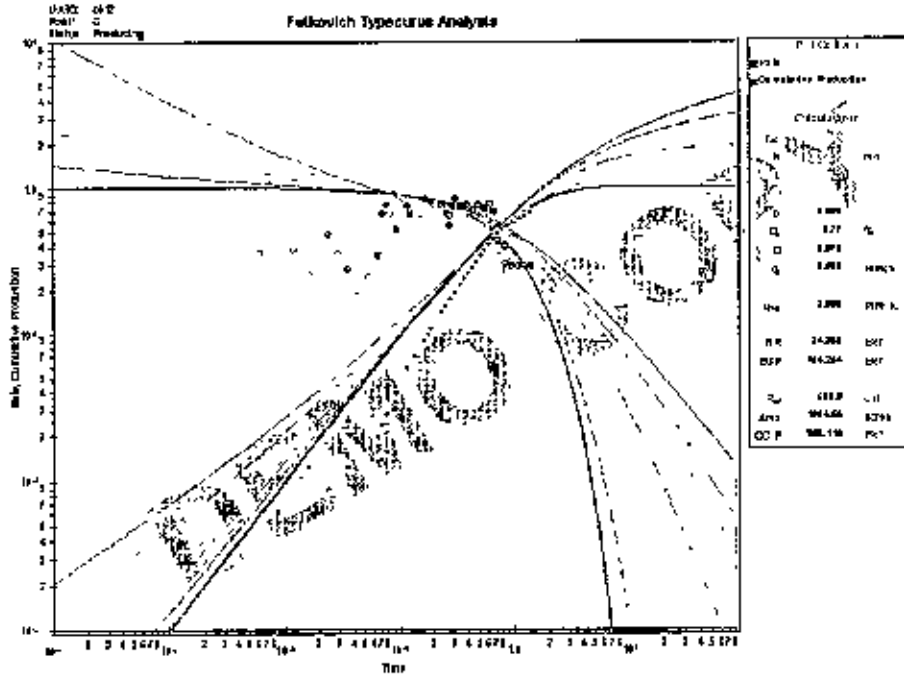


Fig 6.5 Fetkovich Typecurve Analysis of BK3 at G Sand

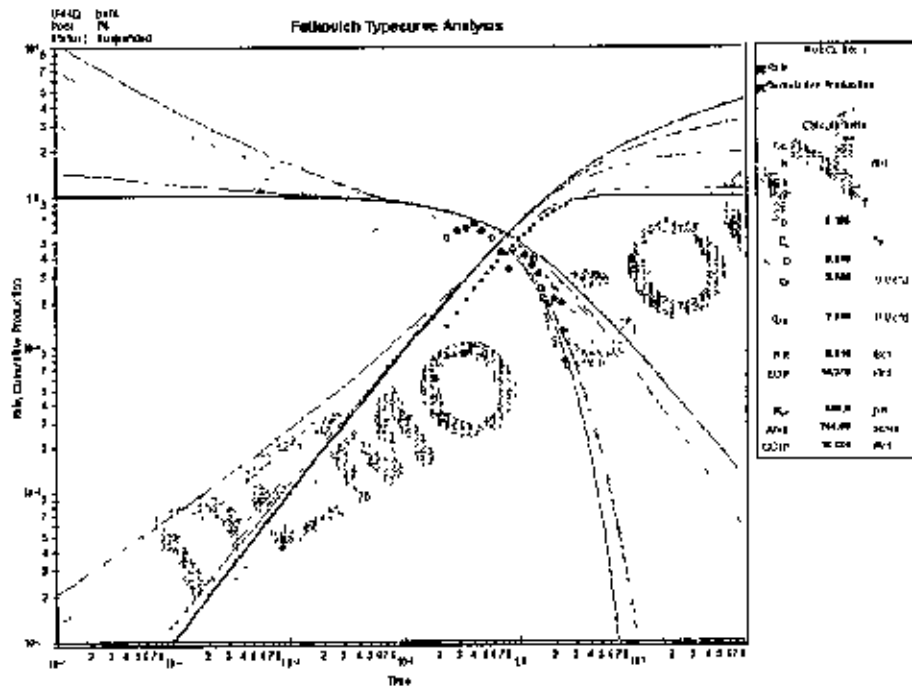


Fig 6.6 Fetkovich Typecurve Analysis of BK4 at G Sand

The transient data of any well do not fit on the Fetkovich curve properly and so cannot be analyzed. The type curve data being very noisy and difficult to interpret, type curve "Data Filter" is also used here for better matching. Portion of data fit on the right hand stem type curves probably due to some constant pressure production at the end of production profile of wells BK3. In the following table summary of results of Fetkovich analysis for the wells of G sand is presented:

Table 6.2 Summary of results of Fetkovich analysis for wells of G Sand:

Wells in G Sand	OGIP bcf	Area acre	FUR bcf	D_i	d_i %	b
BK 3	203.116	1664.55	164.254	0.070099	6.77	0
BK 4G	18.884	256.6	14.27	0.545288		0.1

6.1.3 DL Sand

There are 2 wells in DL sand: BK2 and BK5. Fetkovich typecurve analysis of individual wells of DL Sand is given below:

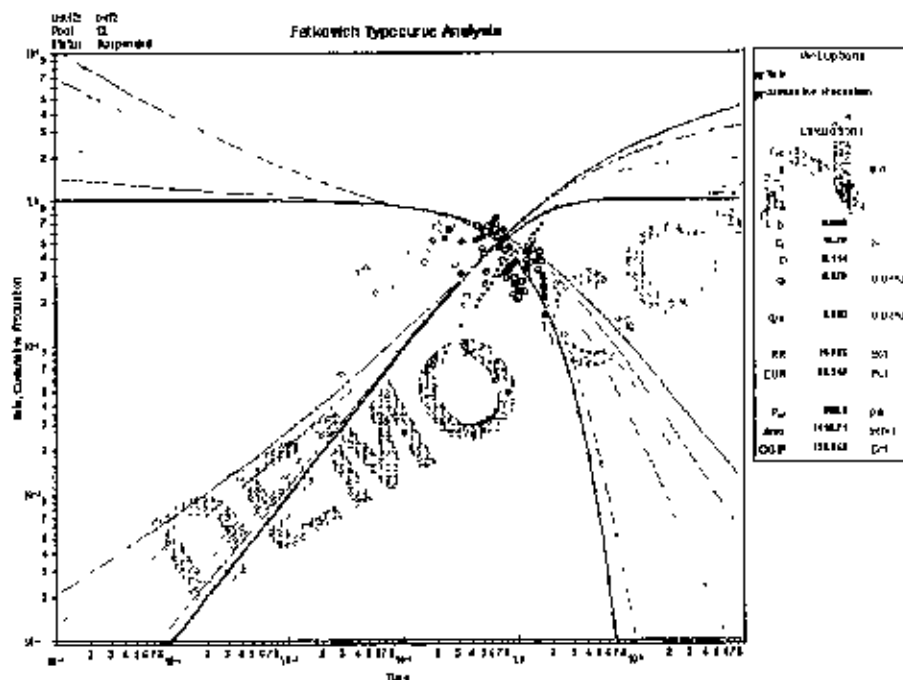


Fig 6.7 Fetkovich Typecurve Analysis of BK2 at DL Sand

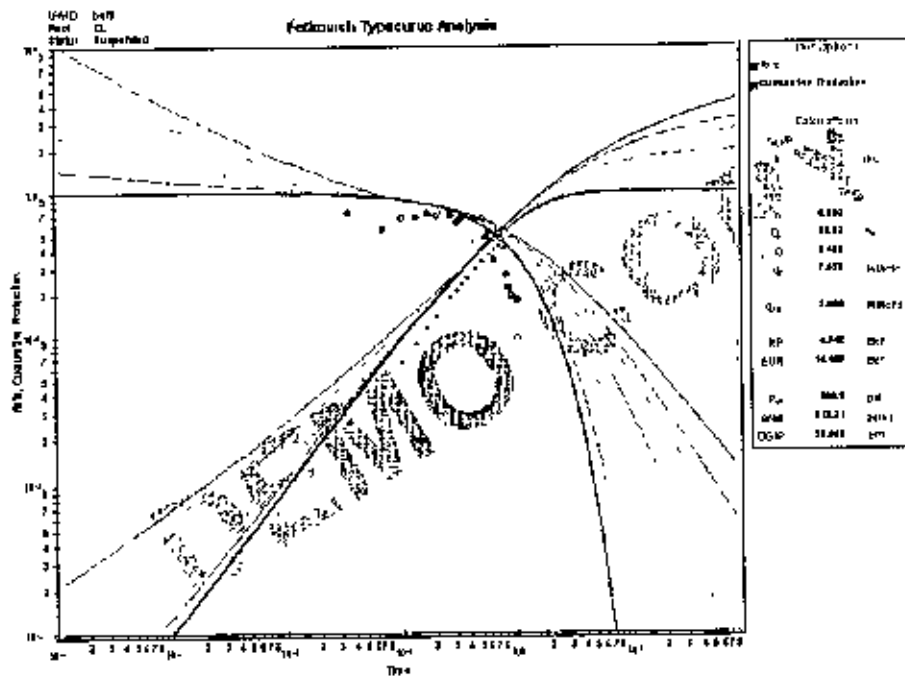


Fig 6.8 Fetkovich Typecurve Analysis of BK5 at DL Sand

The transient data of any well do not fit on the Fetkovich curve properly and so cannot be analyze. The type curve data being very noisy and difficult to interpret, type curve “Data Filter” is also used here for better matching. But boundary dominated data also do not fit on the right hand stem type curves for any well. In the following table summary of results of Fetkovich analysis for the wells of DL sand is presented:

Table 6.3 Summary of results of Fetkovich analysis for wells of DL Sand:

Wells in DL Sand	OGIP bcf	Area acre	EUR bcf	D_i	d_i %	b
BK 2	123.953	1410.71	98.249	0.114137	10.79	0
BK 5	20.666	312.21	14.469	0.408241	33.52	0

6.1.4 DU Sand

There is only one well in DU sand; BK4. Fetkovich typecurve analysis of this well of DU Sand is given bellow:

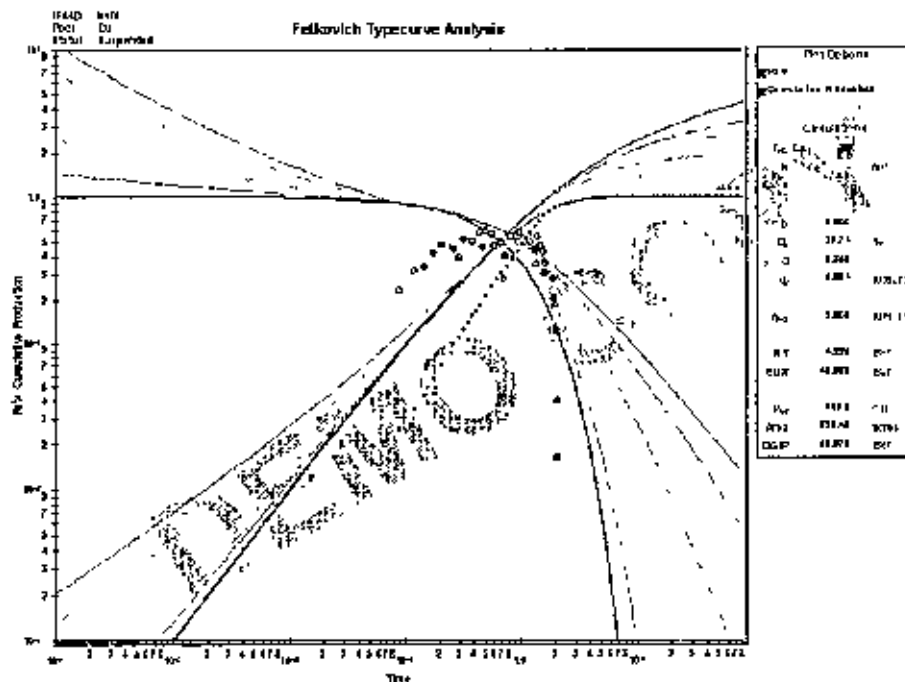


Fig 6.9 Fetkovich Typecurve Analysis of BK4 at DU Sand

The transient data of this well do not fit on the Fetkovich curves properly and so cannot be analyzed properly. The type curve data being very noisy and difficult to interpret, type curve “Data Filter” is also used here for better matching. Only boundary dominated data hardly fit on the right hand stem type curves for this well. In the following table summary of results of Fetkovich analysis for the well BK4 of DU sand is presented:

Table 6.4 Summary of results of Fetkovich analysis for well BK4 of DU Sand:

Wells in DU Sand	OGIP bcf	Area acre	EUR bcf	D _i	d _i %	b
BK 4	60.97	828.43	48.985	0.352571	29.71	0

6.1.5 B Sand

There is only one well in B Sand: BK5. Fetkovich typecurve analysis of this well of B Sand is given bellow:

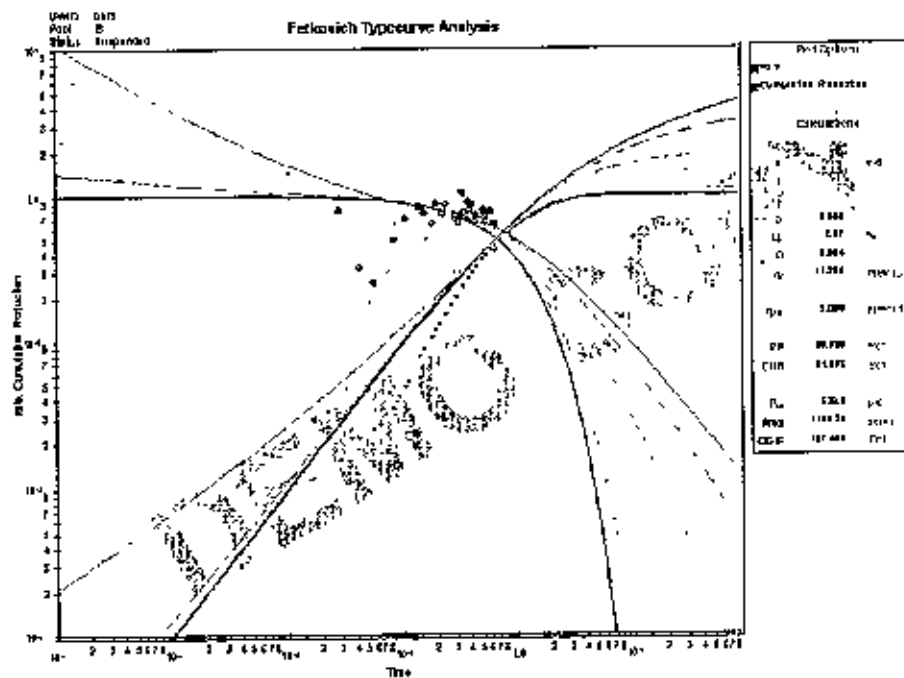


Fig 6.10 Fetkovich Typecurve Analysis of BK5 at B Sand

The transient data of this well do not fit on the Fetkovich curves properly and so cannot be analyzed properly. The type curve data being very noisy and difficult to interpret, type curve "Data Filter" is also used here for better matching. Only some portion of boundary dominated data fit on the right hand stem type curves for this well. In the following table summary of results of Fetkovich analysis for the well BK5 of B sand is presented:

Table 6.5 Summary of results of Fetkovich analysis for well BK4 of B Sand:

Wells in B Sand	OGIP bcf	Area acre	EUR bcf	D_1	d_1 %	b
BK 5	107.466	1196.24	81.898	0.084124	8.07	0

6.2 Blasingame Typecurve Analysis

In this method depletion analysis is analytical. Concepts of normalized rate, material balance time and pseudo time are used here. Using Normalizing Rate data and Material Balance Time allows reservoir to be analyzed independently of production constraints (variable rate / pressure profiles). This method is valid for single-phase volumetric reservoirs and primarily applicable to wells with good quality production and flowing pressure data. A model (radial, fractured, horizontal) is selected first and three rate functions are plotted against material balance pseudo time t_{ca} . For gas wells, material balance pseudo time is defined as follow:

$$t_{ca} = \frac{\mu_i c_{Ri}}{q} \int_0^t \frac{q}{\mu(\bar{p}) c_i(\bar{p})} dt = \frac{\mu_i c_{Ri} z_i G_i (p_{pr} - p_p)}{2q p_i} \quad \dots \quad (6.12)$$

To use this method some data preparation is required: calculation of normalized rate by dividing q by Δp_p for gas reservoirs. Normalized Rate for gas wells is defined as follows:

$$\frac{q}{\Delta p_p} = \frac{q}{p_i - p_{pwi}} \quad \dots \quad (6.13)$$

The rate integral is defined at any point in the production life of a well, as the average rate at which the well has produced until that moment in time. The normalized rate integral is defined as follows:

$$q_i = \left(\frac{q}{\Delta p_p} \right)_i = \frac{1}{t_{ca}} \int_0^{t_{ca}} \frac{q}{\Delta p_p} dt_{ca} \quad \dots \quad (6.14)$$

The rate integral derivative is defined as the semi logarithmic derivative of the rate integral function, with respect to material balance time. It is defined as follows:

$$q_{id} = \left(\frac{q}{\Delta p_p} \right)_{id} = - \frac{d \left(\frac{q}{\Delta p_p} \right)_i}{d \ln t_{ca}} = - t_{ca} \frac{d \left(\frac{q}{\Delta p_p} \right)_i}{dt_{ca}} \quad \dots \quad (6.15)$$

Now a data plot of normalized rate ($q/\Delta p_p$) versus material balance (pseudo) time (t_{ca}) have to be plotted logarithmically. Then $q/\Delta p_p$ vs. t_{ca} data plot is matched to q_{Dd} vs. t_{Dd} (constant rate typecurves in Fetkovich dimensionless format) and a transient ($t_{eD} = r_e/r_{wa}$) stem is sought out. A Rate-Integral (q_i) data plot and a Rate-Integral Derivative (q_{id}) data plot are constructed. Then 'complimentary' typecurves (q_{Dd} and q_{Ddid} curves) are matched by q_i and

q_{id} data to try and fine tune and to confirm match. Matching is similar to previous type curve matching. Unlike the Fetkovich analysis, Blasingame does not require 'b' (hyperbolic exponent) values. Instead, the data are matched on the single depletion (material balance) stem. Given a curve match, the reservoir parameters k , s (from transient match) and Area, OGIP (from boundary dominated match) can be obtained if μ , h , c_v , ϕ , and r_w are known.

k is obtained from rearranging the definition of q_{Dd}

$$q_{Dd} = \frac{q}{\Delta p_p} \left(\frac{1.417E6 * T}{kh} \right) \left(\ln \left(\frac{r_e}{r_{wa}} \right)_{match} - \frac{1}{2} \right) \quad \dots \quad (6.16)$$

$$k = \left(\frac{q / \Delta p_p}{q_{Dd}} \right)_{match} \left(\frac{1.417E6 * T}{h} \right) h_{1,wa} \quad \dots \quad (6.17)$$

Solving for r_{wa} from the definition of t_{Dd} :

$$t_{Dd} = \frac{0.006328kt}{\frac{1}{2} \phi \mu c_v r_{wa}^2 \left(\left(\frac{r_e}{r_{wa}} \right)_{match}^2 - 1 \right) \left(\ln \left(\frac{r_e}{r_{wa}} \right)_{match} - \frac{1}{2} \right)} \quad \dots \quad (6.18)$$

$$r_{wa} = \sqrt{\left(\frac{t_{ca}}{t_{Dd}} \right)_{match} \frac{0.006328k}{\phi \mu c_v \frac{1}{2} \left(\left(\frac{r_e}{r_{wa}} \right)_{match}^2 - 1 \right) \left(\ln \left(\frac{r_e}{r_{wa}} \right)_{match} - \frac{1}{2} \right)}} \quad \dots \quad (6.19)$$

$$s = \ln \left(\frac{r_w}{r_{wa}} \right) \quad \dots \quad (6.20)$$

$$A = \frac{\pi r_e^2}{43560} \text{ (acres)} \quad \dots \quad (6.21)$$

$$G_i = \frac{2p_i}{(z\mu c_i)_i} \left(\frac{t_{ca}}{t_{Dd}} \right)_{match} \left(\frac{q / \Delta p_p}{q_{Dd}} \right)_{match} \text{ (bcf)} \quad \dots \quad (6.22)$$

The q_i and q_{id} curves exhibit a unique signature for boundary dominated production, when matched simultaneously with the normalized rate data. Concept of rate-integral allows for a relatively smooth derivative typecurve, which is not normally possible for drawdown data.

In Blasingame typecurves, Rate-integral calculations are very sensitive to early-time errors. The q_i and q_{id} curves can contain large cumulative deviations due to relatively insignificant

early-time errors. Rate-integral-derivative (q_{ID}) does not readily display the different flow regimes but it is useful for pattern recognition.

Sand-wise Blasingame typecurve analysis

In this section the results of Blasingame typecurve analysis of different wells of different sands have been presented.

6.2.1 J Sand

There are 4 wells in J sand: BK1, BK6, BK7 and BK8. The first step in performing a Blasingame analysis is to choose the correct model. For analyzing the data of Bakhrabad Gas Field, radial model is selected. Then this analysis provides a reliable and versatile method for estimating early time parameters (k , s) and also estimating OGIP and drainage area. Blasingame typecurve analysis of individual wells of J Sand is given below:

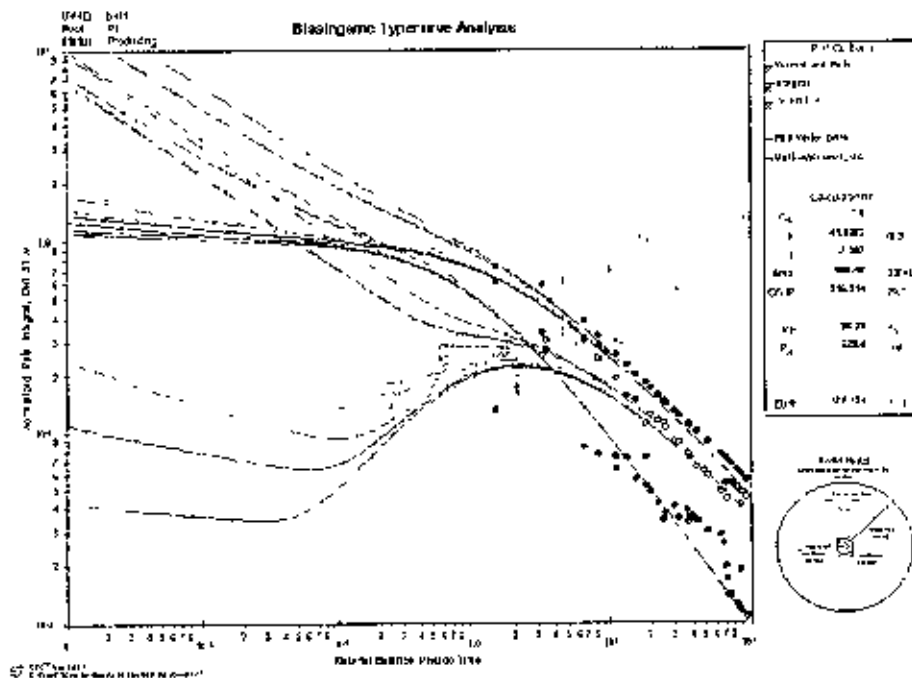


Fig 6.11 Blasingame Typecurve Analysis of BK1 at J Sand

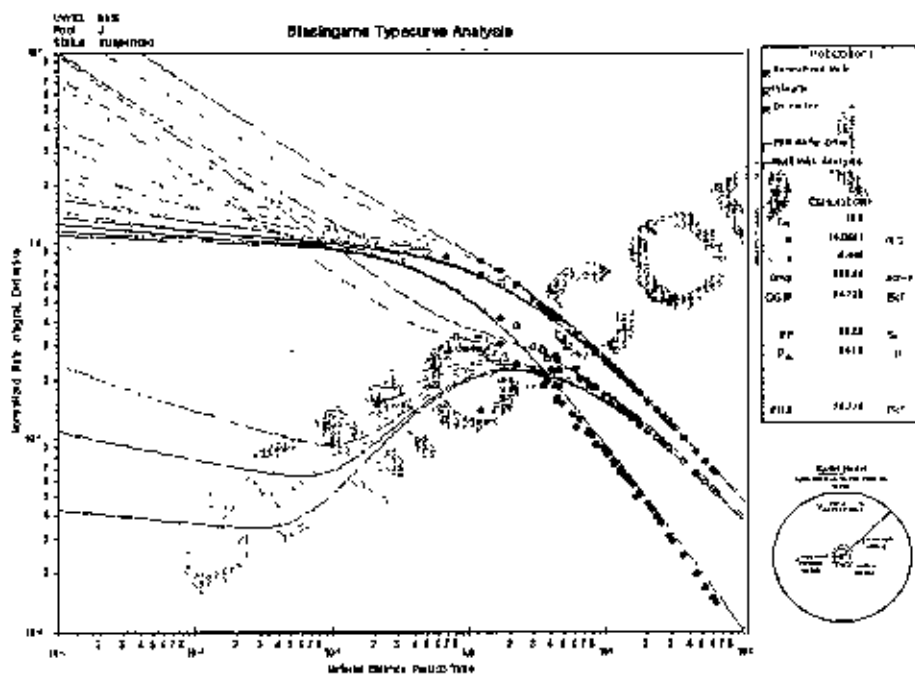


Fig 6.12 Blasingame Typecurve Analysis of BK6 at J Sand

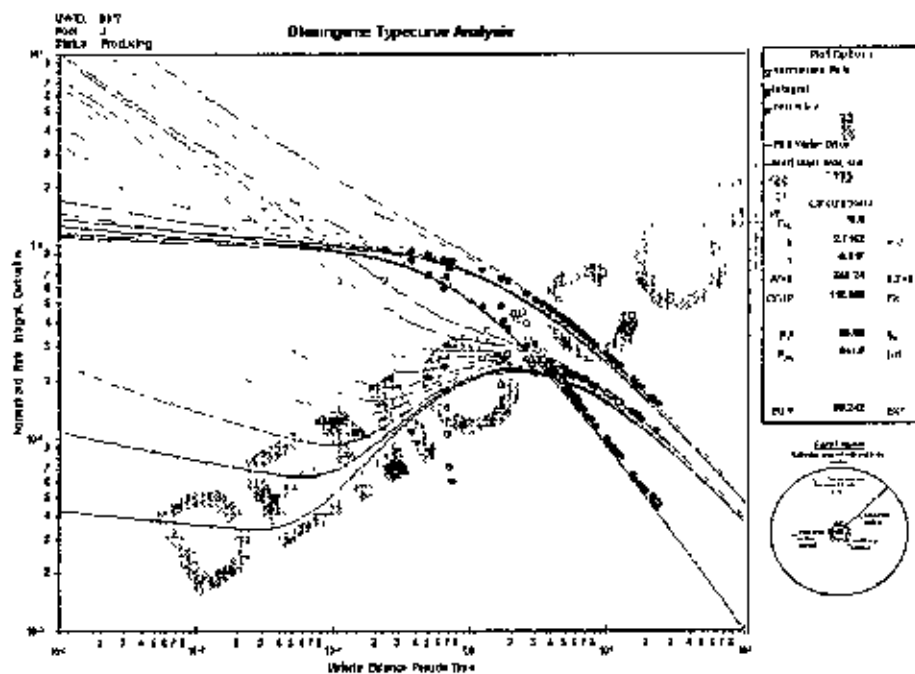


Fig 6.13 Blasingame Typecurve Analysis of BK7 at J Sand

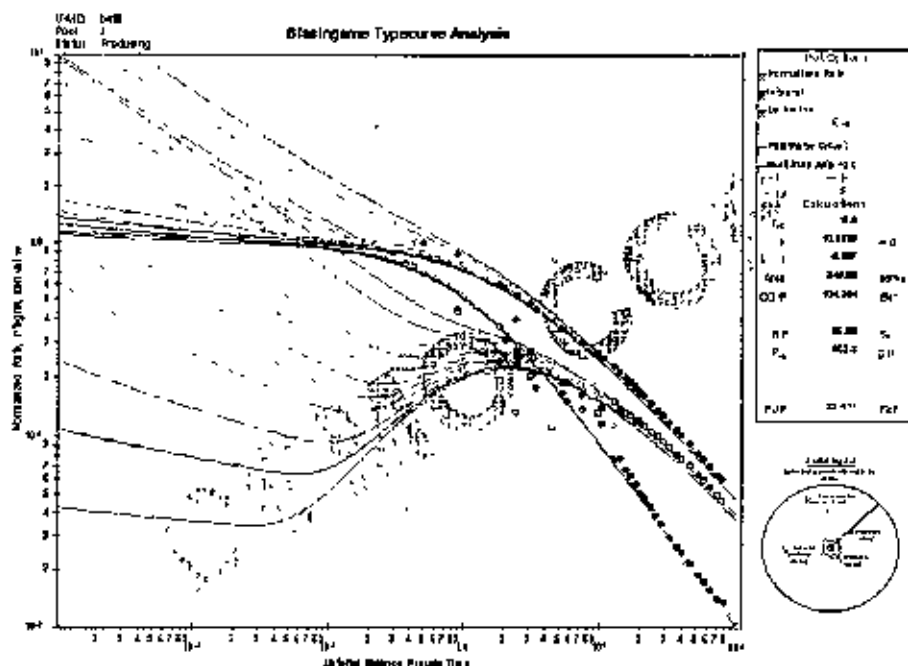


Fig 6.14 Blasingame Typecurve Analysis of BK8 at J Sand

107249

Due to the issue of non-uniqueness, analysis of production data is performed by simultaneous matching of multiple type curves (i.e. normalized rate, integral and derivative). The integral curve smoothes out noisy data, while the derivative exaggerates changes in the character of the data. Blasingame plots show good match for all wells in J Sand. Thus the results of this analysis are more reliable than Fetkovich analysis.

Table 6.6 Summary of results of Blasingame analysis for all wells of J Sand:

Wells in J Sand	r_{eD}	OGIP bcf	Area acre	EUR bcf	k md	s
BK 1	7	215.214	639.43	179.124	41.8032	-7.26724
BK 6	18	94.723	830.56	75.779	14.0661	-6.44478
BK 7	18	112.802	353.24	90.242	2.7152	-6.0173
BK 8	18	104.264	346.08	83.411	10.3339	-6.00707

6.2.2 G Sand

There are 2 wells in G sand: BK3 and BK4. Blasingame typecurve analysis of individual wells of G Sand is given below:

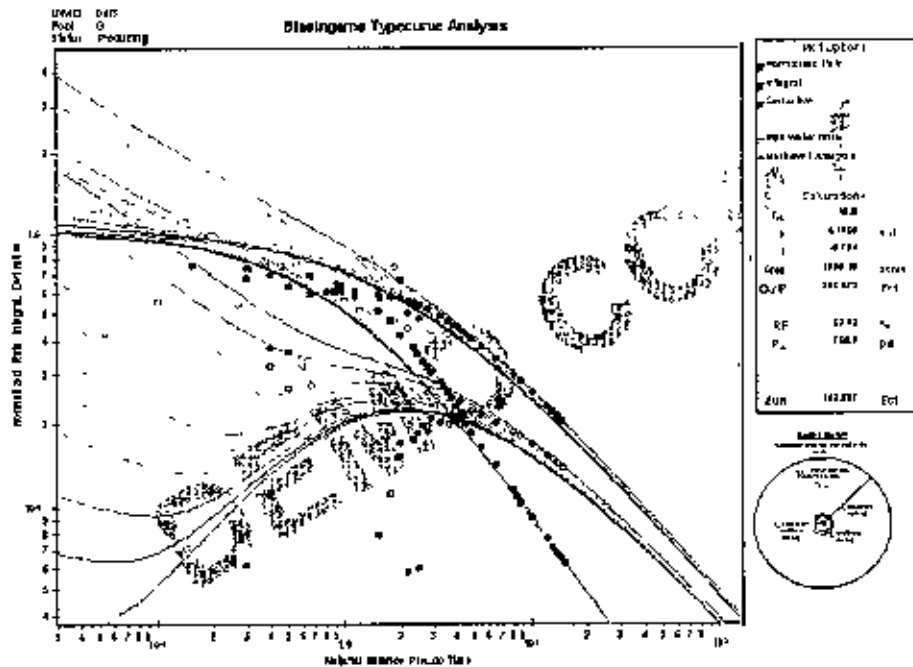


Fig 6.15 Blasingame Typecurve Analysis of BK3 at G Sand

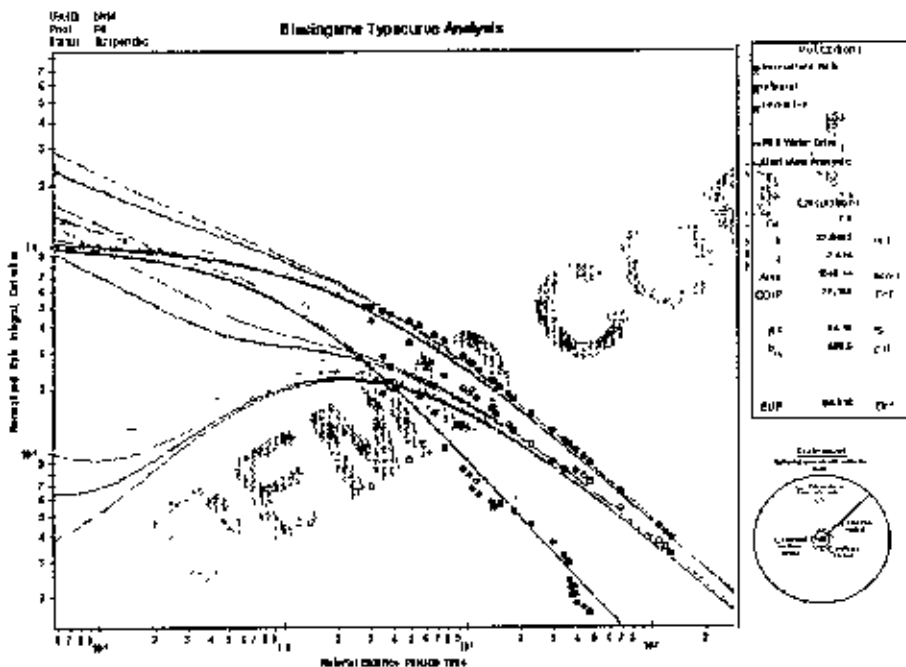


Fig 6.16 Blasingame Typecurve Analysis of BK4 at G Sand

The transient data of BK3 are very noisy although type curve "Data Filter" is used here for better matching. Later portion of data of BK4 deflected from the boundary stem in

normalized rate type curve. In the following table summary of results of Blasingame analysis for the wells of G sand is presented:

Table 6.7 Summary of results of Blasingame analysis for wells of G Sand:

Wells in G Sand	r_{eD}	OGIP bcf	Area acre	EUR bcf	k md	s
BK 3	18	203.672	1669.1	162.937	4.1685	-6.79375
BK 4G	7	77.139	1048.14	64.913	37.0468	-7.51434

6.2.3 DL Sand

There are 2 wells in DL sand: BK2 and BK5. Blasingame typecurve analysis of individual wells of DL Sand is given below:

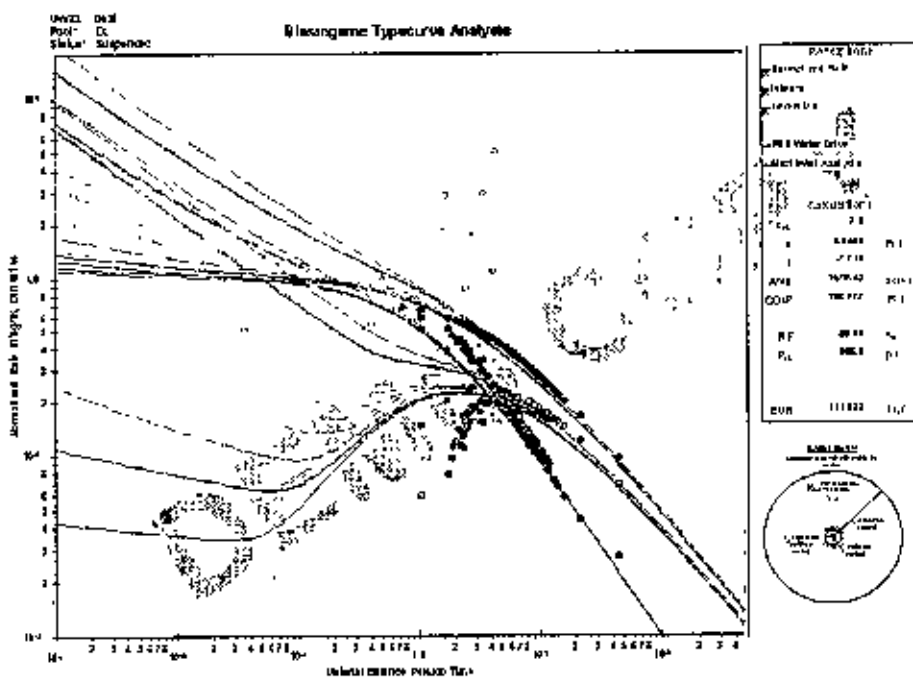


Fig 6.17 Blasingame Typecurve Analysis of BK2 at DL Sand

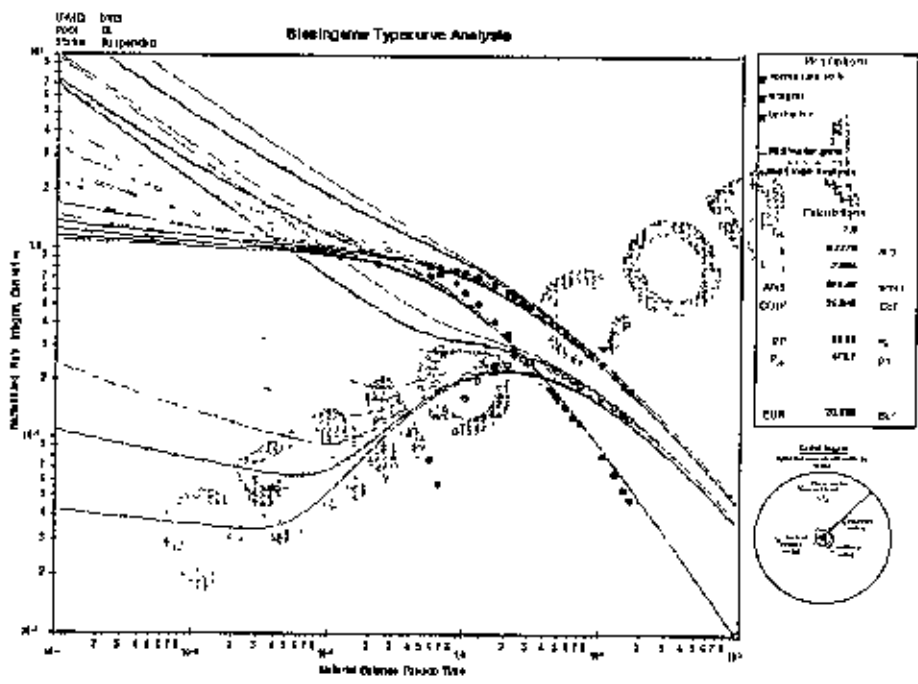


Fig 6.18 Blasingame Typecurve Analysis of BK5 at DL Sand

There is some data scatter in transient data of BK2. But Blasingame plots show good match for BK2 and BK5. In the following table summary of results of Blasingame analysis for the wells of DL sand is presented:

Table 6.8 Summary of results of Blasingame analysis for wells of DL Sand:

Wells in DL Sand	r_{eD}	OGIP bcf	Area acre	EUR bcf	k md	s
BK 2	7	138.777	1579.42	111.022	4.0496	-7.71936
BK 5	7	25.048	378.42	20.038	6.7779	-7.00495

6.2.4 DU Sand

There is only one well in DU sand: BK4. Blasingame typecurve analysis of this well of DU Sand is given below:

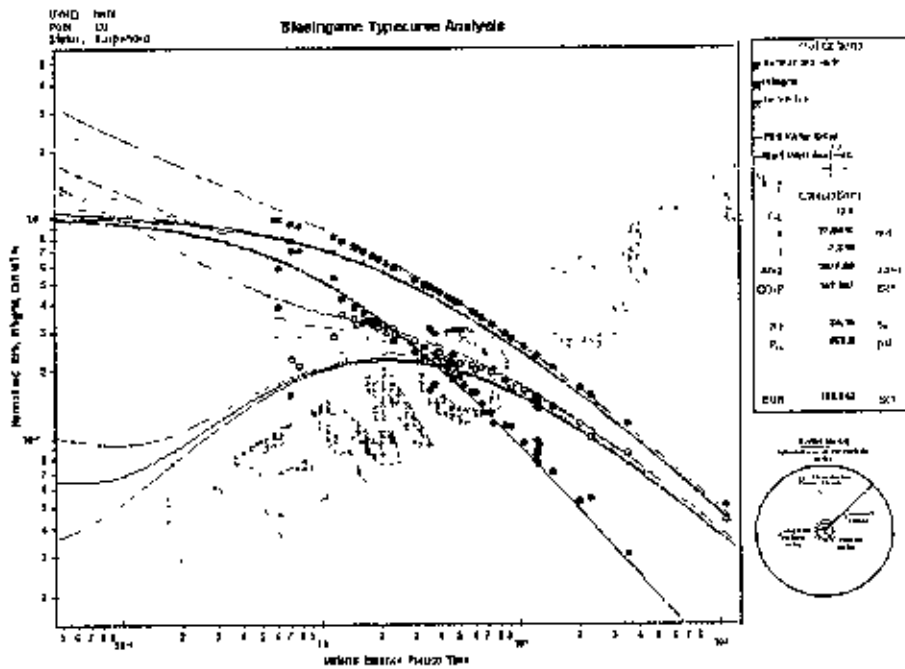


Fig 6.19 Blasingame Typecurve Analysis of BK4 at DU Sand

Data of BK4 in DU Sand shows good match in Blasingame typecurves. In the following table summary of results of Blasingame analysis for the well BK4 of DU sand is presented:

Table 6.9 Summary of results of Blasingame analysis for well BK4 of DU Sand:

Wells in DU Sand	r_{eD}	OGIP bcf	Area acre	EUR bcf	k md	s
BK 4	12	152.867	2077.09	128.64	27.061	-7.31049

6.1.5 B Sand

There is only one well in B Sand: BK5. Blasingame typecurve analysis of this well of B Sand is given below:

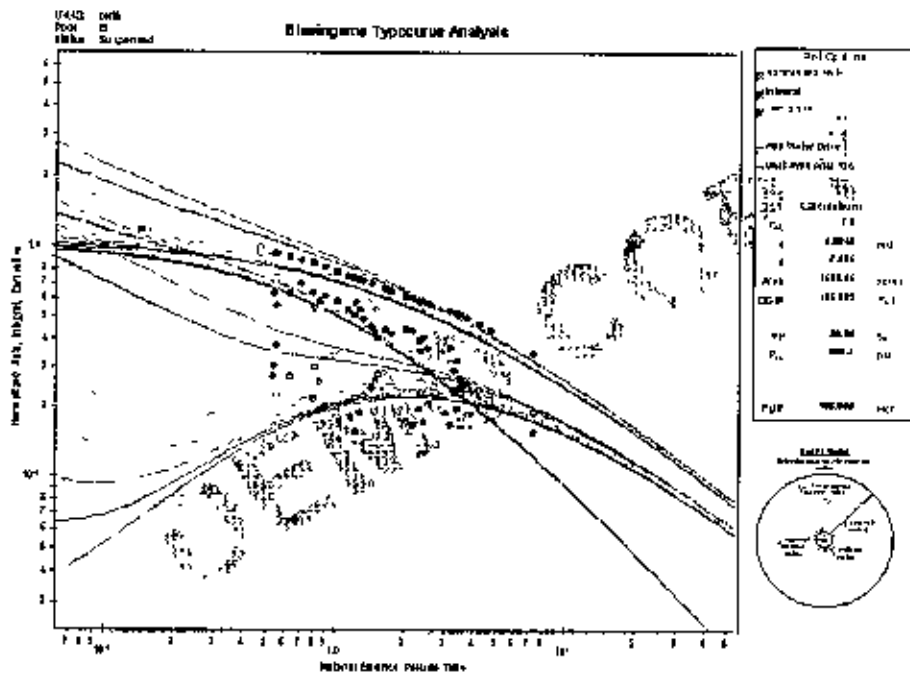


Fig 6.20 Blasingame Typecurve Analysis of BK5 at B Sand

Data of BK5 in B Sand shows good match in Blasingame typecurves. In the following table summary of results of Blasingame analysis for the well BK5 of B sand is presented:

Table 6.10 Summary of results of Blasingame analysis for well BK4 of B Sand:

Wells in B Sand	r_{ED}	OGIP bcf	Area acre	EUR bcf	k md	s
BK 5	7	135.082	1503.65	108.066	5.0248	-7.69478

6.3 Agarwal-Gardner Rate-Time Typecurve Analysis

Agarwal and Gardner method is build upon the work of both Fetkovich and Palacio-Blasingame, utilizing the concepts of the equivalence between constant rate and constant pressure solutions. They present new typecurves with dimensionless variables based on the conventional welltest definitions, as opposed to the Fetkovich dimensionless definitions used by Blasingame et al. They also include primary and semi log pressure derivative plots (in inverse format for decline analysis). Furthermore, they present their decline curves in additional formats to the standard normalized rate versus time plot. These include the rate versus cumulative and cumulative versus time analysis plots.

Similar to previous analysis, in this procedure a model (radial, fractured, horizontal) is selected first. Then $q/\Delta p_p$ vs. $t_c(a)$ data plot is matched to q_D vs. t_{DA} (constant rate typecurves in welltest format) and a transient (r_{eD}) stem is sought out. The dimensionless pressure for standard welltest analysis is defined as

$$P_D = \frac{141.2kh(p_i - p_{wf})}{qB\mu} \quad \dots \quad \dots \quad (6.23)$$

The dimensionless flow rate is simply the inverse of the above equation (in the welltest literature, q_D has a slightly different definition)

$$q_D = \frac{1}{P_D} \quad \dots \quad \dots \quad (6.24)$$

Normalized Rate for gas wells is defined as follows:

$$\frac{q}{\Delta p_p} = \frac{q}{p_i - p_{wf}} \quad \dots \quad \dots \quad (6.25)$$

Inverse-pressure-derivative (1/DER) for gas wells is defined as follows:

$$\frac{1}{DER} = \frac{1}{\frac{\partial \frac{\Delta p_p}{q}}{\partial \ln(t_{ca})}} = \left(t_{ca} \frac{d\left(\frac{\Delta p_p}{q}\right)}{dt_{ca}} \right)^{-1} \quad \dots \quad \dots \quad (6.26)$$

The inverse-pressure-derivative plots are constructed. Then 'complimentary' typecurve (1/DER) are matched by data plot to fine tune the match.

For gas wells, q_D is defined as follows:

$$q_D = \frac{1.417 E 6 T_R}{kh} \frac{q}{\Delta p_p} \quad \dots \quad \dots \quad (6.27)$$

The permeability (k) is calculated from above, as follows:

$$k = \frac{1.417 E 6 T_R}{h} \left(\frac{q / \Delta p_p}{q_D} \right)_{match} \quad \dots \quad \dots \quad (6.28)$$

From the definition of t_{DA} ,

$$t_{DA} = \frac{0.00634}{\pi \phi \mu_r c_{it}} \frac{kt_{cu}}{r_e^2} \quad \dots \quad \dots \quad (6.29)$$

r_e is calculated as follows:

$$r_e = \sqrt{\frac{0.00634 kt_{cu}}{\pi \phi \mu_r c_{it}} \left(\frac{t_{cu}}{t_{DA}} \right)_{match}} \quad \dots \quad \dots \quad (6.30)$$

Additional reservoir parameters are calculated as follows:

$$r_{wa} = \frac{r_e}{(r_e / r_{wa})_{match}} \quad \dots \quad \dots \quad (6.31)$$

$$s = \ln \left(\frac{r_w}{r_{wa}} \right) \quad \dots \quad \dots \quad (6.32)$$

$$A = \frac{\pi r_e^2}{43560} \text{ (acres)} \quad \dots \quad \dots \quad (6.33)$$

$$G = \frac{\pi r_e^2 \phi h s_g p_i T_w}{z_i T P_w} * E - 9 \text{ (bcf)} \quad \dots \quad \dots \quad (6.34)$$

In Agarwal-Gardner method Inverse-Pressure Derivative typecurve has similar functionality to Pressure Transient Derivative (simply the inverse). Thus, different transient flow regimes can be more easily distinguished. The transition from infinite acting to boundary dominated flow occurs at a t_{DA} of 0.1, which is a single vertical line, common to all typecurves on the plot. (Such a line cannot be drawn on the Blasingame plot.)

Inverse-pressure derivative is usually too noisy to gain any meaningful interpretation. A suggested improvement to this method is to calculate a pressure integral (i.e. NPI typecurves) and base the inverse-pressure derivative on this. The resulting derivative plot retains most of the characteristics of the 'raw data' derivative, but has much less scatter. Overall, tends to be more non-unique than Blasingame.

Sand-wise Agarwal-Gardner typecurve analysis

In this section the results of Agarwal-Gardner typecurve analysis of different wells of different sands have been presented.

6.3.1 J Sand

There are 4 wells in J sand: BK1, BK6, BK7 and BK8. The first step in performing an Agarwal-Gardner analysis is to choose the correct model. For analyzing the data of Bakhrabad Gas Field, radial model is selected. The AG rate vs. time plot can be used in conjunction with the Blasingame plot for helping to firm up estimates of OGIP and early time parameters (permeability and skin). Agarwal-Gardner typecurve analysis of individual wells of J Sand is given below:

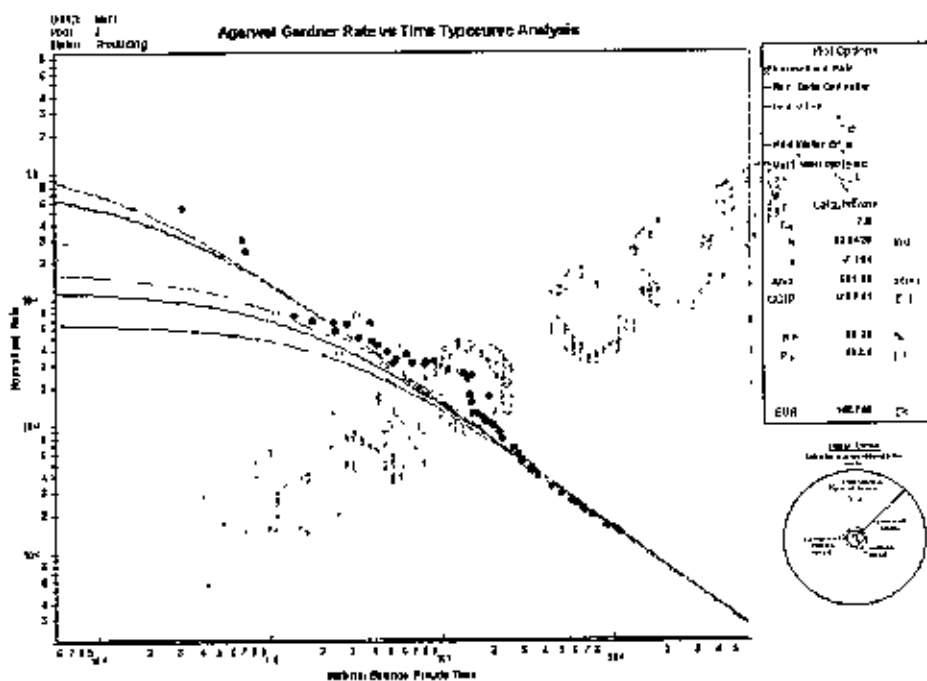


Fig 6.21 Agarwal-Gardner Typecurve Analysis of BK1 at J Sand

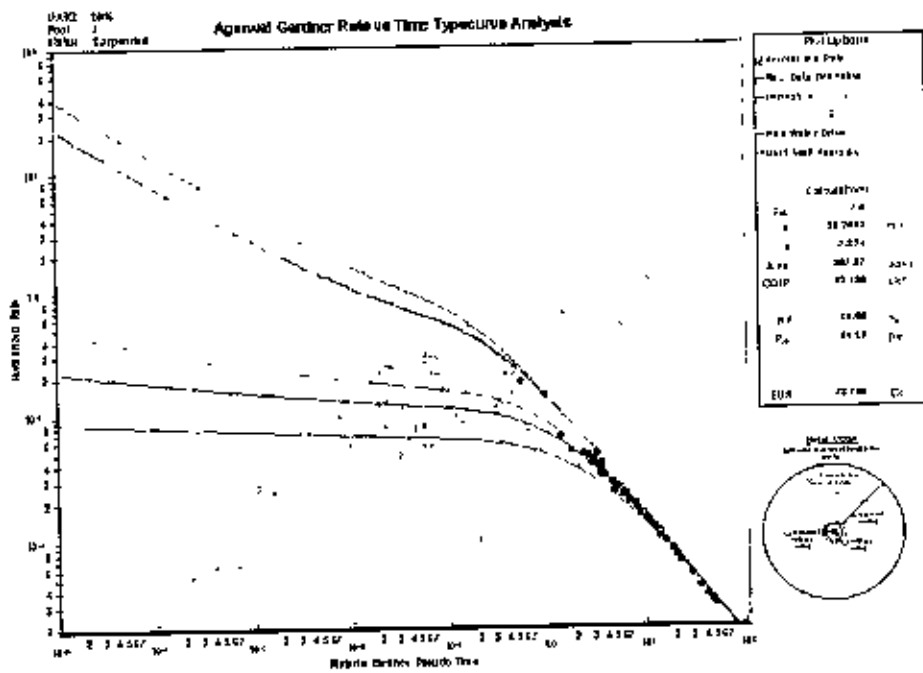


Fig 6.22 Agarwal-Gardner Typecurve Analysis of BK6 at J Sand

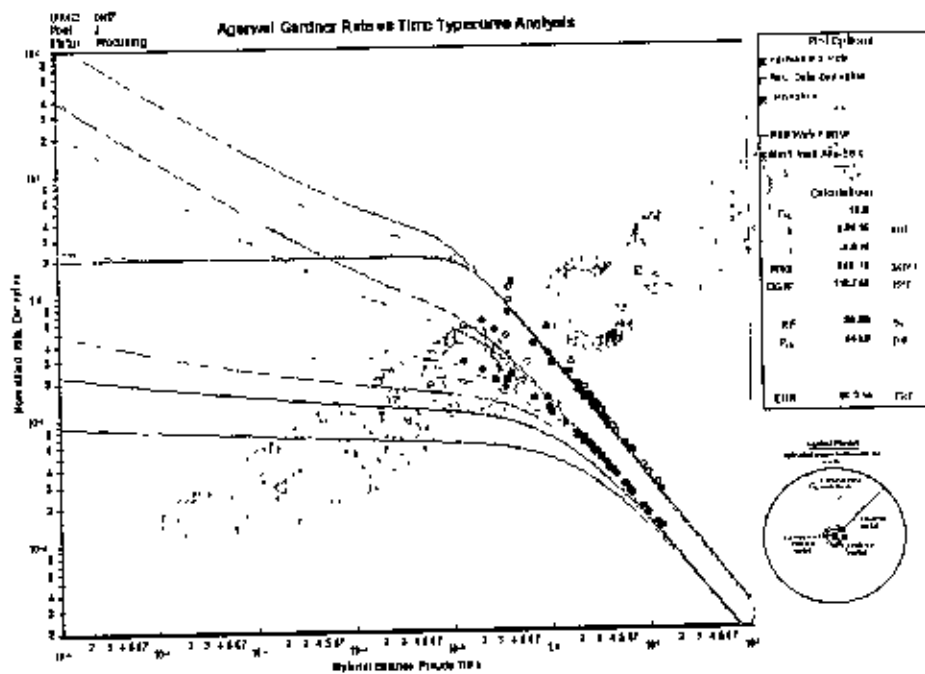


Fig 6.23 Agarwal-Gardner Typecurve Analysis of BK7 at J Sand

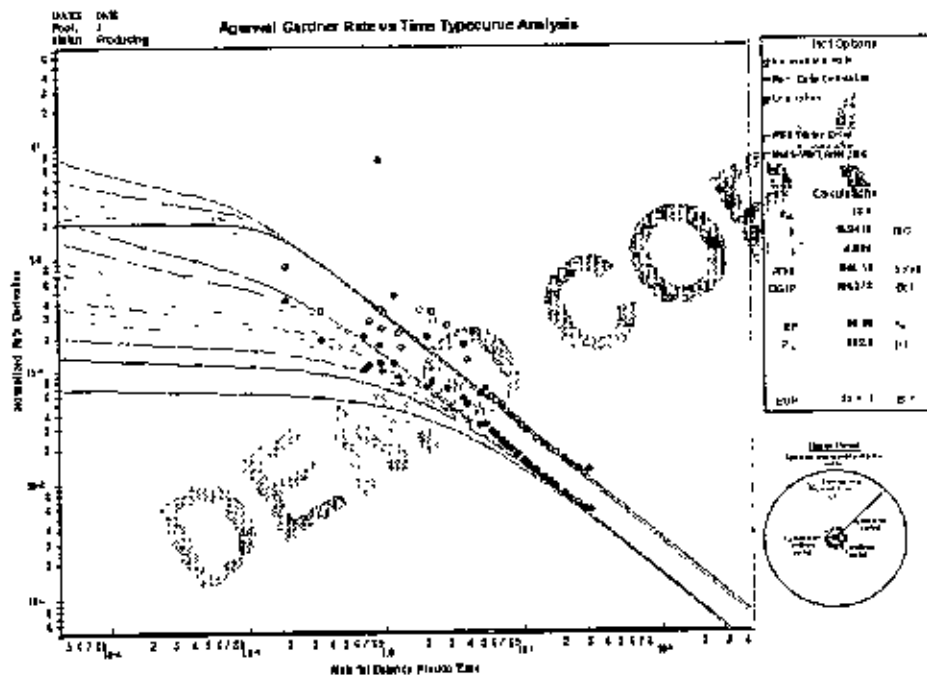


Fig 6.24 Agarwal-Gardner Typecurve Analysis of BK8 at J Sand

Due to the issue of non-uniqueness, analysis of production data is performed by simultaneous matching of multiple type curves (i.e. normalized rate and derivative). AG plots show good match for all wells in J Sand. In the following table summary of results of Agarwal-Gardner analysis for the wells of J sand is presented:

Table 6.11 Summary of results of Agarwal-Gardner analysis for all wells of J Sand:

Wells in J Sand	r_{cD}	OGIP bcf	Area acre	EUR bcf	k md	s
BK 1	7	178.741	531.06	148.768	32.3429	-7.16408
BK 6	7	92.136	807.87	73.709	28.2492	-7.37385
BK 7	18	112.768	353.13	90.214	3.9515	-6.01561
BK 8	18	104.273	346.11	83.418	10.241	-6.00556

6.3.2 G Sand

There are 2 wells in G sand: BK3 and BK4. Agarwal-Gardner typecurve analysis of individual wells of G Sand is given below:

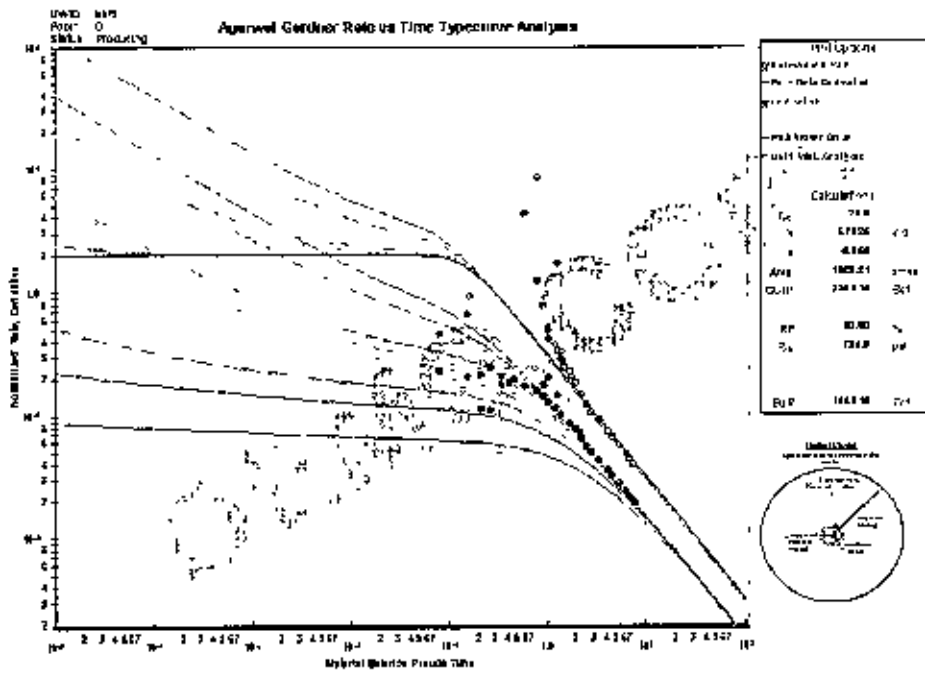


Fig 6.25 Agarwal-Gardner Typecurve Analysis of BK3 at G Sand

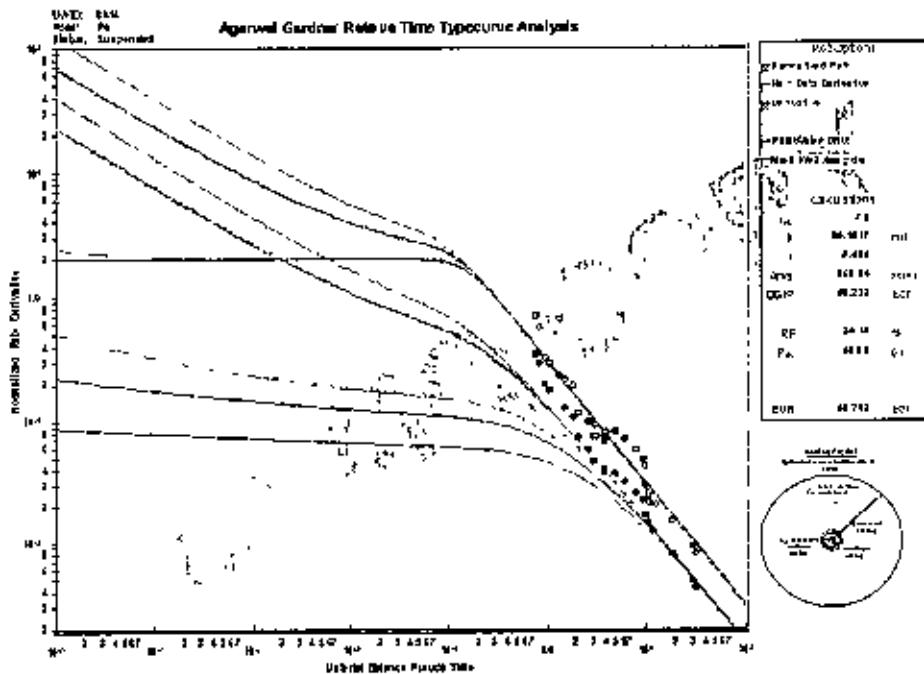


Fig 6.26 Agarwal-Gardner Typecurve Analysis of BK4 at G Sand

The type curve data being very noisy and difficult to interpret, type curve “Data Filter” is used here for better matching. AG plots show good match for all wells in G Sand. In the

following table summary of results of Agarwal-Gardner analysis for the wells of G sand is presented:

Table 6.12 Summary of results of Agarwal-Gardner analysis for wells of G Sand:

Wells in G Sand	r_{GD}	OGIP bcf	Area acre	EUR bcf	k md	s
BK 3	28	206.016	1688.31	164.813	5.7326	-6.35609
BK 4G	7	63.222	859.04	53.202	36.1617	-7.40455

6.3.3 DL Sand

There are 2 wells in DL sand: BK2 and BK5. Agarwal-Gardner typecurve analysis of individual wells of DL Sand is given below:

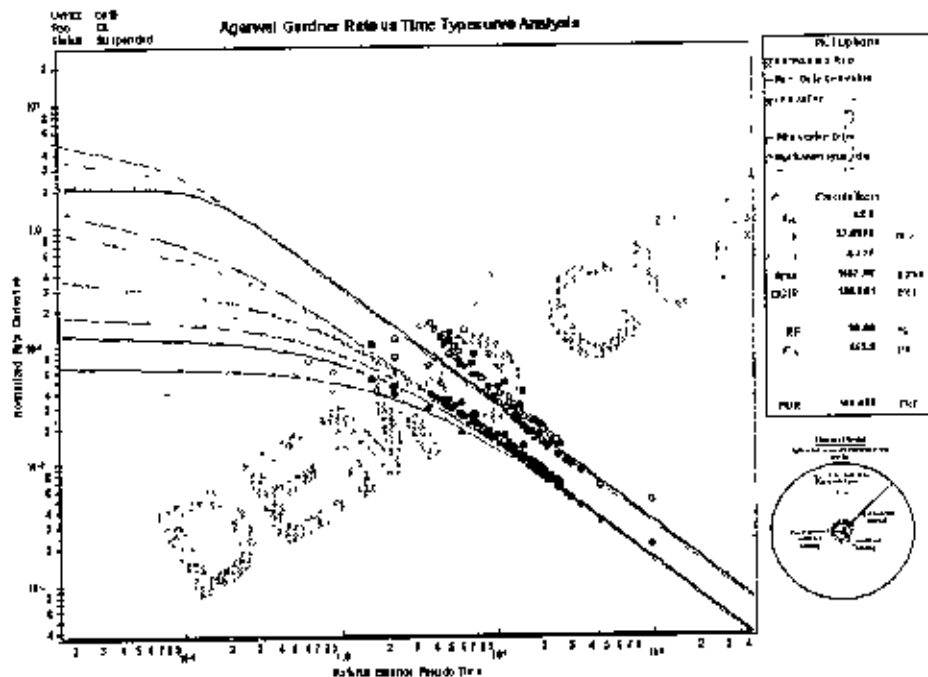


Fig 6.27 Agarwal-Gardner Typecurve Analysis of BK2 at DL Sand

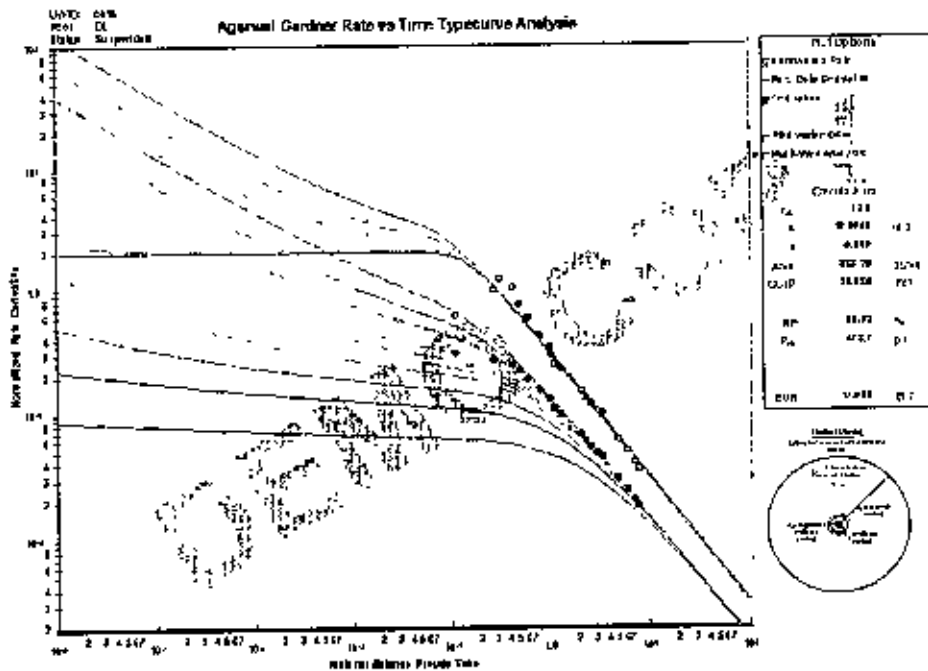


Fig 6.28 Agarwal-Gardner Typecurve Analysis of BK5 at DL Sand

The type curve data being very noisy and difficult to interpret, type curve “Data Filter” is used here for better matching. AG plots show good match for all wells in DL Sand. In the following table summary of results of Agarwal-Gardner analysis for the wells of DL sand is presented:

Table 6.13 Summary of results of Agarwal-Gardner analysis for wells of DL Sand:

Wells in DL Sand	r_{dB}	OGIP bcf	Area acre	EUR bcf	k md	s
BK 2	48	136.861	1557.62	109.489	37.6279	-5.77681
BK 5	12	22.386	338.2	17.909	12.6953	-6.39946

6.3.4 DU Sand

There is only one well in DU sand: BK4. Agarwal-Gardner typecurve analysis of this well of DU Sand is given bellow:

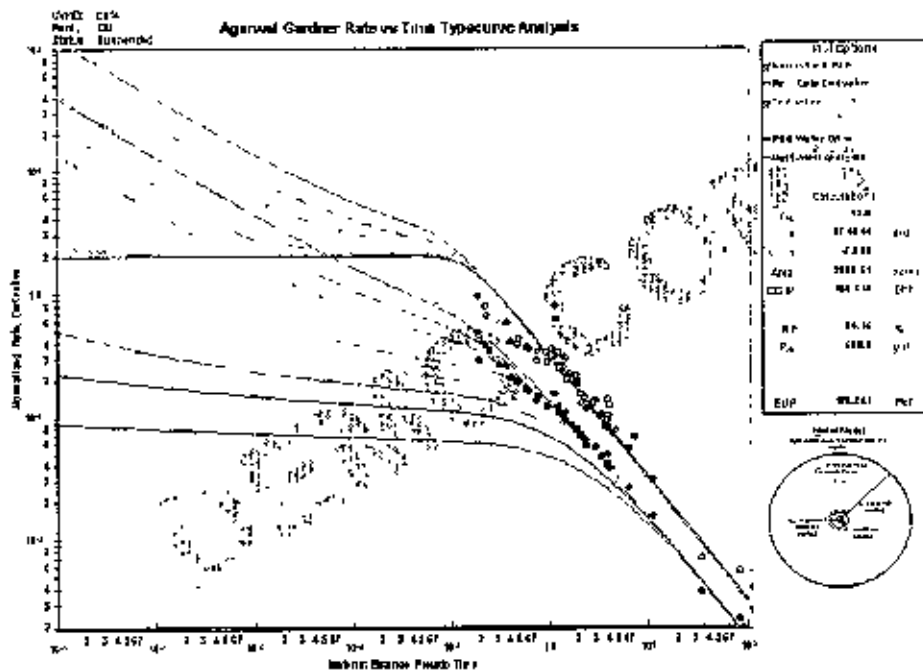


Fig 6.29 Agarwal-Gardner Typecurve Analysis of BK4 at DU Sand

AG plots show good match for BK4 in DU Sand. In the following table summary of results of Agarwal-Gardner analysis for the well BK4 of DU sand is presented:

Table 6.14 Summary of results of Agarwal-Gardner analysis for well BK4 of DU Sand:

Wells in DU Sand	r_{eD}	OGIP bcf	Area acre	EUR bcf	k md	s
BK 4	12	153.119	2080.51	128.851	27.4344	-7.30783

6.3.5 B Sand

There is only one well in B Sand: BK5. Agarwal-Gardner typecurve analysis of this well of B Sand is given below:

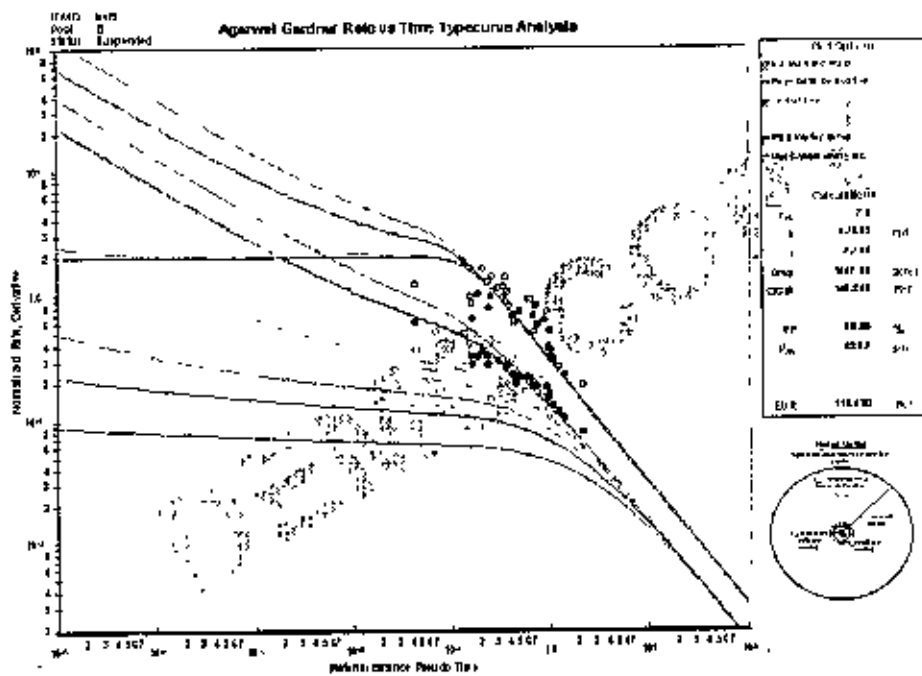


Fig 6.30 Agarwal-Gardner Typecurve Analysis of BK5 at B Sand

AG plots show good match for BK5 in B Sand. In the following table summary of results of Agarwal-Gardner analysis for the well BK5 of B sand is presented:

Table 6.15 Summary of results of Agarwal-Gardner analysis for well BK4 of B Sand:

Wells in B Sand	r_{CD}	OGIP bcf	Area acre	EUR bcf	k md	s
BK 5	7	140.85	1567.85	112.68	6.7392	-7.70538

6.4 NPI (Normalized Pressure Integral) Typecurve Analysis

Blasingame et al (1989) developed the Normalized Pressure Integral (NPI) analysis. This method uses normalized pressure instead of normalized rate. Analysis is the inverse of Agarwal-Gardner Rate-Time Typecurves. The objective of the method was to present a robust diagnostic method for drawdowns that did not suffer from noise and data scatter, as is typical of the standard welltest derivative.

In this analysis procedure, a model (radial, fractured, horizontal) is selected first and three rate functions are plotted against material balance time t_{ca} . For gas wells, material balance time is defined as follow:

$$t_{ca} = \frac{\mu_i c_v}{q} \int_0^{t_{ca}} \frac{q}{\mu(\bar{p}) c_r(\bar{p})} dt \equiv \frac{\mu_i c_v z_i G_i (p_{pr} - p_p)}{2qp_i} \quad \dots \quad \dots \quad (6.35)$$

Normalized Pressure for gas wells is defined as follows:

$$\frac{\Delta p_p}{q} = \frac{p_i - p_{pwf}}{q} \quad \dots \quad \dots \quad (6.36)$$

The pressure integral is defined at any point in the production life of a well, as the average normalized flowing pressure drop at which the well has produced until that moment in time.

The normalized pressure integral is defined as follows:

$$\left(\frac{\Delta p_p}{q} \right)_i = \frac{1}{t_{ca}} \int_0^{t_{ca}} \frac{\Delta p_p}{q} dt \quad \dots \quad \dots \quad (6.37)$$

The pressure integral derivative is defined as the semi logarithmic derivative of the pressure integral function, with respect to material balance time. It is defined as follows:

$$\left(\frac{\Delta p_p}{q} \right)_{id} = \frac{t_{ca} d \left(\frac{\Delta p_p}{q} \right)_i}{dt_{ca}} \quad \dots \quad \dots \quad (6.38)$$

In this analysis procedure a model (radial, fractured, horizontal) is selected. Then $\Delta p_p/q$ vs. t_{ca} data plot is matched to q_D vs. t_{DA} (constant rate typecurves in welltest format) and a transient (τ_{eD}) stem is sought out. A Pressure-Integral (p_i) data plot and a Pressure-Integral Derivative (p_{id}) data plot are constructed and 'complimentary' typecurve (p_{Di}) and (p_{Did}) are matched by data plot to fine tune the match. Given a curve match, the reservoir parameters

k, s (from transient match) and Area, OGIP (from boundary dominated match) can be obtained if μ , h, c_v , ϕ , and r_w are known.

k is obtained from rearranging the definition of p_D

$$p_D = \frac{kh\Delta p_p}{1.417E6Tq} \quad \dots \quad \dots \quad (6.39)$$

$$k = \frac{1.417E6T}{h} \left(\frac{p_D}{\Delta p_p / q} \right)_{match} \quad \dots \quad \dots \quad (6.40)$$

Solving for r_e from the definition of t_{DA} :

$$t_{DA} = \frac{0.00634kt_{ca}}{\pi\phi\mu_i c_v r_e^2} \quad \dots \quad \dots \quad (6.41)$$

$$r_e = \sqrt{\frac{0.00634k}{\pi\phi\mu_i c_v} \left(\frac{t_{ca}}{t_{DA}} \right)_{match}} \quad \dots \quad \dots \quad (6.42)$$

$$r_{wu} = \frac{r_e}{\left(\frac{r_e}{r_{wu}} \right)_{match}} \quad \dots \quad \dots \quad (6.43)$$

$$s = \ln \left(\frac{r_w}{r_{wu}} \right) \quad \dots \quad \dots \quad (6.44)$$

$$G = \frac{(0.00634)(1.417E6)s_g p_i T_{sc}}{(z\mu c_i)_{p_{sc}}} \left(\frac{t_{ca}}{t_{DA}} \right)_{match} \left(\frac{p_D}{\Delta p_p / q} \right)_{match} * 10^9 \text{ (bcf)} \dots \quad (6.45)$$

Sand-wise NPI typecurve analysis

In this section the results of NPI typecurve analysis of different wells of different sands have been presented.

6.4.1 J Sand

There are 4 wells in J sand: BK1, BK6, BK7 and BK8. The first step in performing a NPI analysis is to choose the correct model. For analyzing the data of Bakhrabad Gas Field,

radial model is selected. Then this analysis provides a reliable and versatile method for estimating early time parameters (k, s) and also estimating OGIP and drainage area. NPI typecurve analysis of individual wells of J Sand is given below:

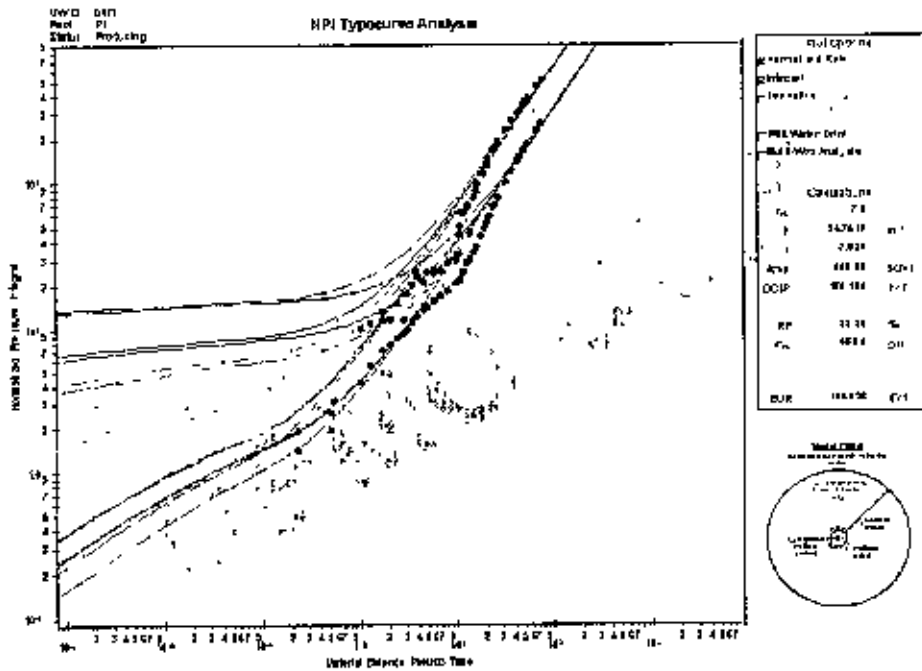


Fig 6.31 NPI Typecurve Analysis of BK1 at J Sand

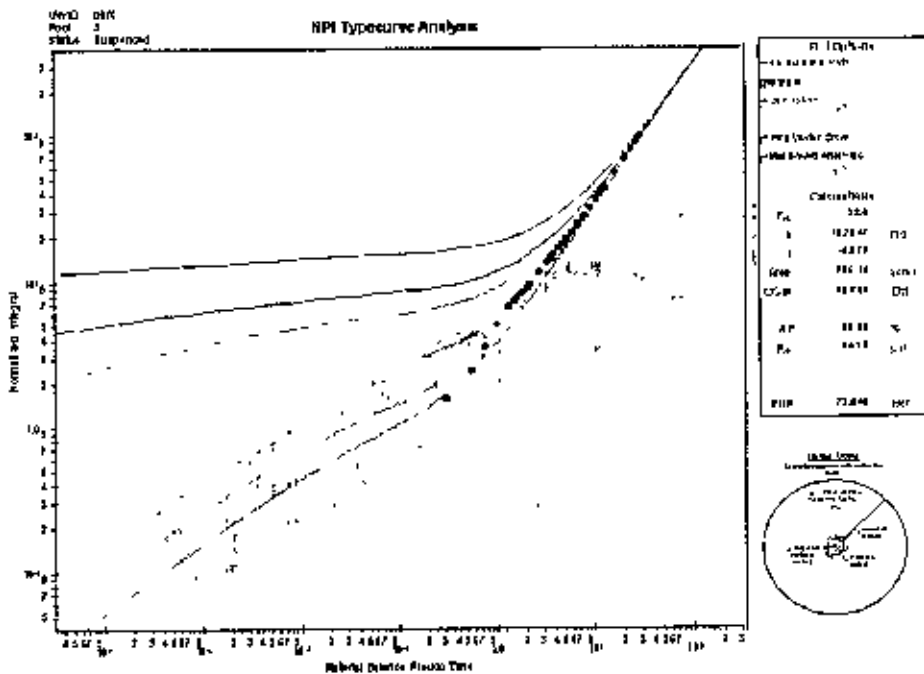


Fig 6.32 NPI Typecurve Analysis of BK6 at J Sand

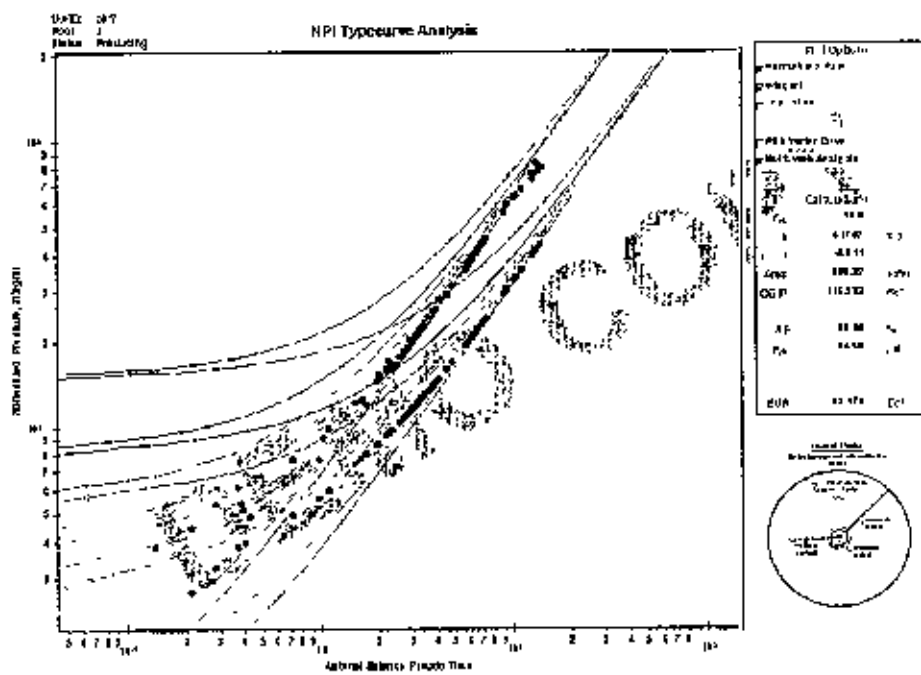


Fig 6.33 NPI Typecurve Analysis of BK7 at J Sand

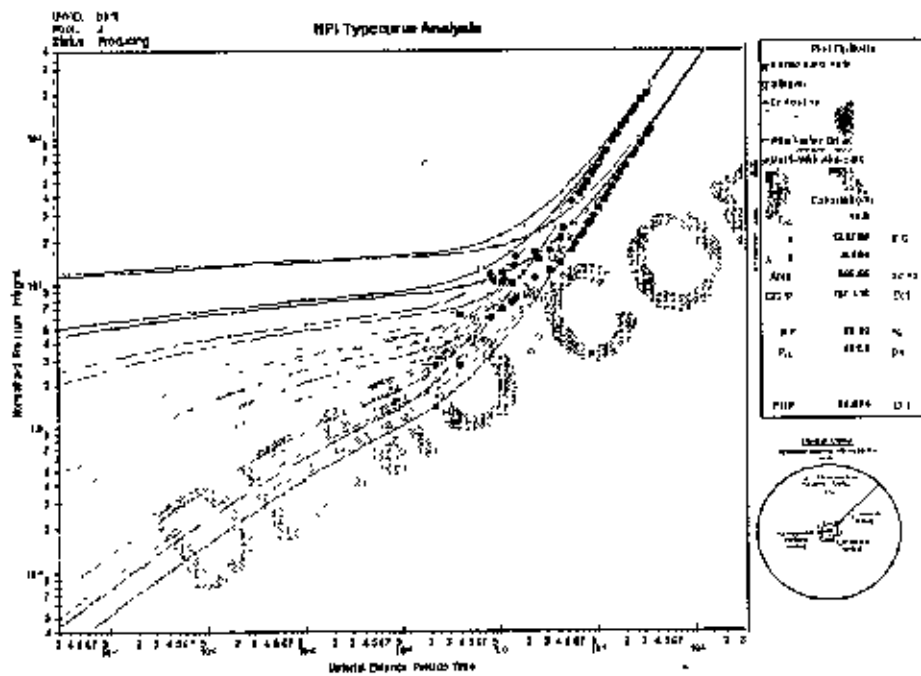


Fig 6.34 NPI Typecurve Analysis of BK8 at J Sand

Due to the issue of non-uniqueness, analysis of production data is performed by simultaneous matching of multiple type curves (i.e. normalized rate and integral). NPI plots show good

match for all wells in J Sand. In the following table summary of results of NPI analysis for the wells of J sand is presented:

Table 6.16 Summary of results of NPI analysis for all wells of J Sand:

Wells in J Sand	r_{eD}	OGIP bcf	Area acre	LUR bcf	k md	s
BK 1	7	186.136	553.03	154.923	24.7519	-7.92923
BK 6	28	90.685	795.14	72.548	15.7547	-6.37866
BK 7	18	115.222	360.82	92.178	4.1757	-6.51113
BK 8	18	107.118	355.55	85.694	12.0786	-6.50378

6.4.2 G Sand

There are 2 wells in G sand: BK3 and BK4. NPI typecurve analysis of individual wells of G Sand is given below:

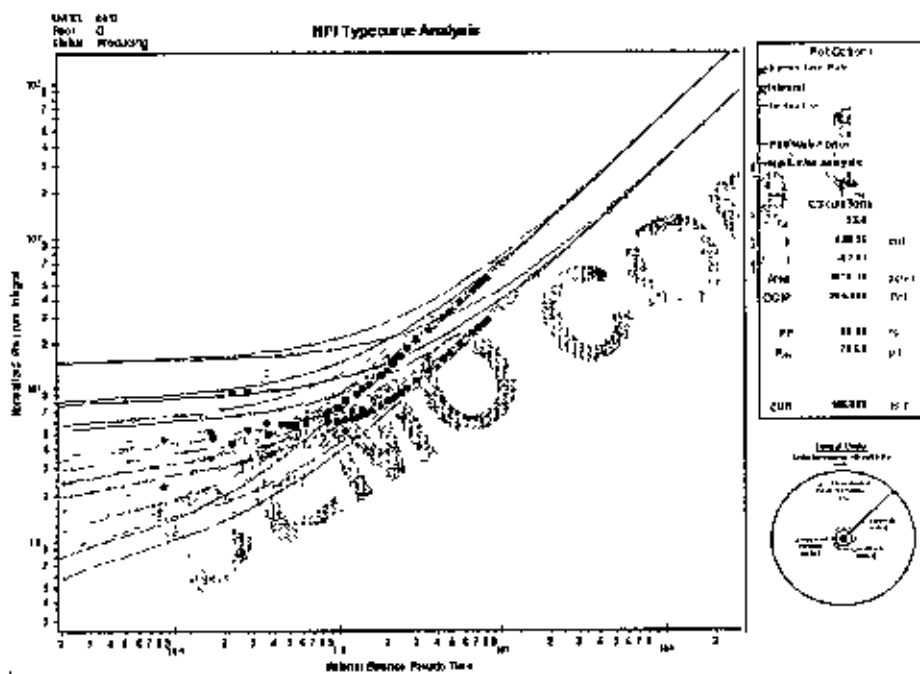


Fig 6.35 NPI Typecurve Analysis of BK3 at G Sand

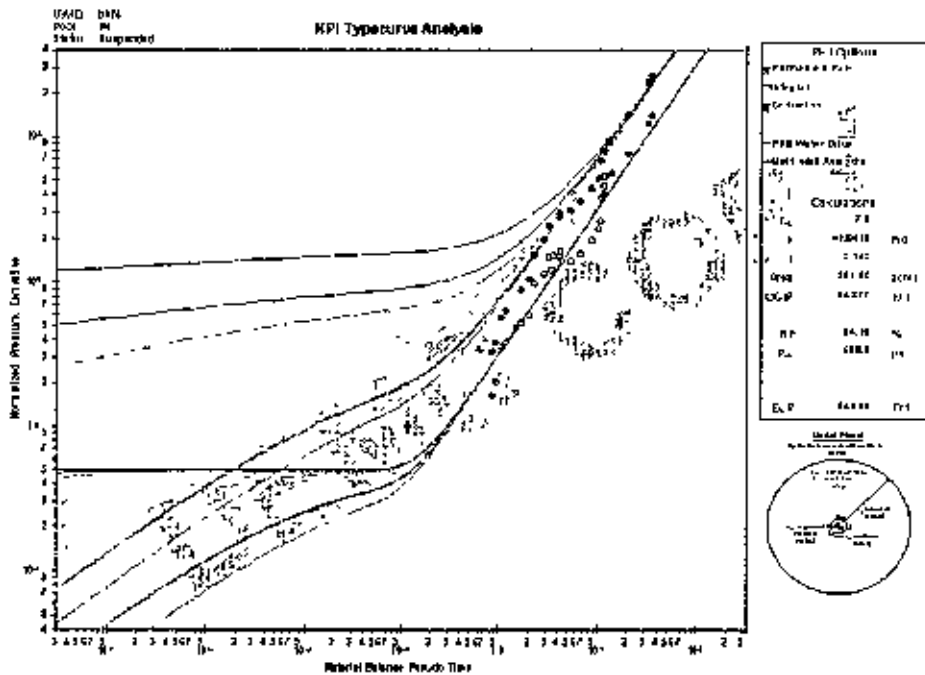


Fig 6.36 NPI Typecurve Analysis of BK4 at G Sand

The type curve data being very noisy and difficult to interpret, type curve “Data Filter” is used here for better matching. NPI plots show good match for all wells in G Sand. In the following table summary of results of NPI analysis for the wells of G sand is presented:

Table 6.17 Summary of results of NPI analysis for wells of G Sand:

Wells in G Sand	r_{eD}	OGIP bcf	Area acre	EUR bcf	k md	s
BK 3	28	204.163	1673.13	163.33	6.0325	-6.75062
BK 4G	7	64.877	881.53	54.595	41.8413	-8.16235

6.4.3 DL Sand

There are 2 wells in DL sand: BK2 and BK5. NPI typecurve analysis of individual wells of DL Sand is given bellow:

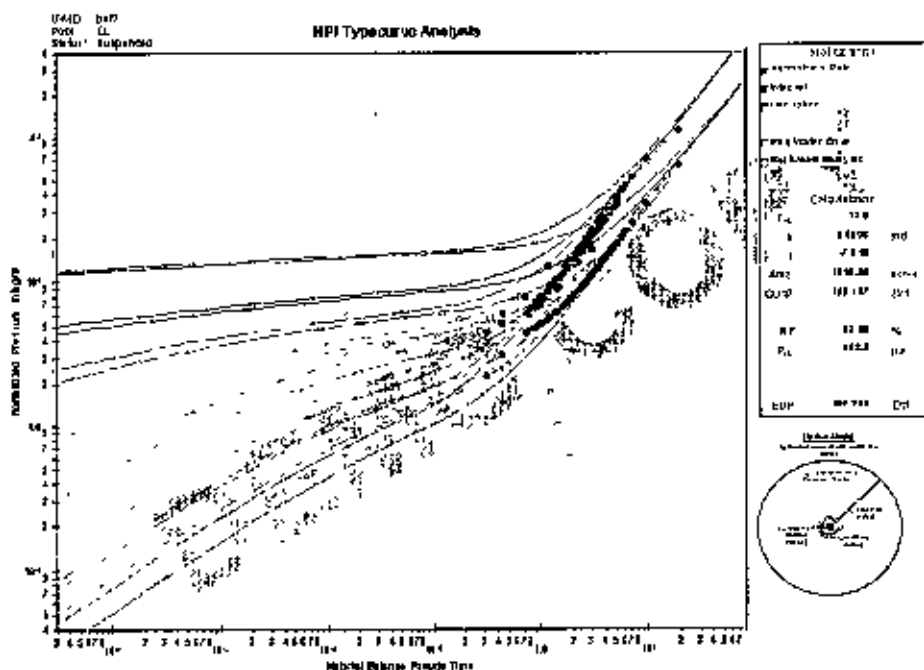


Fig 6.37 NPI Typecurve Analysis of BK2 at DL Sand

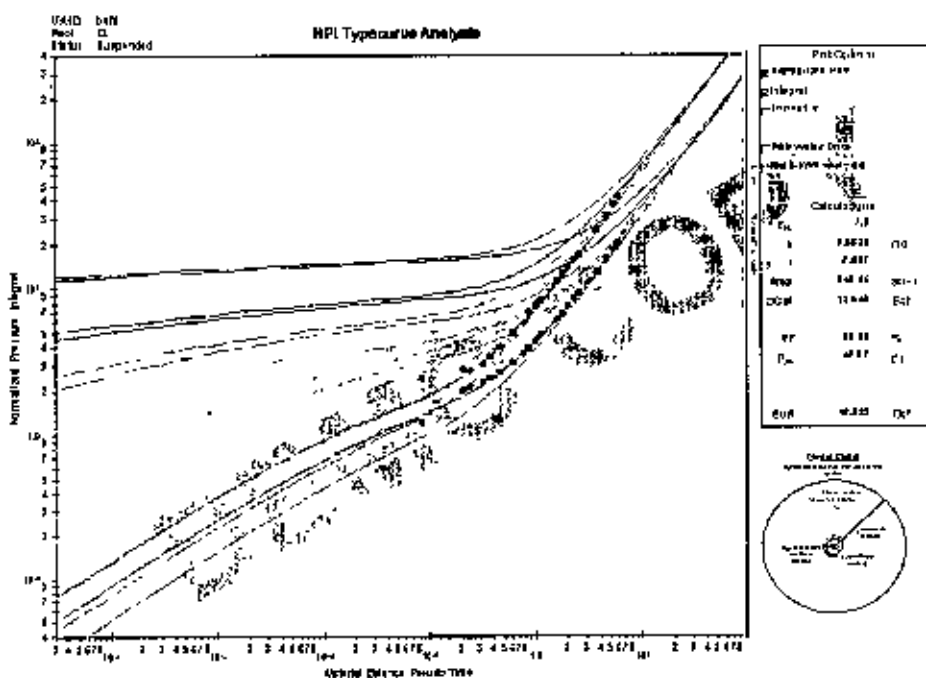


Fig 6.38 NPI Typecurve Analysis of BK5 at DL Sand

NPI plots show good match for all wells in DL Sand. In the following table summary of results of NPI analysis for the wells of DL sand is presented:

Table 6.18 Summary of results of NPI analysis for wells of DL Sand:

Wells in DL Sand	r_{cD}	OGIP bcf	Area acre	EUR bcf	k md	s
BK 2	12	159.107	1810.8	127.286	8.5608	-7.81805
BK 5	7	22.548	340.65	18.038	9.5826	-7.68695

6.4.4 DU Sand

There is only one well in DU sand: BK4. NPI typecurve analysis of this well of DU Sand is given below:

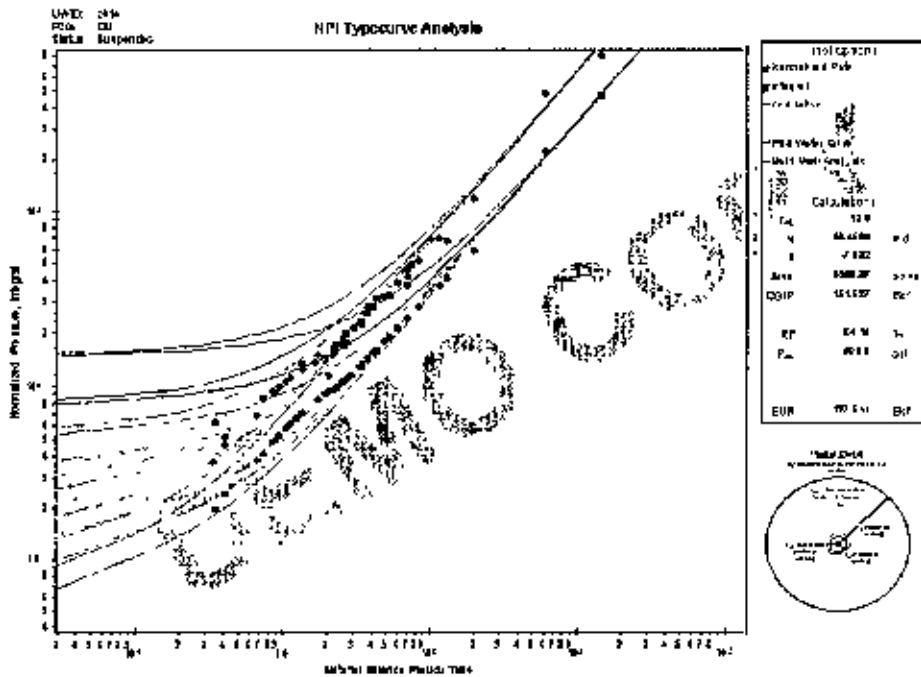


Fig 6.39 NPI Typecurve Analysis of BK4 at DU Sand

NPI plots show good match for BK4 in DU Sand. In the following table summary of results of NPI analysis for the well BK4 of DU sand is presented:

Table 6.19 Summary of results of NPI analysis for well BK4 of DU Sand:

Wells in DU Sand	r_{cD}	OGIP bcf	Area acre	EUR bcf	k md	s
BK 4	12	151.527	2058.87	127.511	49.4506	-7.88224

6.4.5 B Sand

There is only one well in B Sand: BK5. NPI typecurve analysis of this well of B Sand is given below:

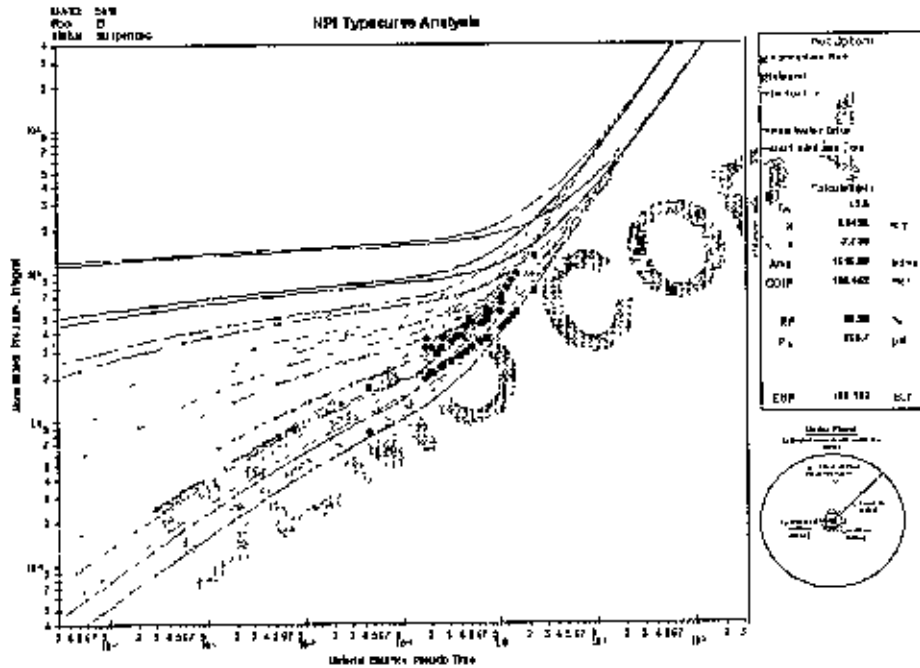


Fig 6.40 NPI Typecurve Analysis of BK5 at B Sand

NPI plots show good match for BK5 in B Sand. In the following table summary of results of NPI analysis for the well BK5 of B sand is presented:

Table 6.20 Summary of results of NPI analysis for well BK4 of B Sand:

Wells in B Sand	r_{wi}	OGIP bcf	Area acre	EUR bcf	k md	s
BK 5	12	136.452	1518.89	109.162	6.9433	-7.73015

6.5 Transient Typecurve Analysis

The transient typecurve analysis method is not a new method of data analysis. Rather, it provides an alternative perspective that is ideal for analysis of very short (early) production periods, and/or analysis of very low permeability reservoirs.

In the Blasingame, Agarwal-Gardner and NPI analyses, the typecurves are scaled such that there is convergence onto a single boundary dominated stem (unit slope). This is achieved through the use of a dimensionless time that is based on area (t_{DA} or t_{DD}). One consequence of this type of scaling is that there are numerous transient stems. If a dimensionless time based on well radius (t_D) is chosen instead, there will be a single transient stem with a series of boundary dominated curves. When viewing all the typecurves together, the transient presentation provides a more convenient base for analysis of transient data. Thus the transient presentation of the typecurves provides a more unique typecurve match as transient data works better with the Transient format (q_D vs t_D). The accepted time-superposition function for Rate Transient Analysis is Material Balance Time (MBT). Since MBT is rigorous for boundary dominated flow, it is a natural standard for evaluating variable rate production data. When dealing with only transient data, the standard time-superposition for transient flow (pressure transient analysis) is radial superposition time.

In this methodology, the horizontal axis is material balance pseudo time, which is defined as follows:

$$t_{ca} = \frac{\mu_i c_{vi}}{q} \int_0^t \frac{q}{\mu(\bar{p}) c_v(\bar{p})} dt \quad \dots \quad \dots \quad (6.46)$$

on the vertical axis, two variables are plotted, namely Normalized Rate and Inverse of Semi-log Derivative. Normalized Rate for gas wells is:

$$\frac{q}{\Delta p_p} = \frac{q}{p_i - p_{pwf}} \quad \dots \quad \dots \quad (6.47)$$

and Inverse of Semi-log Derivative is:

$$\frac{1}{DER} = \frac{1}{\frac{\partial \Delta p_p}{\partial \ln(t_{ca})} \frac{q}{\Delta p_p}} \quad \dots \quad \dots \quad (6.48)$$

The normalized rate and inverse semi-log derivative data are plotted against material balance time on a log-log scale of the same size as the type curves. This plot is called the "data plot". The data plot is moved over the type curve plot, while the axes of the two plots are kept parallel, until a good match is obtained. Type curve analysis is done by selecting a match point, and reading its co-ordinates off the data plot ($q/\Delta p_p$ and t_{DA})_{match}, and off the type curve plot (q_D and t_D)_{match}. At the same time the stem value " r_c/r_{wa} " of the matching curve is noted.

In radial basis of analysis, k is obtained from rearranging the definition of q_D

$$q_D = \frac{1.417 E 6 T_R}{kh} \frac{q}{\Delta p_p} \quad \dots \quad \dots \quad (6.49)$$

The permeability (k) is calculated from above, as follows:

$$k = \frac{1.417 E 6 T_R}{h} \left(\frac{q / \Delta p_p}{q_D} \right)_{match} \quad \dots \quad \dots \quad (6.50)$$

From the definition of t_{DA} ,

$$t_D = \frac{0.00634 k t_{ca}}{\phi \mu c_h r_{wa}^2} \quad \dots \quad \dots \quad (6.51)$$

r_{wa} is calculated as follows:

$$r_{wa} = \sqrt{\frac{0.00634 k t_{ca}}{\phi \mu c_h} \left(\frac{1.417 E 6 T_R}{h} \right) \left(\frac{t_{ca}}{t_D} \right)_{match} \left(\frac{q / \Delta p_p}{q_D} \right)_{match}} \quad \dots \quad (6.52)$$

Skin is calculated as follows:

$$s = \ln \left(\frac{r_w}{r_{wa}} \right) \quad \dots \quad \dots \quad (6.53)$$

Volume and area parameters are calculated as follows:

$$G = \frac{\pi (0.00634) (1.417 E 6) s_g p_i T_{sc}}{\mu c_h z_i P_{sc}} \left(\frac{t_{ca}}{t_D} \right)_{match} \left(\frac{q / \Delta p_p}{q_D} \right)_{match} (r_{wa})_{match}^2 * E - 9 \text{ (bcf)} \quad \dots \quad (6.54)$$

$$A = \frac{G z_i T_{sc}}{\phi h s_g p_i T_w} \frac{1}{43560} \text{ (acres)} \quad \dots \quad \dots \quad (6.55)$$

It should be noted that boundary dominated flow analysis is not advised using this method.

Sand-wise Transient typecurve analysis

In this section the results of Transient typecurve analysis of different wells of different sands have been presented.

6.5.1 J Sand

There are 4 wells in J sand: BK1, BK6, BK7 and BK8. The first step in performing a Transient analysis is to choose the correct model. For analyzing the data of Bakhrabad Gas Field, radial model is selected. Then this analysis provides a reliable and versatile method for estimating early time parameters (k , s) and also estimating OGIP and drainage area. Transient typecurve analysis of individual wells of J Sand is given below:

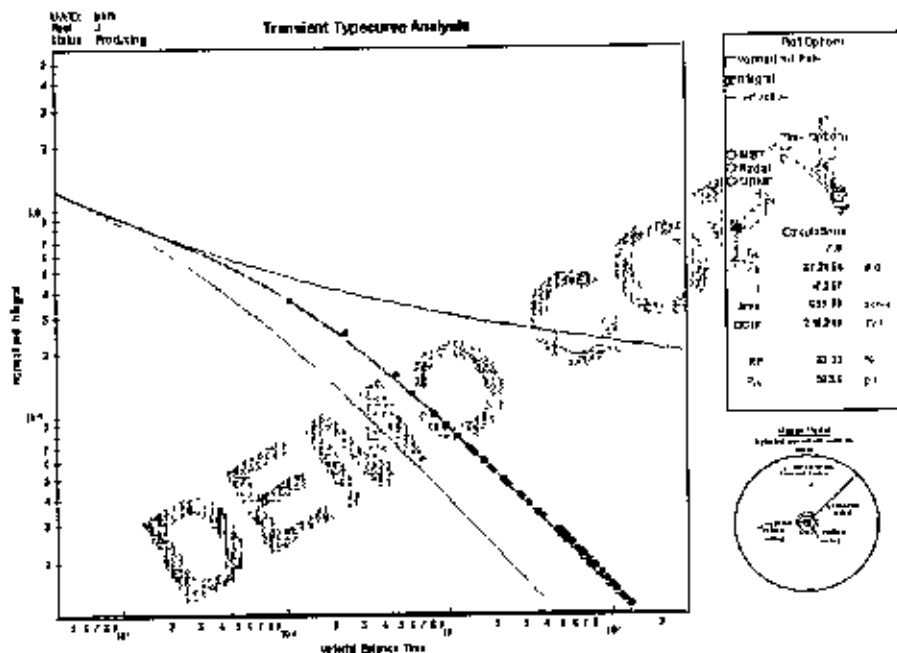


Fig 6.41 Transient Typecurve Analysis of BK1 at J Sand

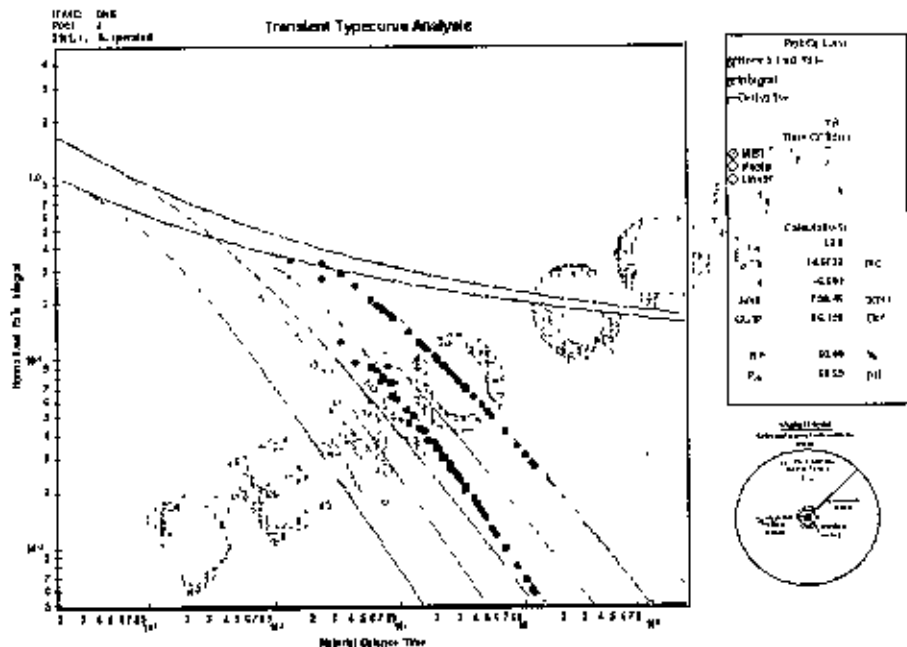


Fig 6.42 Transient Typecurve Analysis of BK6 at J Sand

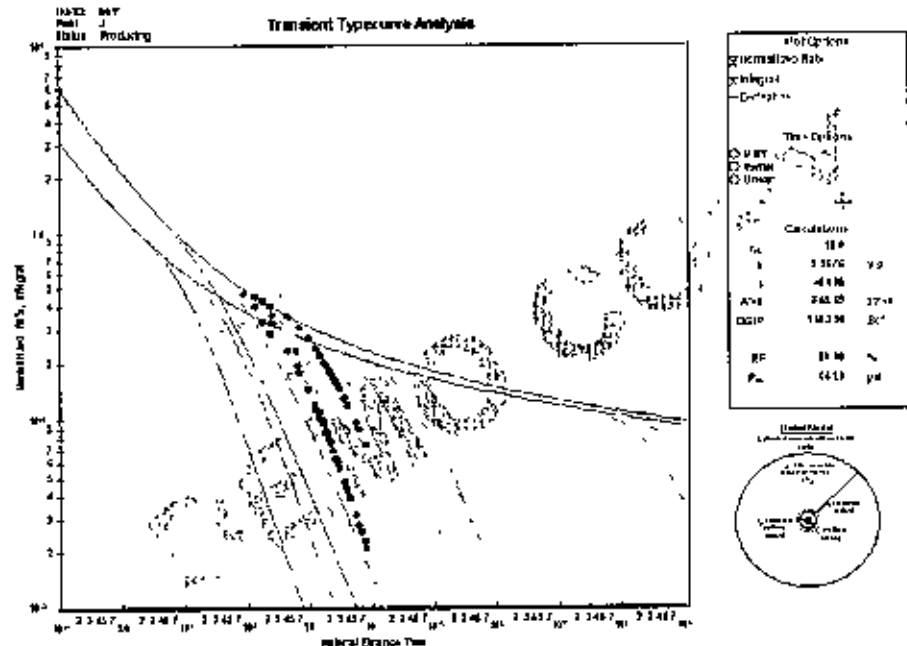


Fig 6.43 Transient Typecurve Analysis of BK7 at J Sand

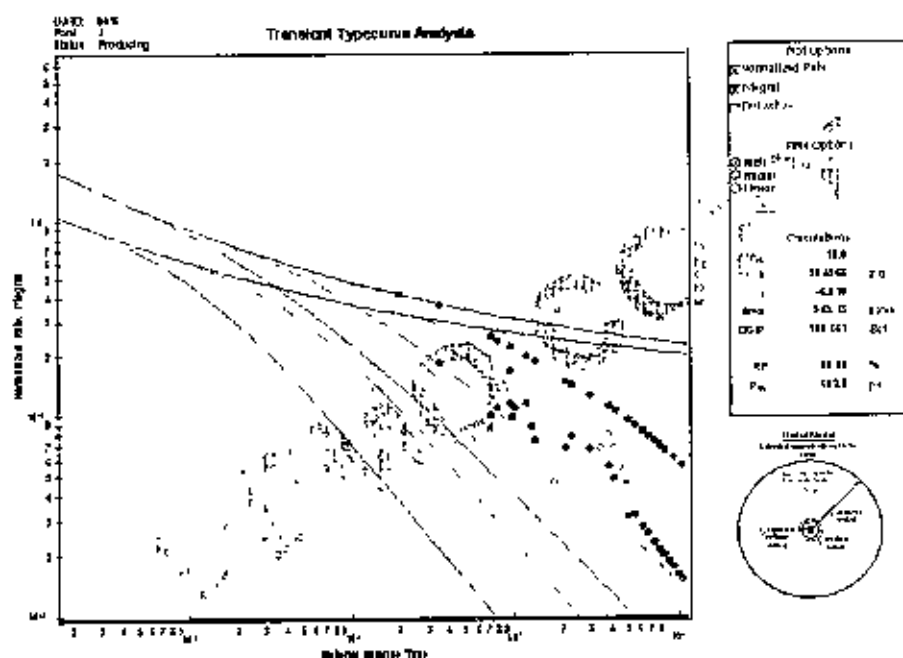


Fig 6.44 Transient Typecurve Analysis of BK8 at J Sand

Due to the issue of non-uniqueness, analysis of production data is performed by simultaneous matching of multiple type curves (i.e. normalized rate and integral). Transient plots show good match for all wells in J Sand. In the following table summary of results of Transient analysis for the wells of J sand is presented:

Table 6.21 Summary of results of Transient analysis for all wells of J Sand:

Wells in J Sand	r _{eD}	OGIP bcf	Area acre	FUR bcf	k md	s
BK 1	7	215.2	639.39	179.113	87.2054	-7.2569
BK 6	12	86.159	755.46	68.927	14.6723	-6.80131
BK 7	18	110.39	345.69	88.312	2.3676	-6.00495
BK 8	18	105.181	349.13	84.145	10.4968	-6.0099

6.5.2 G Sand

There are 2 wells in G sand: BK3 and BK4. Transient typecurve analysis of individual wells of G Sand is given below:

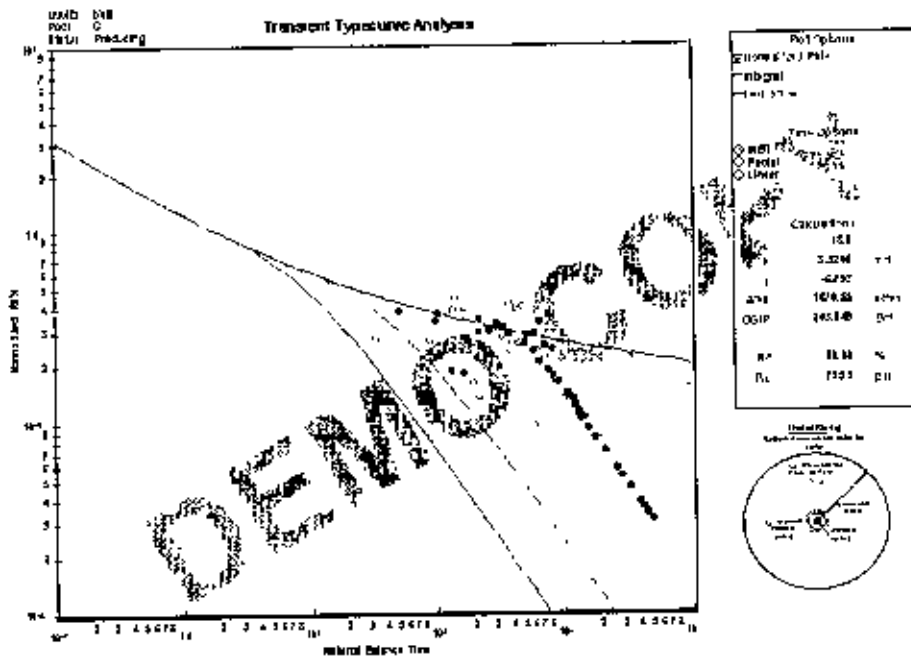


Fig 6.45 Transient Typecurve Analysis of BK3 at G Sand

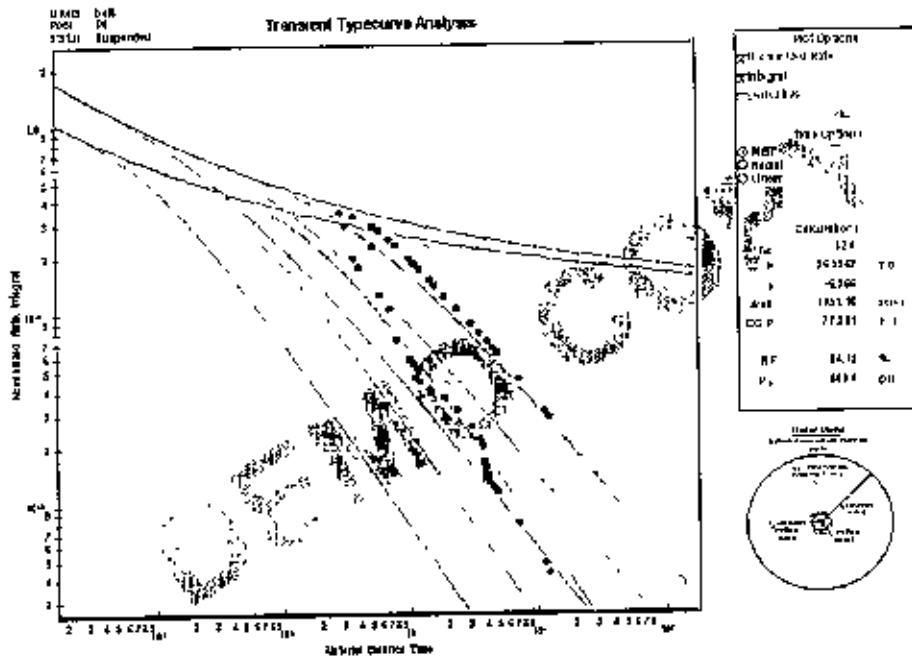


Fig 6.46 Transient Typecurve Analysis of BK4 at G Sand

The type curve data being very noisy and difficult to interpret, type curve "Data Filter" is used here for better matching. Transient plots show good match for all wells in G Sand. In

the following table summary of results of Transient analysis for the wells of G sand is presented:

Table 6.22 Summary of results of Transient analysis for wells of G Sand:

Wells in G Sand	r_{cD}	OGIP bcf	Area acre	EUR bcf	k md	s
BK 3	18	203.849	1670.55	163.079	3.5205	-6.79264
BK 4G	12	77.361	1051.16	65.1	36.9542	-6.96647

6.5.3 DL Sand

There are 2 wells in DL sand: BK2 and BK5. Transient typecurve analysis of individual wells of DL Sand is given below:

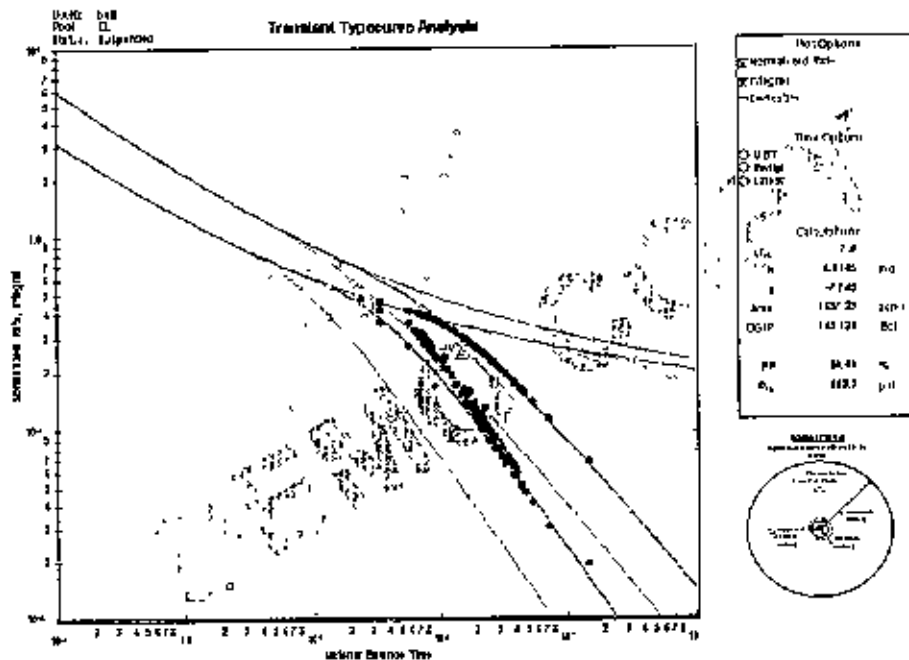


Fig 6.47 Transient Typecurve Analysis of BK2 at DL Sand

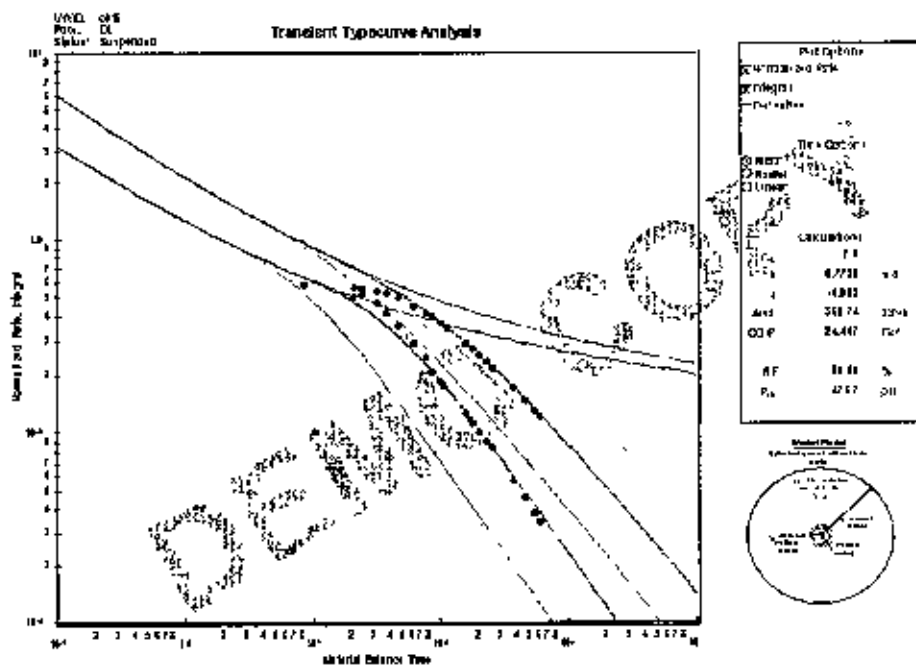


Fig 6.48 Transient Typecurve Analysis of BK5 at DL Sand

The type curve data being very noisy and difficult to interpret, type curve “Data Filter” is used here for better matching. Transient plots show good match for all wells in DL Sand. In the following table summary of results of Transient analysis for the wells of DL sand is presented:

Table 6.23 Summary of results of Transient analysis for wells of DL Sand:

Wells in DL Sand	r_{ef}	OGIP bcf	Area acre	EUR bcf	k md	s
BK 2	7	149.128	1697.23	119.302	4.0145	-7.74502
BK 5	7	24.407	368.74	19.526	6.7728	-6.98169

6.5.4 DU Sand

There is only one well in DU sand: BK4. Transient typecurve analysis of this well of DU Sand is given bellow:

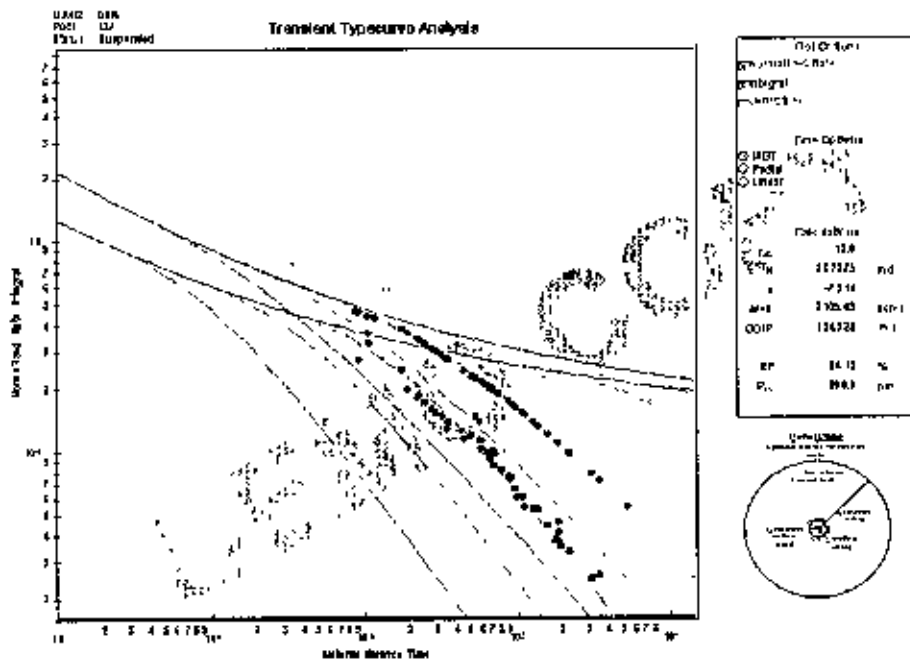


Fig 6.49 Transient Typecurve Analysis of BK4 at DU Sand

Transient plots show good match for BK4 in DU Sand. In the following table summary of results of Transient analysis for the well BK4 of DU sand is presented:

Table 6.24 Summary of results of Transient analysis for well BK4 of DU Sand:

Wells in DU Sand	r_{eD}	OGIP bcf	Area acre	EUR bcf	k md	s
BK 4	12	154.928	2105.09	130.374	28.7375	-7.3137

6.5.5 B Sand

There is only one well in B Sand: BK5. Transient typecurve analysis of this well of B Sand is given bellow:

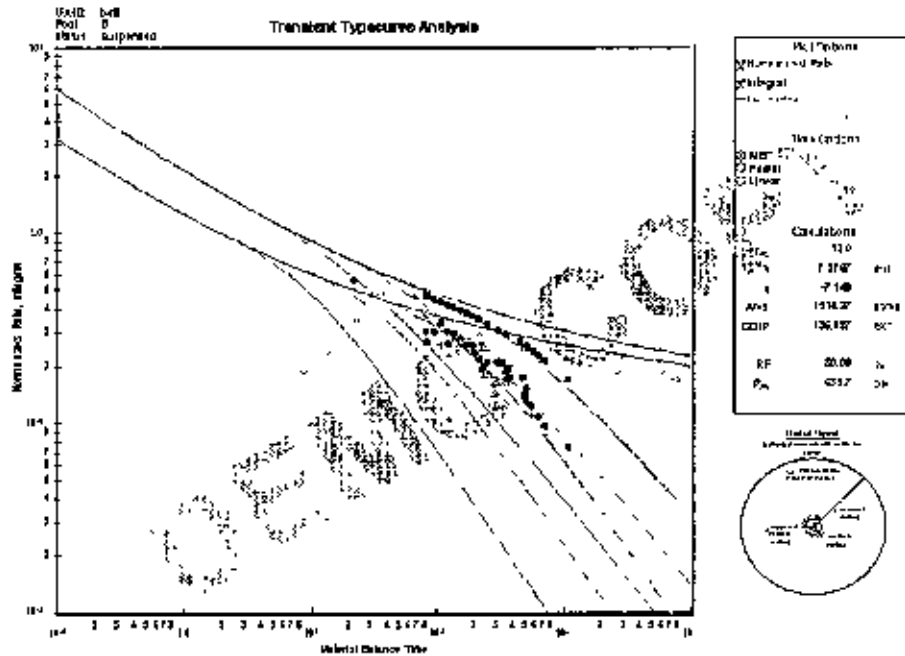


Fig 6.50 Transient Typecurve Analysis of BK5 at B Sand

Transient plots show good match for BK5 in B Sand. In the following table summary of results of Transient analysis for the well BK5 of B sand is presented:

Table 6.25 Summary of results of Transient analysis for well BK4 of B Sand:

Wells in B Sand	r_{eD}	OGIP bcf	Area acre	EUR bcf	k md	s
BK 5	12	136.037	1514.27	108.83	7.2767	-7.14899

All the type curve methods (except Fetkovich) showed extraordinary agreement between data and reservoir model (radial) for Bakhrabad Gas Field's different wells (both producing and suspended). AG. Balasingame, NPI and Transient typecurve methods yield similar values of skin (which is negative) and closer values of permeability of different wells. In the case of negative skin the effective wellbore radius is greater than the actual radius (due to stimulation results). This result complies with the sand production problems of Bakhrabad Gas Field. The dominant flow regimes for different wells are also determined excellently by these type curve methods and they firmly agree with the pressure versus rate diagnosis performed in Chapter 3. Gas in place values and EUR values of different wells are also very similar in different analysis for respective wells.

Chapter 7

NON -TYPECURVE ANALYSES

The non-typecurve methods are considered to be more suitable for quantitative analysis of reserves, because they are Cartesian plots (late-time data does not get compressed by the time scale). The fluid-in-place analysis is performed once the presence of boundary dominated flow is confirmed from the previous diagnostics.

7.1 Arps (Traditional) Decline Analysis

Arps decline analysis is easy and convenient to apply and does not require knowledge of pressure data or reservoir parameters. It provides production forecast and estimates the expected ultimate recovery (EUR) (at current operating conditions) using Arps decline curve theory. The semi-log rate versus time plot is used in conjunction with the linear rate versus cumulative production plot, which helps to ensure that periods of shut-in are not included as part of the decline.

According to F.A.S.T. RTA Technical Documentation (2005), there are some common Decline Analysis Concerns:

- If hyperbolic forecast is used, it is better to set the duration of the forecast (and thus the EUR) limiting no longer than 10 years, rather than setting an economic limit. This prevents unrealistically high estimates of EUR.
- It is better to be aware of the historical flowing pressure trend when forecasting production. If the trend shows steeply declining pressures, even the most conservative exponential decline will over-predict EUR.
- The 'b' values that exceed 1 should not be used to determine EUR, as it will cause unrealistic results.
- Exponential decline is consistent with the understanding of single-phase, boundary dominated flow, whereas hyperbolic decline is considered to be consistent with the performance of solution-gas drive reservoirs.

Using the following equations, the expected ultimate recovery (EUR), original gas in place (OGIP) and area can be calculated for a variety of situations in exponential decline.

$$EUR = Q_f + \frac{q_f - q_{ab}}{D} \quad \dots \quad \dots \quad (7.1)$$

$$q_f = q_1 e^{-D t_f} \quad \dots \quad \dots \quad (7.2)$$

$$G_f = \frac{EUR \times P_i Z_{wf}}{P_i Z_{wf} - P_{wf} Z_i} \text{ (bcf)} \quad \dots \quad \dots \quad (7.3)$$

$$A = \frac{Z_i T P_{sc} G_f}{\phi h S_g P_i T_{sc} (43560)} \text{ (acres)} \quad \dots \quad \dots \quad (7.4)$$

Where, the 'f' subscript denotes conditions at the beginning of the forecast period, and:

q_1 – initial rate. This is the starting rate of the period preceding the forecast

q_{ab} – abandonment rate

q_f – rate at the beginning of the forecast period

Q_f – cumulative production at the start of the forecast

D – decline rate

Sand-wise Arps Decline Analysis

In this section the results of Arps Decline analysis of different wells of J, G, DL, DU and B sands have been presented.

7.1.1 J Sand

There are 4 wells in J sand: BK1, BK6, BK7 and BK8. The Traditional page consists of two plots: Semilog Rate vs. Time and Rate vs. Cumulative Production. The left-hand side data table of each plot shows the decline (nominal decline “d” and exponential decline “D”) and output parameters (EUR- Expected Ultimate Recovery and RR- Remaining Reserves). When the wellbore flowing pressure is entered (P_{wf}), an OGIP is back calculated from the EUR. Arps Decline analysis of individual wells of J Sand is given bellow:

Well: AR0118	
Current	
Operator: O&A AR0118-1	
Analysis Interval:	
Type	Hydrocarbon
b	3.64
D	3.67
Q	7.42
Q _h	%
Start	05/01/2000
End	05/01/2001
Q	7.42
Q _h	0.00
End	05/01/2001
Q	7.42
Q _h	0.00
Factors:	
EUR	44.00
RR	33.00
PL	0.00
ARR	5.10
CCP	0.40
Production Interval:	
T ₀	05/01/2000
Q _h	0.00
N _h	0.00
W _h	0.00

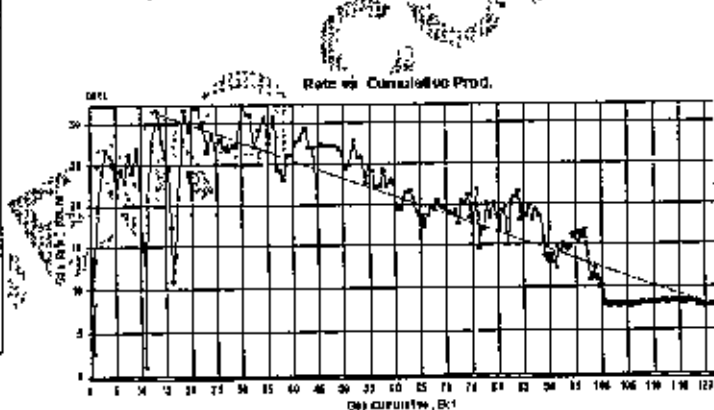
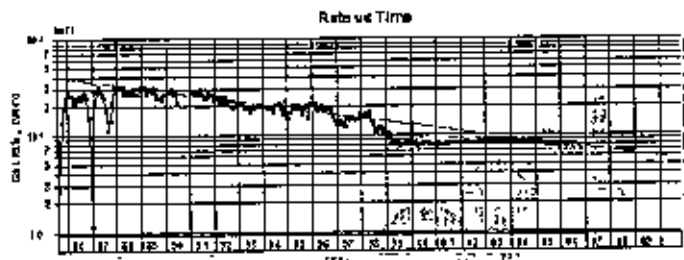


Fig 7.1 Arps Decline Analysis of BK1 at J Sand

Well: AR0118	
Current	
Operator: O&A AR0118-1	
Analysis Interval:	
Type	Hydrocarbon
b	0.00
D	0.00
Q	0.00
Q _h	%
Start	05/01/2000
End	05/01/2001
Q	0.00
Q _h	0.00
End	05/01/2001
Q	0.00
Q _h	0.00
Factors:	
EUR	44.00
RR	33.00
PL	0.00
ARR	5.10
CCP	0.40
Production Interval:	
T ₀	05/01/2000
Q _h	0.00
N _h	0.00
W _h	0.00

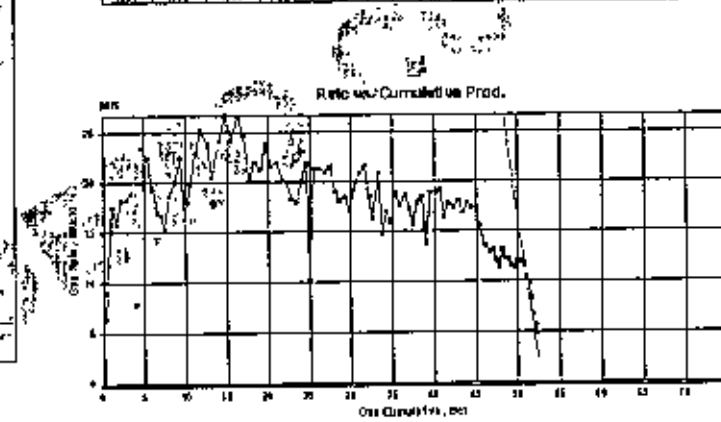
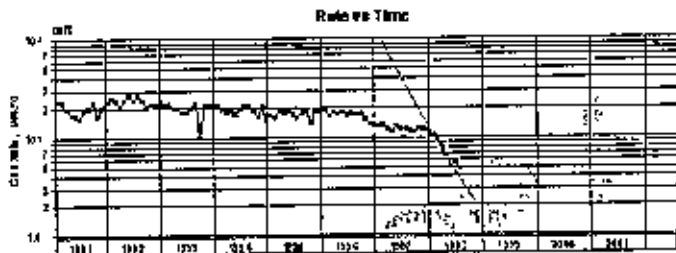


Fig 7.2 Arps Decline Analysis of BK6 at J Sand

Decline Analysis	
Current	Analysis: Gas Analysis 1
Analysis Parameters	
Type	Hyperbolic
b	0.027
D	1.964
L _h	41.91 %
D _h	%
Start	01/01/2000 01:00:00 AM
Q	14.000 MMSCFD
Q _h	7.2000 MMSCFD
End	01/01/2011 01:00:00 AM
Q ₁	3.000 MMSCFD
Q ₂	0.5000 MMSCFD
Results	
LGR	33.000 %
R.R.	24.000 %
P _h	400.00 %
API	146.21 %
COIP	110.000 %
Production History	
T ₁	01/01/2000 01:00:00 AM
Q ₁	14.000 MMSCFD
T ₂	01/01/2011 01:00:00 AM
Q ₂	0.5000 MMSCFD

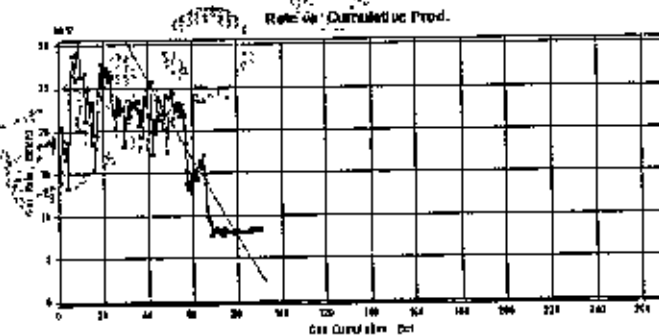
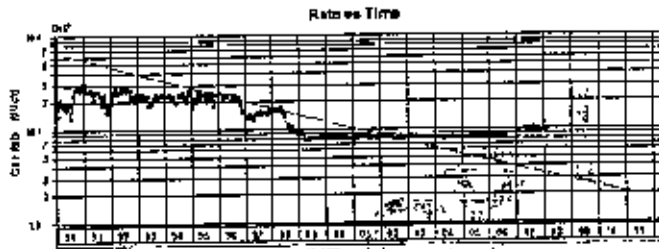


Fig 7.3 Arps Decline Analysis of BK7 at J Sand

Decline Analysis	
Current	Analysis: Gas Analysis 1
Analysis Parameters	
Type	Hyperbolic
b	0.791
D	4.117
L _h	17.94 %
D _h	%
Start	01/01/2000 01:00:00 AM
Q	7.200 MMSCFD
Q _h	41.174 MMSCFD
End	01/01/2011 01:00:00 AM
Q ₁	7.000 MMSCFD
Q ₂	16.000 MMSCFD
Results	
LGR	55.000 %
R.R.	60.000 %
P _h	100.00 %
API	200.00 %
COIP	100.000 %
Production History	
T ₁	01/01/2000 01:00:00 AM
Q ₁	7.200 MMSCFD
T ₂	01/01/2011 01:00:00 AM
Q ₂	16.000 MMSCFD

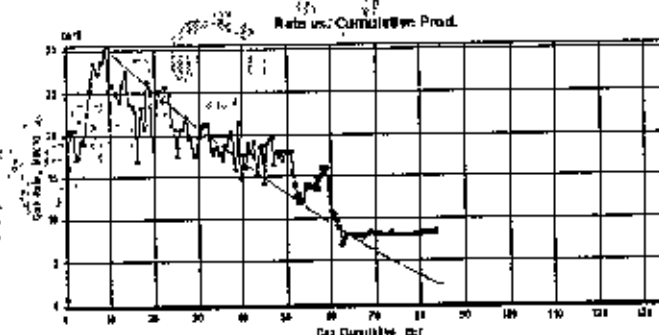


Fig 7.4 Arps Decline Analysis of BK8 at J Sand

All the wells of J Sand show hyperbolic type of decline in Arps Decline Analysis. But the hyperbolic exponent "b" is very close to zero value except well BK8. This kind of anomaly in results is probably due to the inclusion of restricted rate data at the end portion of

producing wells. In the following table summary of results of Arps analysis for all wells of J sand is presented:

Table 7.1 Summary of results of Arps analysis for all wells of J Sand:

Wells in J Sand	OGIP bcf	Area acre	EUR bcf	D_1	d_1 %	b
BK 1	174.977	519.88	149.188	0.077069	7.42	0.036032
BK 6	62.298	546.24	52.398	2.033206	86.91	0.063296
BK 7	110.556	346.21	92.986	0.164392	15.16	0.037
BK 8	102.263	339.44	85.037	0.117087	11.05	0.260864

7.1.2 G Sand

There are 2 wells in G sand: BK3 and BK4. Arps Decline analysis of individual wells of G Sand is given below:

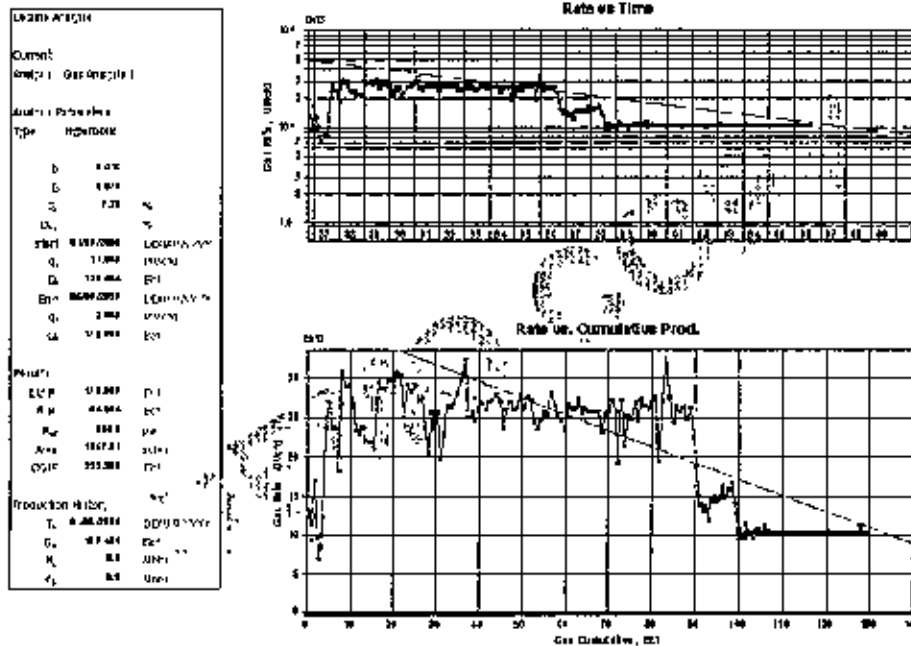


Fig 7.5 Arps Decline Analysis of BK3 at G Sand

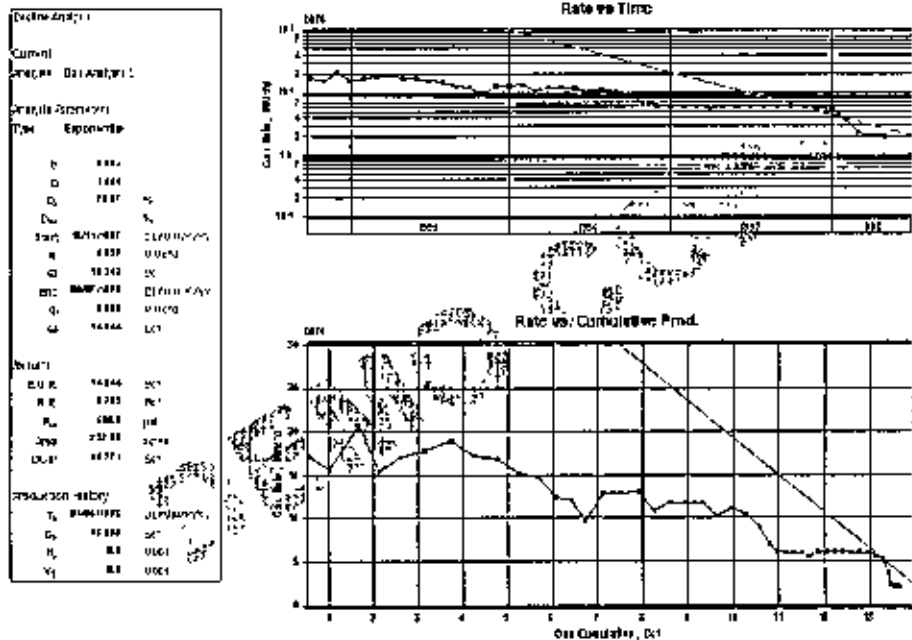


Fig 7.6 Arps Decline Analysis of BK4 at G Sand

In the following table summary of results of Arps analysis for the wells of G sand is presented:

Table 7.2 Summary of results of Arps analysis for wells of G Sand:

Wells in G Sand	OGIP bcf	Area acre	EUR bcf	D _i	d _i %	b
BK 3	202.233	1657.31	173.909	0.075046	7.23	0.0096
BK 4	16.771	227.88	14.044	1.554499	78.87	0

7.1.3 DL Sand

There are 2 wells in DL sand: BK2 and BK5. Arps Decline analysis of individual wells of DL Sand is given below:

Decline Analysis	
Current	
Analysis	Decline Analysis 1
Analysis Parameters	
Type	Exponent
D	0.334
D	0.333
U	0.667
Q _u	%
Start	1/18/2008
Q	3000
Q _u	3000
End	1/18/2008
Q	3000
Q _u	3000
Results	
EUR	11700
EUR	11700
P _u	6000
APIP	11700
OCIP	11700
Production Ratio	
T _u	1/18/2008
Q _u	3000
N _u	11700
N _u	11700

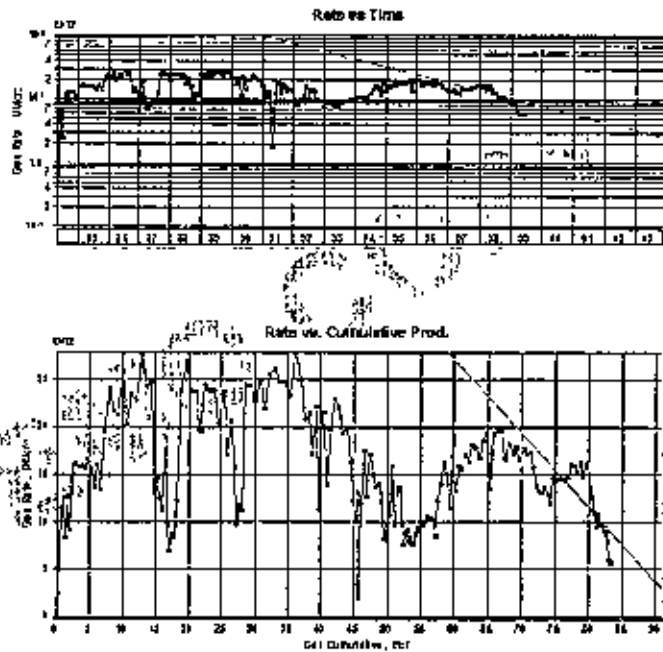


Fig 7.7 Arps Decline Analysis of BK2 at DL Sand

Decline Analysis	
Current	
Analysis	Decline Analysis 1
Analysis Parameters	
Type	Exponent
D	0.337
D	0.336
U	0.663
Q _u	%
Start	1/18/2008
Q	3000
Q _u	3000
End	1/18/2008
Q	3000
Q _u	3000
Results	
EUR	11700
EUR	11700
P _u	6000
APIP	11700
OCIP	11700
Production Ratio	
T _u	1/18/2008
Q _u	3000
N _u	11700
N _u	11700

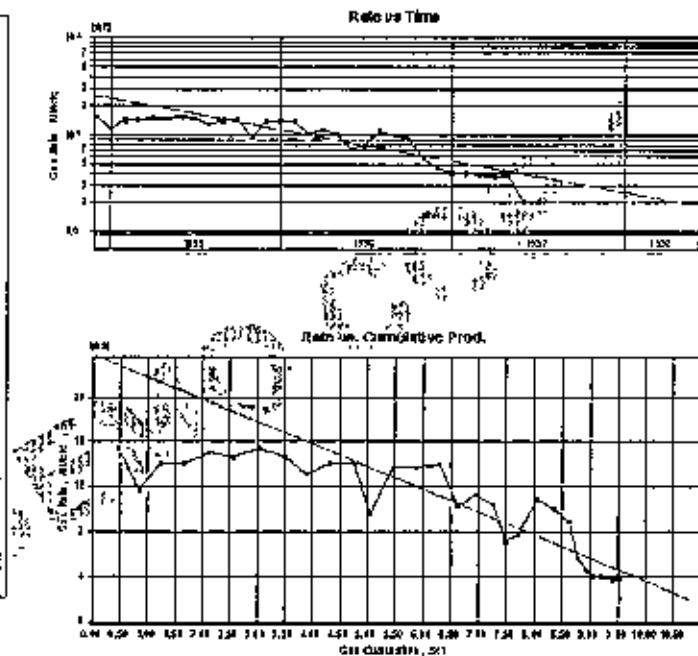


Fig 7.8 Arps Decline Analysis of BK5 at DL Sand

In the following table summary of results of Arps analysis for the wells of DL sand is presented:

Table 7.3 Summary of results of Arps analysis for wells of DL Sand:

Wells in DL Sand	OGIP bcf	Area acre	EUR bcf	D_1	d_1 %	b
BK 2	110.501	1257.62	93.289	0.286919	24.94	0
BK 5	13.72	207.28	10.794	0.742678	52.42	0

7.1.4 DU Sand

There is only one well in DU sand: BK4. Arps Decline analysis of this well of DU Sand is given below:

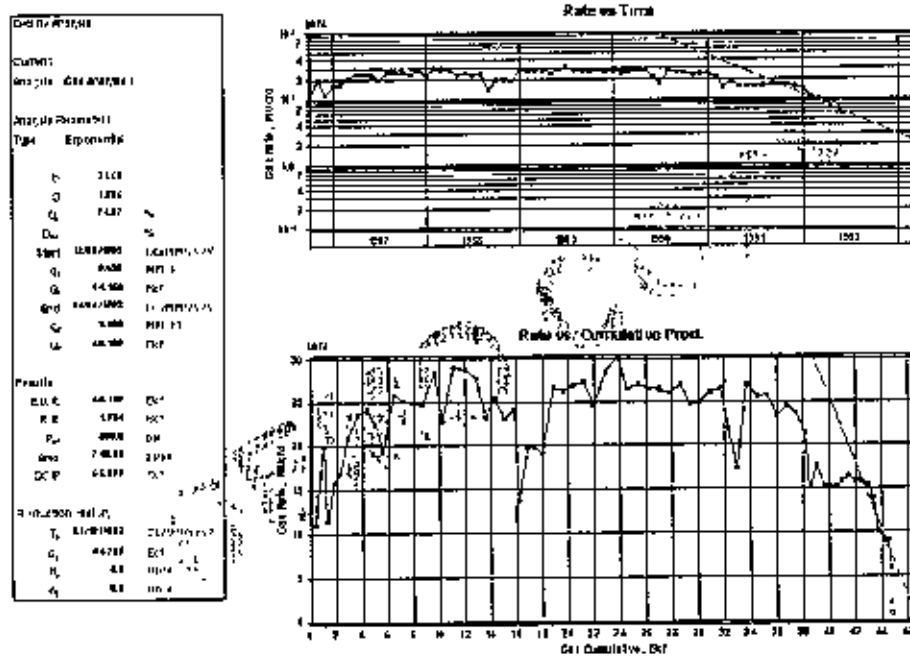


Fig 6.9 Arps Decline Analysis of BK4 at DU Sand

In the following table summary of results of Arps analysis for the well BK4 of DU sand is presented:

Table 7.4 Summary of results of Arps analysis for well BK4 of DU Sand:

Wells in DU Sand	OGIP bcf	Area acre	EUR bcf	D_1	d_1 %	b
BK 4	55.099	748.66	46.139	1.385232	74.97	0

7.1.5 B Sand

There is only one well in B Sand: BK5. Arps Decline analysis of this well of B Sand is given below:

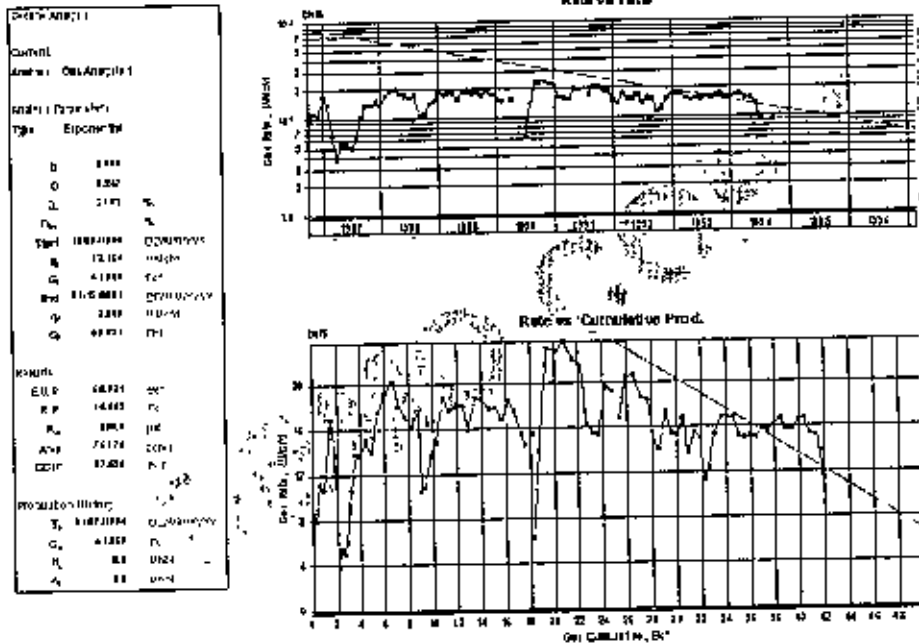


Fig 7.10 Arps Decline Analysis of BK5 at B Sand

In the following table summary of results of Arps analysis for the well BK5 of B sand is presented:

Table 7.5 Summary of results of Arps analysis for well BK4 of B Sand:

Wells in B Sand	OGIP bcf	Area acre	EUR bcf	D ₁	d ₁ %	b
BK 5	67.536	751.76	56.921	0.247386	21.92	0

7.2 Flowing Material Balance

The Flowing Material Balance (FMB) is a straightforward and intuitive method of production data analysis based on a modified version of the Agarwal-Gardner Rate-Cumulative typecurves and its functionality is similar to conventional gas material balance. The method is similar to a conventional material balance analysis, but requires no shut-in pressure data

(except initial reservoir pressure). Instead, it uses the concepts of pressure normalized rate and material balance (pseudo) time to create a simple linear plot, which extrapolates to fluids-in-place. This method is superior to typecurve methods for estimating fluids-in-place, because data are plotted on a linear scale. Late-time data on typecurves tend to be somewhat compressed, due to the logarithmic nature of the plot.

In FMB analysis procedure first Gas-in-place (OGIP) is estimated. Then pseudo-time (t_e) for gas wells is calculated using previous equation. Then the normalized cumulative production (Q_n) is calculated using the following equation:

$$Q_n = \frac{Q}{c_i \Delta p} \quad \dots \quad \dots \quad (7.5)$$

Then a plot of normalized rate ($q/\Delta p$) versus Q_n is constructed and best-fit line is extrapolated to get OGIP. New OGIP is used in the repeated procedure. Once convergence on OGIP is achieved, the EUR (based on a specified abandonment pressure) can be estimated using the following equation:

$$EUR = \frac{z_i}{P_i} \left(\frac{P_i}{z_i} - \frac{P_{ab}}{z_{ab}} \right) OGIP \quad \dots \quad \dots \quad (7.6)$$

This FMB can only be applied to reservoirs in depletion (similar to p/z plot).

Sand-wise Flowing Material Balance Analysis

In this section the results of FMB analysis of different wells of these sands have been presented.

7.2.1 J Sand

There are 4 wells in J sand: BK1, BK6, BK7 and BK8. Unlike other analysis, AG FMB is not a type curve analysis. Rather, its functionality is similar to both the Arps Rate versus Cumulative Production analysis and the P/Z versus Cumulative Production (conventional gas material balance) plot. The x-axis of the graph is "Normalized Cumulative Production" and the y-axis is "Normalized Rate". An alternative, or compliment to the AG FMB, is the flowing P/Z plot. When the AG FMB and Flowing P/Z analyses are displayed simultaneously, the AG FMB plot is dominant (it is the active analysis and the p/z simply responds to its position). FMB analysis of individual wells of J Sand is given bellow:

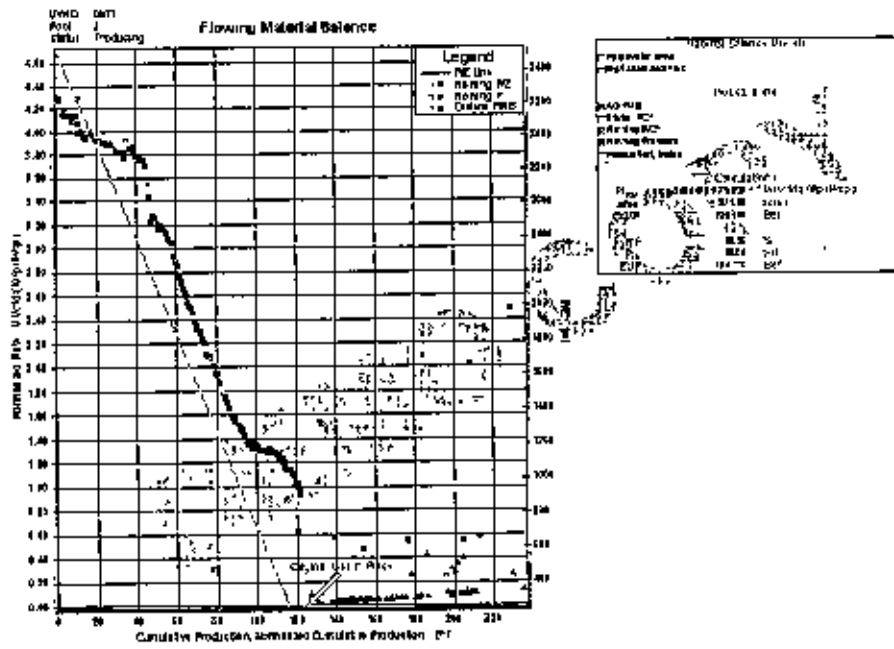


Fig 7.11 FMB Analysis of BK1 at J Sand

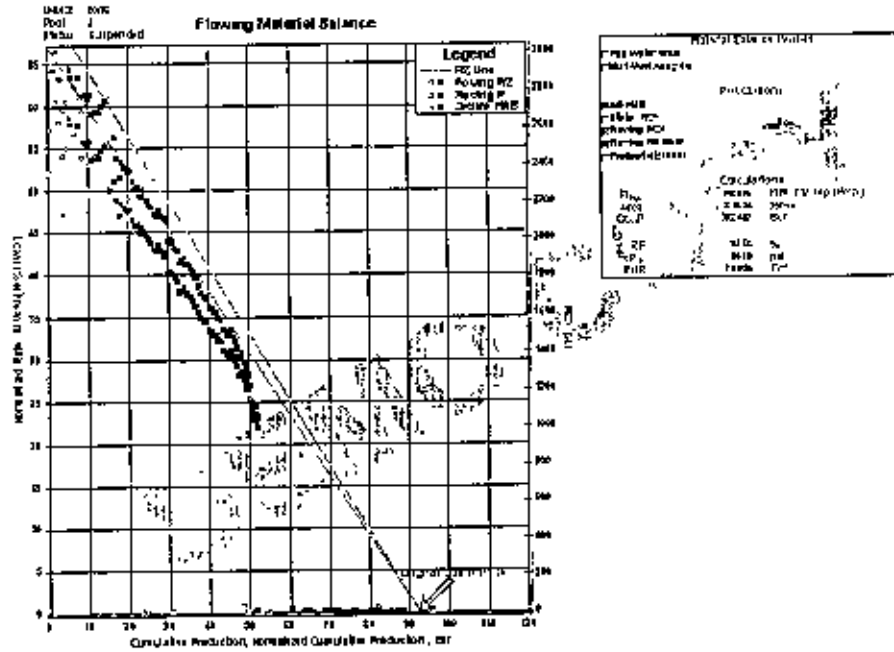


Fig 7.12 FMB Analysis of BK6 at J Sand

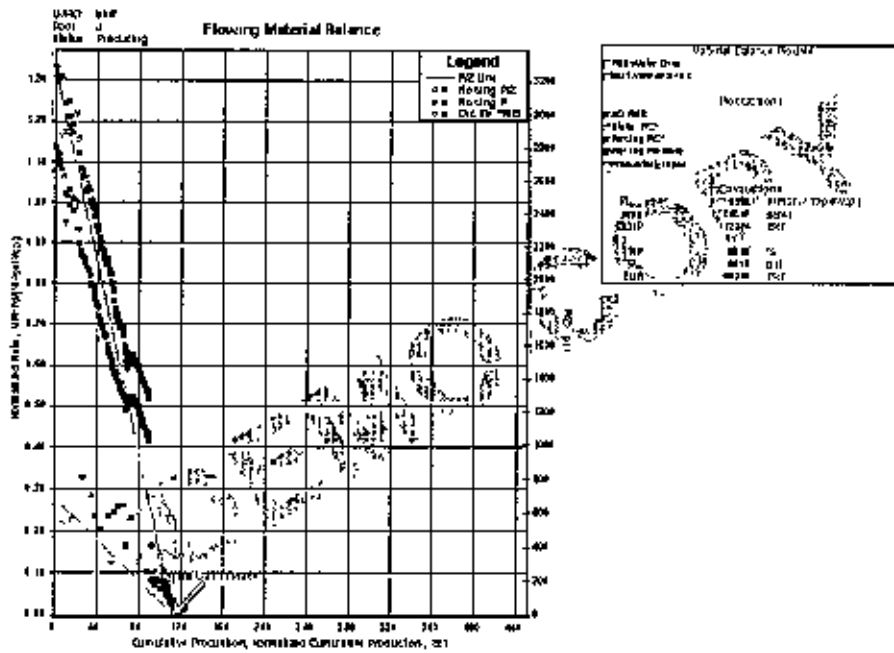


Fig 7.13 FMB Analysis of BK7 at J Sand

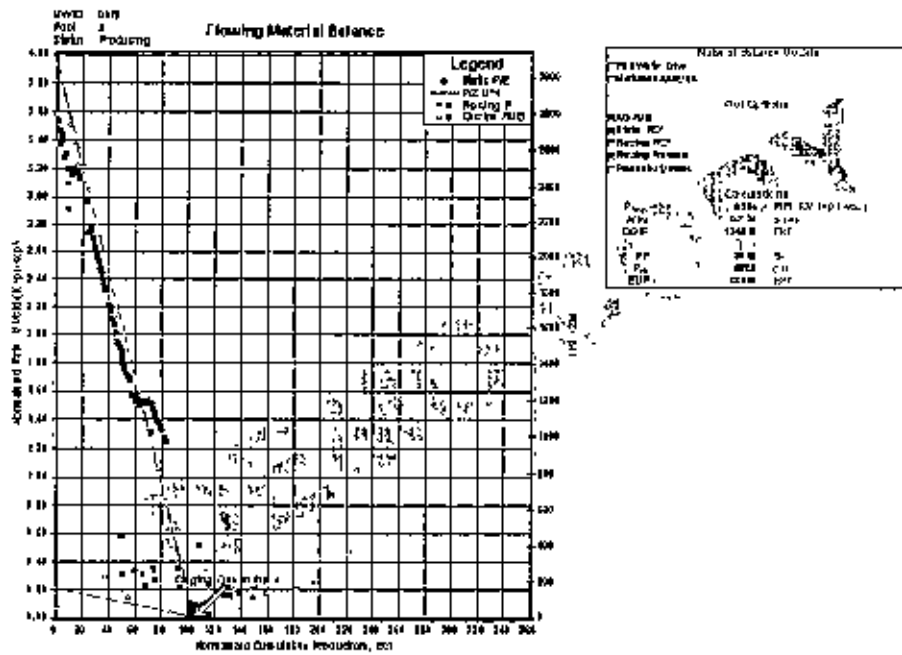


Fig 7.14 FMB Analysis of BK8 at J Sand

Table 7.6 Summary of results of FMB analysis for all wells of J Sand:

Wells in J Sand	OGIP bcf	Area acre	EUR bcf
BK 1	125.158	371.86	104.17
BK 6	92.407	810.24	73.925
BK 7	112.874	353.47	90.299
BK 8	104.615	347.25	83.692

7.2.2 G Sand

There are 2 wells in G sand: BK3 and BK4. FMB analysis of individual wells of G Sand is given below:

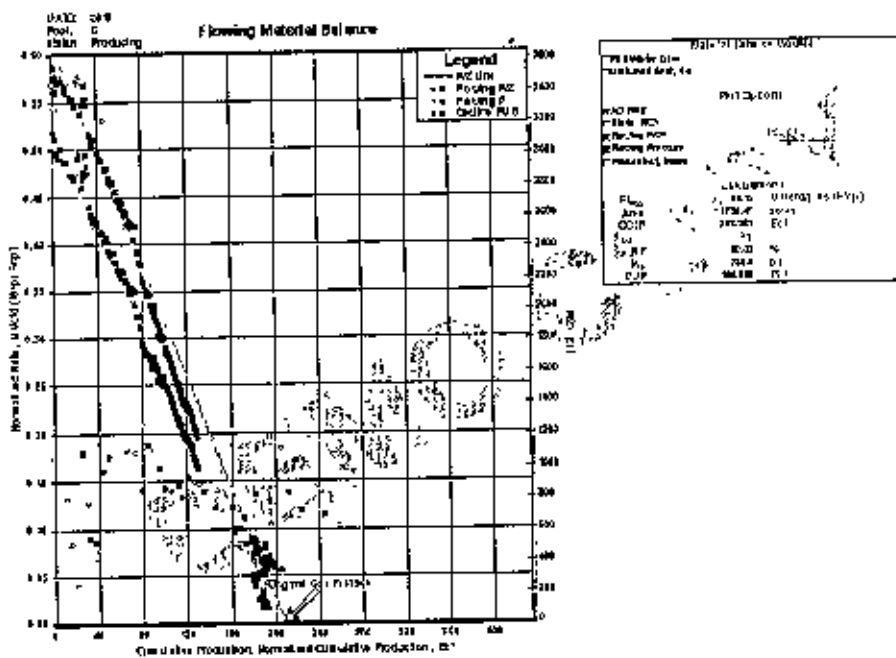


Fig 7.15 FMB Analysis of BK3 at G Sand

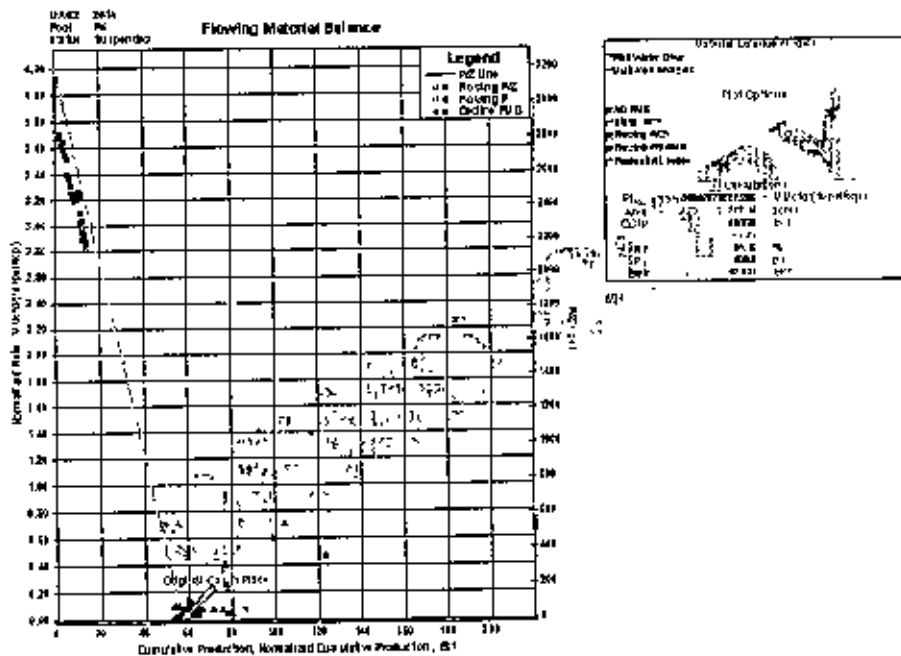


Fig 7.16 FMB Analysis of BK4 at G Sand

In the following table summary of results of FMB analysis for the wells of G sand is presented:

Table 7.7 Summary of results of FMB analysis for wells of G Sand:

Wells in G Sand	OGIP bcf	Area acre	EUR bcf
BK 3	208.231	1706.47	166.585
BK 4	56.828	772.16	47.821

7.2.3 DL Sand

There are 2 wells in DL sand: BK2 and BK5. FMB analysis of individual wells of DL Sand is given below:

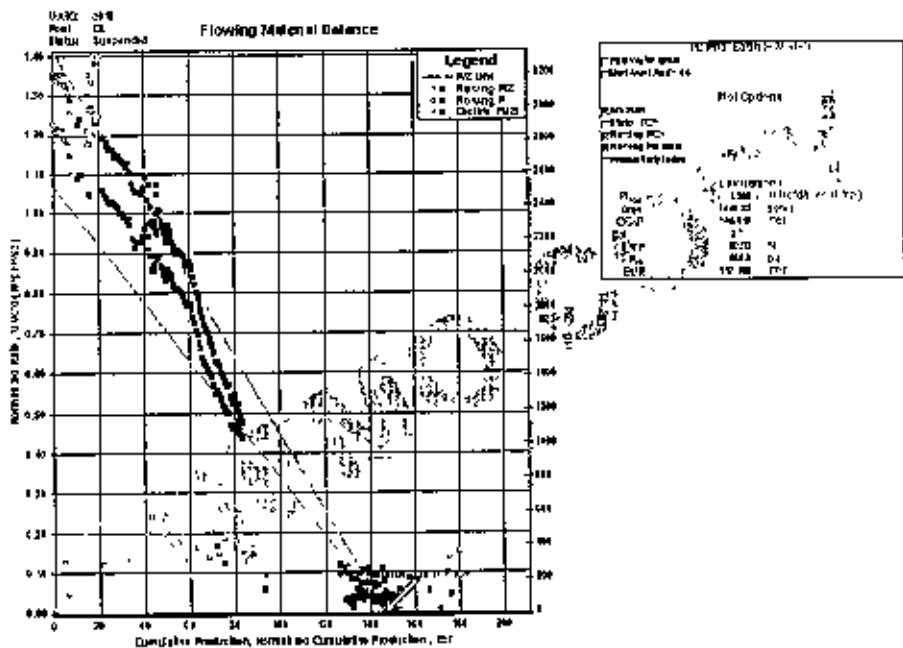


Fig 7.17 FMB Analysis of BK2 at DL Sand

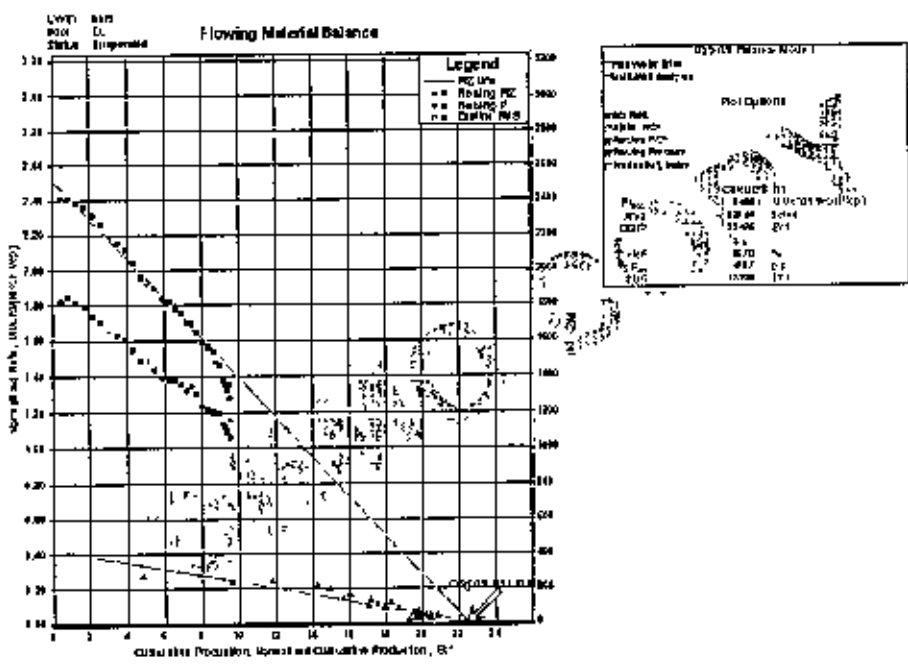


Fig 7.18 FMB Analysis of BK5 at DL Sand

In the following table summary of results of FMB analysis for the wells of DL sand is presented:

Table 7.8 Summary of results of FMB analysis for wells of DL Sand:

Wells in DL Sand	OGIP bcf	Area acre	EUR bcf
BK 2	146.413	1666.32	117.13
BK 5	22.475	339.54	17.98

7.2.4 DU Sand

There is only one well in DU sand: BK4. FMB analysis of this well of DU Sand is given below:

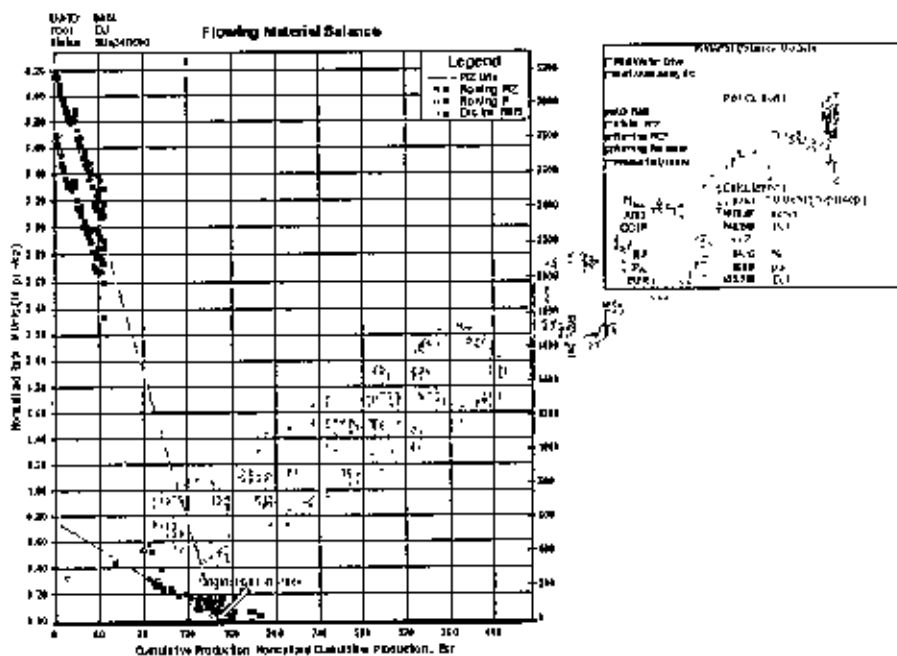


Fig 7.19 FMB Analysis of BK4 at DU Sand

In the following table summary of results of FMB analysis for the well BK4 of DU sand is presented:

Table 7.9 Summary of results of FMB analysis for well BK4 of DU Sand:

Wells in DU Sand	OGIP bcf	Area acre	EUR bcf
BK 4	145.249	1973.57	122.229

7.2.5 B Sand

There is only one well in B Sand: BK5. FMB analysis of this well of B Sand is given below:

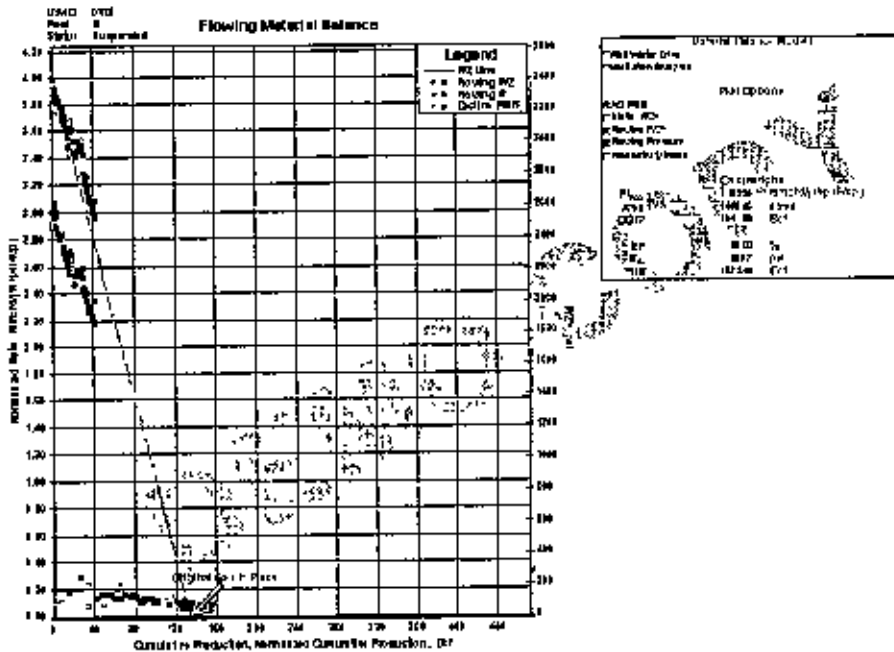


Fig 6.20 FMB Analysis of BK5 at B Sand

In the following table summary of results of FMB analysis for the well BK5 of B sand is presented:

Table 7.10 Summary of results of FMB analysis for well BK4 of B Sand:

Wells in B Sand	OGIP bcf	Area acre	EUR bcf
BK 5	134.18	1493.6	107,344

Non-typecurve methods (traditional and FMB) provide quantitative analysis of reserves of different sands of Bakhrabad Gas Field. Arps (traditional) analysis firmly comply with the decline diagnosis of chapter 4 and justifies exponential decline type production of the wells of different sands. FMB also fully agrees with the AWMB analysis and confirmed volumetric drive mechanism in wells of different sands. The use of traditional decline analysis in concert with the FMB provides an excellent indicator of whether historical and current production conditions are sufficient for the well to attain optimum recovery of gas in place.

A systematic approach to production data analysis using the best methods available enables one to obtain a full picture of the reserve. In the following table comparison of gas in place (bcf) of different sands of Bakhrabad Gas Field using typecurve, non-typecurve and AWMB methods are presented:

Table 7.11 Comparison of gas in place (bcf) of different sands of Bakhrabad Gas Field using typecurve, non-typecurve and AWMB methods:

Sands	Typecurve methods					Typecurveless methods		AWMB
	AG	Blasingame	Fetkovich	NPI	TRANSIENT	ARPS	FMB	
J	487.918	527.003	573.212	499.161	516.93	450.094	435.054	452
G	269.238	280.811	222	269.04	281.21	219.004	265.059	218
DL	159.247	163.825	144.619	181.655	173.535	124.221	168.888	144.7
DU	153.119	152.867	60.97	151.527	154.928	55.099	145.249	130
B	140.85	135.082	107.466	136.452	136.037	67.536	134.18	115
Total	1210.372	1259.588	1108.267	1237.835	1262.64	915.954	1148.43	1059.7

In this study several modern decline curve methods and material balance methods are presented for estimating the original gas in-place using flowing data (pressure and production). Up to August 2006, cumulative production of Bakhrabad Gas Field was 670.073 bcf and an abandonment pressure of 600 psia was assumed in different analysis procedure, as there is compression facility in this field. From the above table, based on Transient typecurve method, highest gas in place estimate is 1262.64 bcf, which yields a recovery of 53.07% for the field, whereas based on traditional decline analysis, lowest gas in place estimate is 915.954 bcf, which yields a recovery of 73.15% for Bakhrabad Gas Field. Gas in place value estimated using AWMB method is 1059.7 bcf, which yields a recovery of 63.23% for Bakhrabad.

Chapter 8

CONCLUSIONS AND RECOMMENDATIONS

8.1 Conclusions

Following conclusions are made based on the findings of this study:

1. Pressure versus rate diagnostic plot successfully discerns reservoir flow behavior with approximate duration of flow regimes for the wells of different sands of Bakhrabad Gas Field. It is found that Infinite Acting flow period existed for a time in all producing sands. Presently PSS flow regime is predominant in the producing sands. Current production behavior of Bakhrabad gas field is boundary dominated, which indicates Bakhrabad to be a mature field.
2. Multiple wells in the same sand exhibited the same slope on the pressure-rate ($p-q$) plot; suggesting reservoir connectivity. Therefore there is no compartment in the major sands of Bakhrabad Gas Field.
3. From decline analysis, a sharp exponential decline is noticed at the end of the production profiles of all the wells. This is common for both producing wells (before rate restriction) and for suspended wells (before suspension). This is an indication of gas wells undergoing liquid loading- a common phenomenon at the final stage of production of mature gas fields.
4. AWMB method reconfirms the recovery mechanism is volumetric depletion and no evidence of aquifer support exists in this field. Later portion of deflection from straight line in this method probably indicate liquid loading phenomena. It is possible that water is intruding from any upper wet strata, which may happen due to poor cement.
5. Type curve analysis methods showed good agreement between data and reservoir radial model for this field. They also reveal negative skin effect in all wells, which complies with the sand production problem of this field. It suggests the presence of large cavities around the wellbore.
6. The Gas Initially in Place (GIIP) value of this field obtained by different methods ranges from 915.954 BCF to 1262.64 BCF, with the most likely value being 1200

BCF. These values compare well with the previously reported values based on volumetric method, which ranges from 1281 to 1392 BCF.

7. Based on an abandonment pressure of 600 psia, ultimate gas recovery from the Bakhrabad Gas Field ranges from 53 to 73 percent of the initial gas-in-place for the major sands.

8.2 Recommendations

Following recommendations are made from the findings of this study:

1. The systematic approach of reserve estimation procedure showed in this study can be applied to other gas fields of Bangladesh.
2. To be certain about liquid loading problem and to prevent it for suspended wells having such problem, cement evaluation of the wells, especially of the suspended wells may be undertaken.
3. Using the range of GIIP values of different methods of this study, production forecasting can be generated using numerical or analytical models.

REFERENCES

Agarwal, R.G.(1979): "Real Gas Pseudo-Time — A New Function for Pressure Buildup Analysis of MHF Gas Wells", paper SPE 8279, presented at the SPE Annual Technical Conference and Exhibition, Las Vegas, NV, Sept. 23-26.

Agarwal, R.G., Gardner, D.C., Kleinstieber, S.W. and Fussell, D.D.(1998): "Analyzing Well Production Data Using Combined-Type-Curve and Decline-Curve Analysis Concepts", paper 57916, presented at the SPE Annual Technical Conference and Exhibition, New Orleans Sept.27-30.

Agarwal, R.G., Gardner, D.C., Kleinstieber, S.W., and Fussell, D.D. (1999): "Analyzing Well Production Data Using Combined-Type-Curve and Decline-Curve Analysis Concepts", paper SPE 57916, SPEREE 2(5): 478-486.

Al-Hussainy, R., Ramey, H.J., Jr., and Crawford, P.B. (1966): "The Flow of Real Gases Through Porous Media", *JPT* (May 1966) 30-42.

Anderson, D. and Mattar, L. (2004): "Practical Diagnostics Using Production Data and Flowing Pressures", paper SPE 89939, presented at SPE Annual Technical Conference and Exhibition, Houston, Texas, U.S.A., September 26-29.

Arps, J.J. (1945): "Analysis of Decline Curves", *Trans*, AIME 160,228.

Blasingame, T.A and Lee, W.J. (1986): "Variable -Rate Reservoir Limits Testing", paper SPE 15028, prepared for presentation at the SPE Permian Basin Oil and Gas Recovery Conference, Midland, Texas, March 13-14.

Blasingame, T.A., Johnston, J.L., and Lee, W.J. (1989): "Type Curve Analysis Using the Pressure Integral Method", paper SPE 18799, prepared for presentation at the SPE California Regional Meeting, Bakersfield, CA, April 5-7.

Blasingame, T.A., McCray, T.L., and Lee, W.J. (1991): "Decline Curve Analysis for Variable Pressure Drop/Variable Flow Rate Systems", paper SPE 21513, prepared for presentation at the SPE Gas Technology Symposium, Houston, Texas, January 22-23.

Callard, J.G. and Schenewerk, P.A.(1995): "Reservoir Performance History Matching Using Rate/ Cumulative Type Curves", paper SPE 30793, presented at the SPE Annual Technical Conference and Exhibition, Dallas, TX, Oct. 22-25

Carter, R.D. (1985): "Type Curves for Finite Radial and Linear Gas Flow Systems: Constant-Terminal Pressure Case", *SPEJ* (Oct. 1985) 116-121.

Choudhury, Z. (1999): "Reservoir Engineering Study of Bakhrabad Gas Field", M.Sc. thesis, DPMRE, BUET.

Dietz, D.N., (1965): "Determination of Average Reservoir Pressure From Build-Up Surveys", *JPT* 27(8): 955-959; *Trans., AIME*, 234.

Doublet, L.E., Pande, P.K., McCollum, T.J and Blasingame, T.A.(1994): "Decline Curve Analysis Using Type Curves – Analysis of Well Production Data Using Material Balance Time: Application to Field Cases", paper SPE 28688, presented at the Petroleum Conference and Exhibition, Veracruz, Mexico, Oct. 10-13.

Earlougher, R.C., Jr. (1977): "Advances in Well Test Analysis". SPE Monograph Series, 5, 31, Richardson, TX.

F.A.S.T. RTA Technical Documentation, December 2005, Fekete Associates Inc., 54⁰ – 5th Avenue S.W. Calgary, Alberta, Canada.

Fetkovich, M.J. (1980): "Decline Curve Analysis Using Type Curves", JPT (June) 1065.

Fetkovich, M.J., Fetkovich, E.J., and Fetkovich, M.D. (1994): "Useful Concepts for Decline Curve Forecasting, Reserve Estimation, and Analysis", paper SPE 28628, presented at the Petroleum Conference and Exhibition, New Orleans, LA, U.S.A., Sep. 25-28.

Frain, M.L. and Wattenbarger, R.A. (1987): "Gas Reservoir Decline Curve Analysis Using Type Curves with Real-Gas Pseudopressure and Normalized Time", *SPEFE* (Dec. 1987) 671-682; *Trans. AIME*, 290.

Havlena, D. and Odeh, A.S. (1963): "The Material Balance as an Equation of a Straight Line", *Journal of Petroleum Technology (JPT)*, August 1963.

Ikoku, Chi U.: *Natural Gas Reservoir Engineering*, Krieger Publishing Company, Krieger Drive, Malabar, Florida (1992).

Intercomp-Kanata Management Ltd. (IKM) (1990B): "Gas Field Appraisal Project, Reservoir Engineering Report, Bakhrabad Gas Field, Bangladesh", Canadian International Development Agency (CIDA) & Bangladesh Oil, Gas and Minerals Corporation (BOGMC) report.

Jordan, C.L., Fenniak, M.J., and Smith, C.R. (2006): "Case Studies: A Practical Approach to Gas-Production Analysis and Forecasting", paper SPE 99351, presented at the SPE Gas Technology Symposium, Calgary, Alberta, Canada, May 15-17.

Kabir, C.S., Izgec, B. (2006): "Diagnosis of Reservoir Behavior From Measured Pressure/Rate Data", paper SPE 100384, presented at the SPE Gas Technology Symposium, Calgary, Alberta, Canada, May 15-17.

Lee, W.J., and Wattenbarger, R.A.(1996).: *Gas Reservoir Engineering, SPE Textbook Series*, Dallas, Volume 5, 1996, 214-229.

Lewis, J.O., and Beal, C.H. (1918): "Some New Methods for Estimating the Future Productions of Oil Wells", *Trans. AIME* 59, 492-525.

Mattar, L., and McNeil, R. (1997): "The 'Flowing' Gas Material Balance", *J. Can. Pet. Tech.* () 52.

Marhaendrajana, T. (2000): "Modeling and Analysis of Flow Behavior in Single and Multiwell Bounded Reservoirs", PhD Dissertation, Texas A&M University, College Station, Texas.

Marhaendrajana, T., and Blasingame, T.A. (2001): "Decline Curve Analysis Using Type Curve – Evaluation of Well Performance Behavior in a Multiwell Reservoir System", paper SPE 71517, presented at SPE Annual Technical Conference and Exhibition, New Orleans, Louisiana, U.S.A., September 30- October 3.

Marhaendrajana, T. (2005): "A Novel Approach for the Evaluation of Oil and Gas Well Performances in Multiwell Reservoir Systems", paper SPE 93222, prepared for presentation at the SPE Asia Pacific Oil and Gas Conference and Exhibition, Jakarta, Indonesia, April 5-7.

Onur, M. and Serra, K.V. (1988): "Analysis of Pressure-Buildup Data from a Well in a Multiwell System", paper SPE 18123, prepared for presentation at the SPE Annual Technical Conference and Exhibition, Houston, Texas, October 2-5.

Palacio, J.C. and Blasingame, T.A.(1993): "Decline Curve Analysis Using Type Curves: Analysis of Gas Well Production Data", paper SPE 25909, presented at the

SPE Rocky Mountain Regional/Low Permeability Reservoirs Symposium, Denver, CO. April 12-14.

Rodriguez, F. and Cinco-Ley, H. (1993): "A New Model for Production Decline", paper SPE 25480, prepared for presentation at the SPE Production Operations Symposium, Oklahoma City, OK, March 21-23.

Schilthuis, R.J. (1936): "Active Oil and Reservoir Energy", *Trans.*, AIME 118, 33-52.

Sullivan, S.A., Poston, S.W. and Piper, L.D. (1998): "Using Short-Term Pressure Buildup Tests for Gas Reserve Estimation in Tight Gas Reservoirs", paper SPE 17707, presented at the SPE Gas Technology Symposium, Dallas, TX, June 13-15.

Welldrill (UK) Ltd. (1990): "Reserve Report on the Bakhrabad Gas Field."

APPENDIX A

Derivation of p-q Slope for different Flow Regime

AI Multi rate Superposition Equation

Real reservoir systems usually have several wells operating at varying rates. The diffusivity equation, which is a combination of 1) the law of conservation of mass, 2) an equation of state, and 3) Darcy's law; when expressed in radial co ordinates, is linear.

$$\frac{\partial^2 P}{\partial r^2} + \frac{1}{r} \frac{\partial p}{\partial r} = \frac{1}{0.0002637} \frac{\phi \mu c_v}{k} \frac{\partial p}{\partial t} \quad \dots \quad \dots \quad (A1.1)$$

Multiple rate and multiple-well problems can be considered by applying the principle of superposition. The mathematical basis for this technique is explained by Van Everdingen and Hurst, Collins & others.

The superposition principle states that adding solutions to a linear differential equation results in a new solution to that differential equation, but for different boundary conditions.

$$p_i - p(t, r) = 141.2 \frac{q B \mu}{k h} [p_D(t_D, r_D, C_D, geometry, \dots) + s] \quad \dots \quad \dots \quad (A1.2)$$

Equation (A1.2) is a solution of Equation (A1.1) for a single well producing at constant rate q.

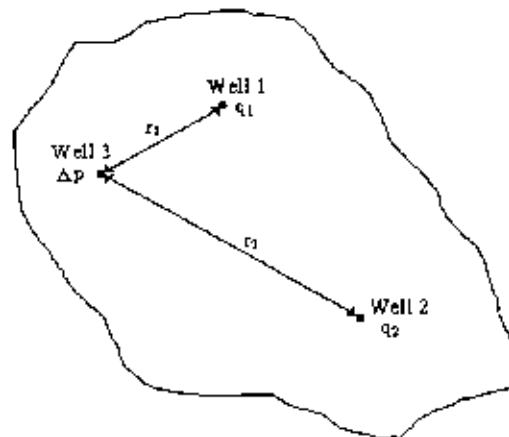


Fig.A1.1: Multiple-well infinite system for superposition explanation.

To illustrate the principle of superposition in space, consider the three-well infinite system in Fig.A1.1. At $t = 0$, Well 1 starts producing at rate q_1 , and Well 2 starts producing at rate q_2 . It is needed to estimate the pressure at the shut-in observation point, Well 3. To do this, it is needed to add the pressure change at Well 3 caused by Well 1 to the pressure change at Well 3 caused by Well 2:

$$\Delta p_3 = \Delta p_{3,1} + \Delta p_{3,2} \quad \dots \quad \dots \quad (A1.3)$$

To use Eq. (A1.3), we must substitute Eq.(A1.2) for Δp . Then, extending to an arbitrary number of wells, $j = 1, 2, \dots, n$,

$$\Delta p(t, r) = \frac{141.2\mu}{kh} \sum_{j=1}^n q_j B_j p_D(t_D, r_{Dj}), \quad \dots \quad \dots \quad (A1.4)$$

where, r_{Dj} is the dimensionless distance from Well j to the point of interest.

It is noted that Eq.(A1.3) and (A1.4) add pressure changes (or dimensionless pressure), not pressures. If the point of interest is an operating well, the skin factor must be added to the dimensionless pressure for that well only.

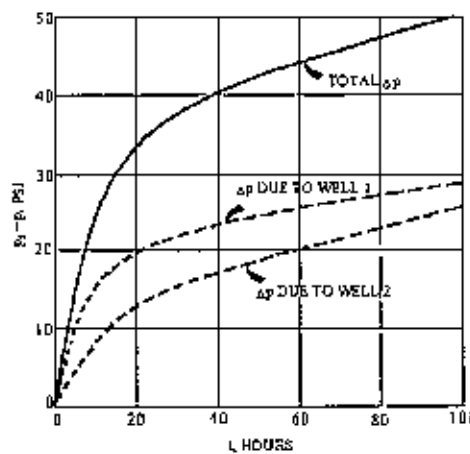


Fig.A1.2: Calculation of pressure change at observation well of Fig: A1.1 for superposition.

Fig.A1.2 graphically illustrates the use of Eq.(A1.3) and (A1.4) for the system of Fig.A1.1 and the exponential integral p_D .

$$p_D(t_D, r_D) = -\frac{1}{2} Ei\left(\frac{-r_D^2}{4t_D}\right) \quad \dots \quad \dots \quad (A1.5a)$$

$$\approx \frac{1}{2} [\ln(t_D / r_D^2) + 0.80907] \quad \dots \quad \dots \quad (A1.5b)$$

Eq.(A1.5b) may be used when $t_D / r_D^2 > 100$

The exponential integral is defined by

$$Ei(-x) = - \int_x^{\infty} \frac{e^{-u}}{u} du \quad \dots \quad \dots \quad (A1.6a)$$

$$Ei(-x) \approx \ln(x) + 0.5772 \text{ for } x < 0.0025 \quad \dots \quad \dots \quad (A1.6b)$$

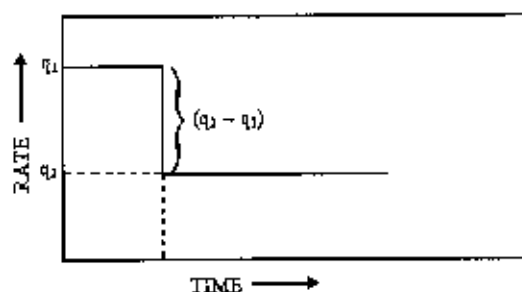


Fig.A1.3: Variable rate schedule for superposition explanation.

To illustrate an application of the principle of superposition to varying flow rates, it is considered a single-well system with the production-rate schedule shown in Fig.A1.3. The production rate is q_1 from $t = 0$ to t_1 and the second (imaginary) well producing at rate $(q_2 - q_1)$, starting at t_1 and continuing for a time period $(t - t_1)$. The net rate after time t_1 would be $q_1 + (q_2 - q_1) = q_2$. As before, Δp 's are added for these conditions. The general form of equation for N rates, with changes at $t_j, j = 1, 2, \dots, N$, is

$$\Delta p = \frac{141.2\mu}{kh} \sum_{j=1}^N \{ (q_j B_j - q_{j-1} B_{j-1}) [p_D ([t - t_{j-1}]_D) + s] \} \quad \dots \quad \dots \quad (A1.7)$$

In Eq.(A1.7), $[t - t_{j-1}]_D$ is the dimensionless time calculated at time $(t - t_1)$. For Fig.A1.3, $N = 2$ and only two terms of the summation are needed.

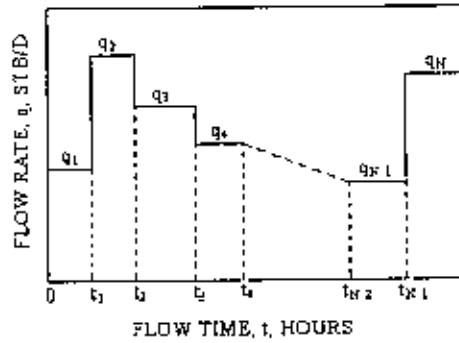


Fig.A1.4: Schematic representation of a variable production-rate schedule

Fig.A1.4 schematically shows a variable-rate history. In the nomenclature of that figure, production (or injection) starts at time 0, the rate remains constant at q_1 until time t_1 , then changes to q_2 until time t_2 etc. Rate q_i ends at time t_i and $t_0 = 0$. The last (and current) rate is always q_N . The pressure at the well (or at any other point for which p_D is known) may be calculated at any time during rate q_N by using the principle of superposition as indicated by Eq.(A1.7). The pressure at the well is

$$\begin{aligned}
 p_{wf}(t) = p_i - \frac{141.2B\mu}{kh} \{ & q_1 [p_D(t_D) + s] \\
 & + (q_2 - q_1) [p_D((t - t_1)_D) + s] + (q_3 - q_2) [p_D((t - t_2)_D) + s] + \dots \\
 & + (q_N - q_{N-1}) [p_D((t - t_{N-1})_D) + s] \} \dots \dots \dots (A1.8)
 \end{aligned}$$

This may be rearranged to

$$\begin{aligned}
 p_{wf}(t) = p_i - \frac{141.2B\mu}{kh} \{ & q_1 [p_D(t_D) - p_D((t - t_1)_D)] \\
 & + q_2 [p_D((t - t_1)_D) - p_D((t - t_2)_D)] + \dots \\
 & + q_{N-1} [p_D((t - t_{N-2})_D) - p_D((t - t_{N-1})_D)] \\
 & + q_N [p_D((t - t_{N-1})_D)] + s \} \dots \dots \dots (A1.9)
 \end{aligned}$$

If the system is infinite-acting and if the logarithmic approximation of the exponential integral, Eq.(A1.5b), applies, Eq.(A1.9) may be written

$$p_{wf}(t) = p_i - \frac{70.60B\mu}{kh} \left\{ q_1 \ln \left(\frac{t}{t - t_1} \right) + q_2 \ln \left(\frac{t - t_1}{t - t_2} \right) \right\}$$

$$+ q_{N-1} \ln\left(\frac{t-t_{N-2}}{t-t_{N-1}}\right) + q_N \left[\ln(t-t_{N-1}) + \ln\left(\frac{k}{\phi\mu c_r r_w^2}\right) - 7.4316 + 2s \right] \} \quad \dots \text{(A1.10)}$$

or

$$p_{wf}(t) = p_i - \frac{162.6B\mu^*}{kh} \left\{ \sum_{j=1}^{N-1} q_j \log\left(\frac{t-t_{j-1}}{t-t_j}\right) + q_N \left[\log(t-t_{N-1}) + \log\left(\frac{k}{\phi\mu c_r r_w^2}\right) - 3.2275 + 0.86859s \right] \right\} \quad \dots \text{(A1.11)}$$

Eq.(A1.8) through (A1.11) are convenient for estimating pressure resulting from multiple-rate histories. However, the form

$$\frac{p_i - p_{wf}(t)}{q_N} = \frac{162.6B\mu^*}{kh} \left\{ \sum_{j=1}^N \left[\left(\frac{q_j - q_{j-1}}{q_N} \right) \log(t-t_{j-1}) \right] + \log\left(\frac{k}{\phi\mu c_r r_w^2}\right) - 3.2275 + 0.86859s \right\} \quad \dots \text{(A1.12)}$$

which results from combining Eq.(A1.8) and Eq.(A1.5b), is more convenient for analyzing multiple- rate data.

A2 Infinite-Acting Flow Period:

During infinite-acting flow period, the generalized multirate superposition equation for liquids is given by Eq.(A1.12). Rearranging this equation

$$\frac{p_i - p_{wf}}{q_n} = \frac{162.6B\mu^*}{kh} \left\{ \sum_{j=1}^n \left[\left(\frac{q_j - q_{j-1}}{q_n} \right) \log(t_n - t_{j-1}) \right] + \log\left(\frac{k}{\phi\mu c_r r_w^2}\right) - 3.23 + 0.869s \right\} \quad \dots \text{(A2.1)}$$

Setting $m = 162.6B\mu^*/kh$, and rearranging Eq. A2.1, we obtain

$$p_{wf} = p_i - m \left\{ \sum_{j=1}^n (q_j - q_{j-1}) \log(t_n - t_{j-1}) \right\} - m q_n \left\{ \log\left(\frac{k}{\phi\mu c_r r_w^2}\right) - 3.23 + 0.869s \right\} \quad \dots \text{(A2.2)}$$

Using the chain rule of differentiation, one can write

$$\frac{dp_{wf}}{dt} = \frac{dp_{wf}}{dq} \frac{dq}{dt} \quad \dots \quad \dots \quad \text{(A2.3)}$$

Rearranging Eq. A2.3, we have

$$\frac{dp_{wf}}{dq} = \frac{dp_{wf}/dt}{dq/dt} \quad \dots \quad \dots \quad (A2.4)$$

Differentiating Eq. A2.2 with respect to t_1 , t_2 , and t_3 , we obtain

$$\frac{d}{dt_1} \{(q_1 - q_0) \log(t_1 - t_0)\} = \frac{1}{(t_1 - t_0)} (q_1 - q_0) \quad \dots \quad \dots \quad (A2.5)$$

$$\frac{d}{dt_2} \{(q_1 - q_0) \log(t_2 - t_0) + (q_2 - q_1) \log(t_2 - t_1)\} = \frac{1}{(t_2 - t_0)} (q_1 - q_0) + \frac{1}{(t_2 - t_1)} (q_2 - q_1) \quad \dots \quad (A2.6)$$

$$\begin{aligned} \frac{d}{dt_3} \{(q_1 - q_0) \log(t_3 - t_0) + (q_2 - q_1) \log(t_3 - t_1) + (q_3 - q_2) \log(t_3 - t_2)\} \\ = \frac{(q_1 - q_0)}{(t_3 - t_0)} + \frac{(q_2 - q_1)}{(t_3 - t_1)} + \frac{(q_3 - q_2)}{(t_3 - t_2)} \end{aligned} \quad \dots \quad (A2.7)$$

Therefore, the general form of time derivative can be written as

$$\frac{d}{dt_n} \left\{ \sum_{j=1}^n (q_j - q_{j-1}) \log(t_n - t_{j-1}) \right\} = \sum_{j=1}^n \frac{q_j - q_{j-1}}{t_n - t_{j-1}} \quad \dots \quad \dots \quad (A2.8)$$

Combining Eqs. AA4 and AA8, we have

$$\frac{dp_{wf}}{dq_n} = \frac{-m \left\{ \sum_{j=1}^n \frac{q_j - q_{j-1}}{t_n - t_{j-1}} \right\} - m \frac{dq_n}{dt_n} \left\{ \log \left(\frac{k}{\phi \mu c_r r_w^2} \right) - 3.23 + 0.869s \right\}}{\frac{dq_n}{dt_n}} \quad \dots \quad (A2.9)$$

For the constant-rate case, we have $dq_n/dt_n = 0$, thereby leading dp_{wf}/dq_n to infinity or the vertical line on the p_{wf}/q graph. Otherwise, the numerator remains negative in Eq. A2.9, suggesting negative slope for the p_{wf}/q graph during infiniteacting flow. Obviously, when a well is produced at constant p_{wf} the slope attains a zero value.

A3 PSS Flow Period:

During PSS flow, the general governing flow equation for variable-rate liquid flow is given by (Blasingame and Lee, 1986)

$$\frac{P_i - P_{wf}}{q_n} = 70.6 \frac{B\mu}{kh} \ln \left(\frac{4A}{e^{\gamma} C_A r_w^2} \right) + \frac{0.2339B}{\phi h c_r A} \sum_{j=1}^n \frac{q_j (t_j - t_{j-1})}{q_n} \dots \quad \dots \quad (A3.1)$$

Rearranging Eq. A3.1, one obtains

$$p_{wf} = p_i - 70.6 \frac{B_i \mu q_n}{kh} \ln \left(\frac{4A}{e^{\gamma} C_A r_w^2} \right) - \frac{0.2339B}{\phi h c_i A} \sum_{j=1}^n q_j (t_j - t_{j-1}) \dots \dots \quad (\text{A3.2})$$

Differentiating Eq. A3.2 with respect to time, one obtains

$$\frac{dp_{wf}}{dt_n} = - \frac{0.2339B}{\phi h c_i A} q_n \dots \dots \quad (\text{A3.3})$$

Differentiating Eq. A3.2 with respect to t_1, t_2 , etc., we can write

$$\frac{d\{q_1(t_1 - t_0)\}}{dt_1} = q_1 \dots \dots \quad (\text{A3.4})$$

for timestep 1, and

$$\frac{d\{q_1(t_1 - t_0) + q_2(t_2 - t_1)\}}{dt_2} = q_2 \dots \dots \quad (\text{A3.5})$$

for timestep 2, and so on.

Therefore, the general form of time-derivative can be written as

$$\frac{d}{dt} \left\{ \sum_{j=1}^n q_j (t_j - t_{j-1}) \right\} = q_n \dots \dots \quad (\text{A3.6})$$

In other words,

$$\frac{dq}{dt} = \frac{q_2 - q_1}{t_2 - t_1} \dots \dots \quad (\text{A3.7})$$

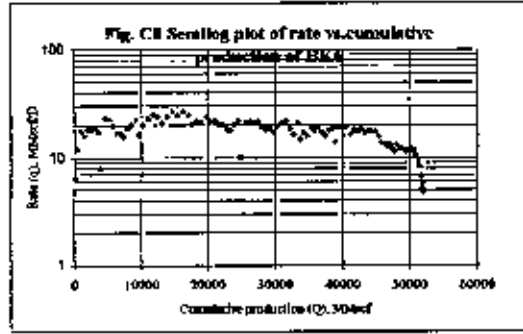
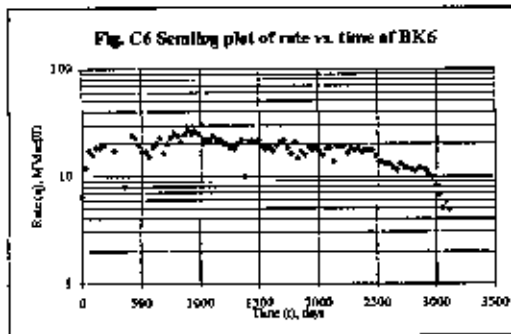
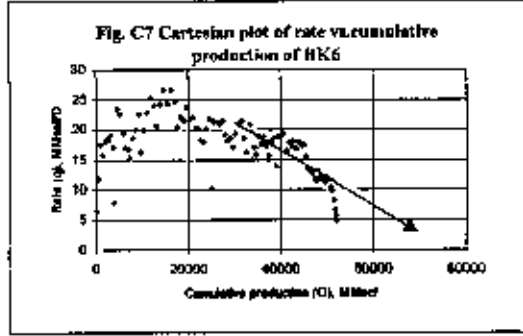
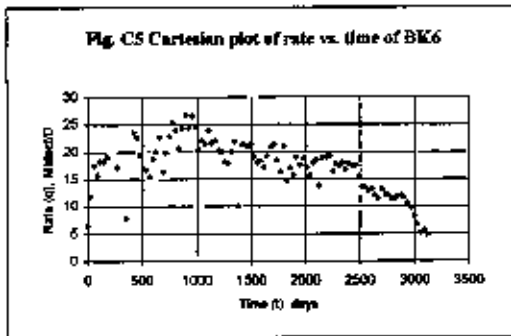
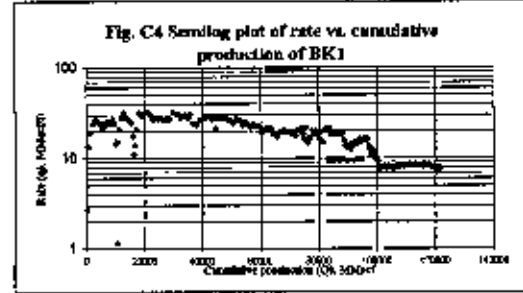
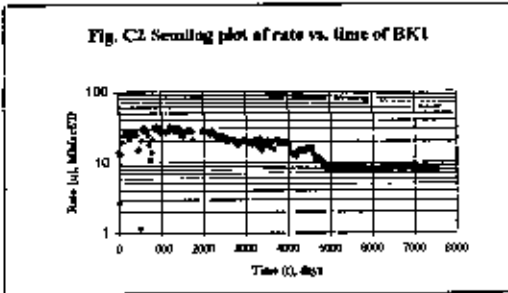
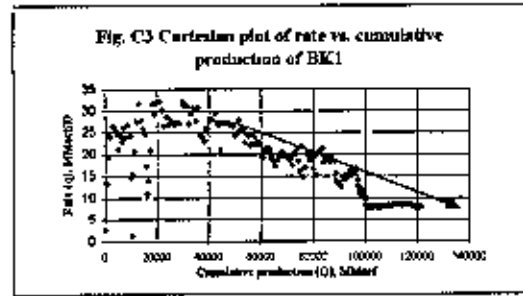
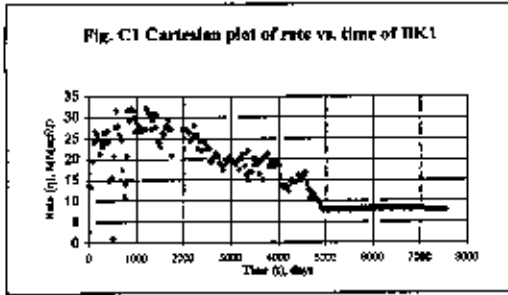
Eq. A3.6 is negative because the numerator is negative, while the denominator is always positive. Therefore, combining Eqs. A2.4, A3.3, and A3.7, we obtain

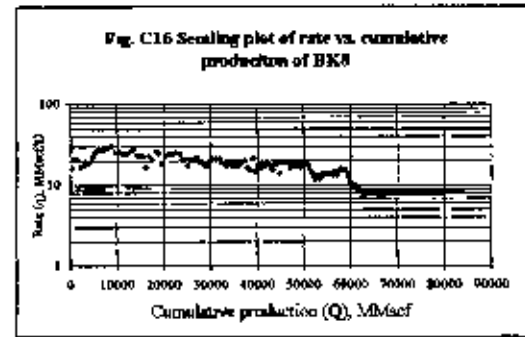
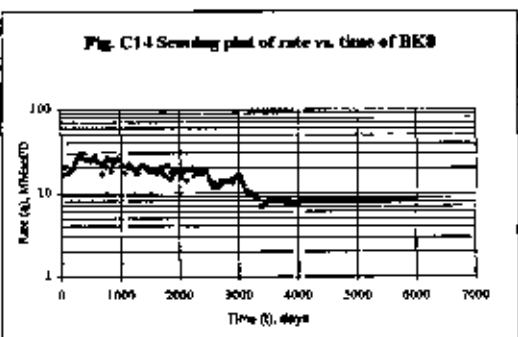
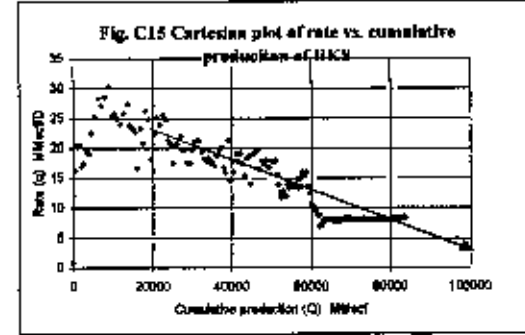
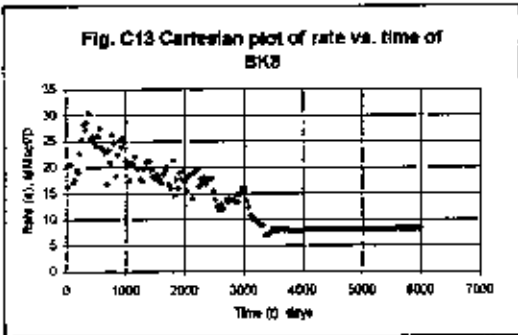
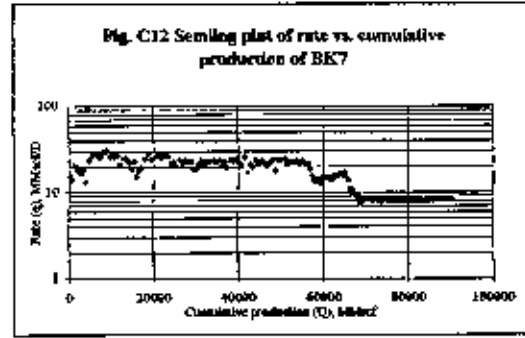
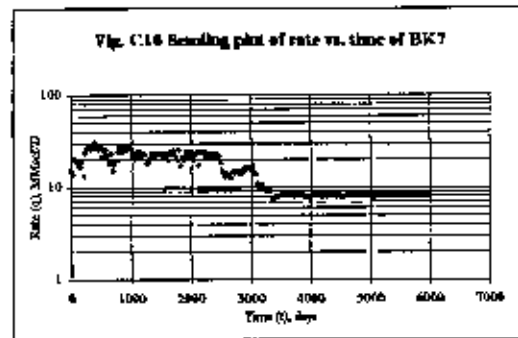
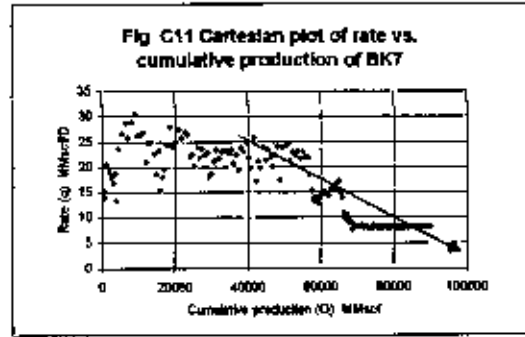
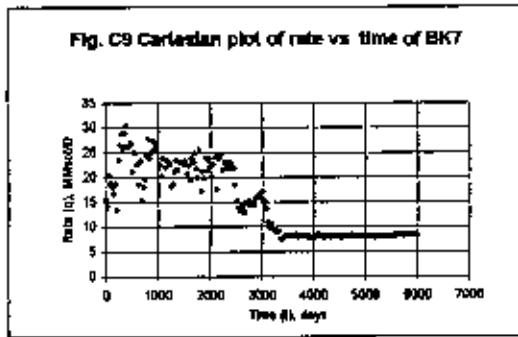
$$\frac{dp_{wf}}{dq_n} = \frac{- \frac{0.2339B}{\phi h c_i A} q_n}{- \frac{dq_n}{dt_n}} \dots \dots \quad (\text{A3.8})$$

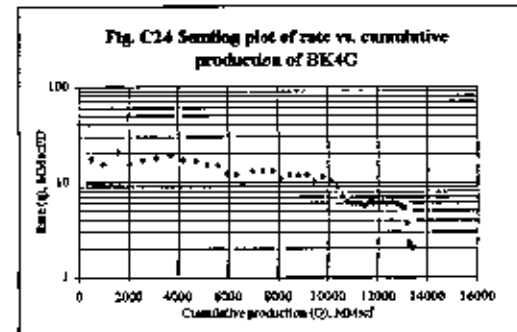
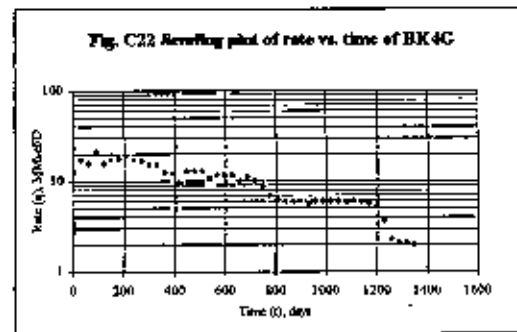
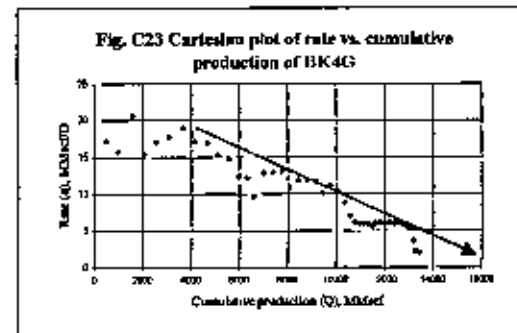
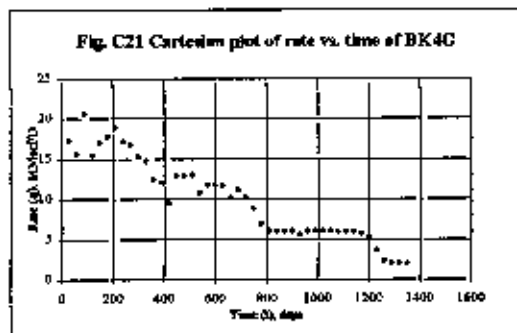
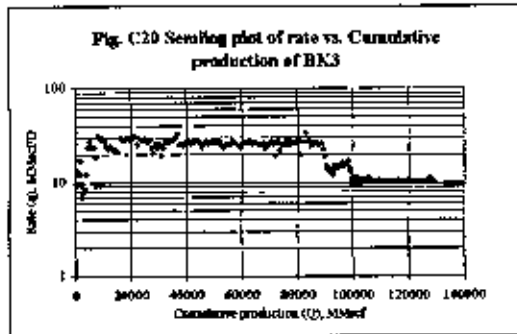
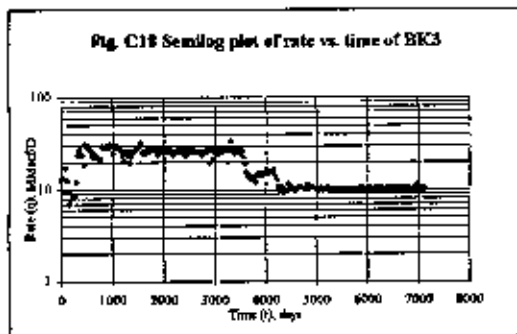
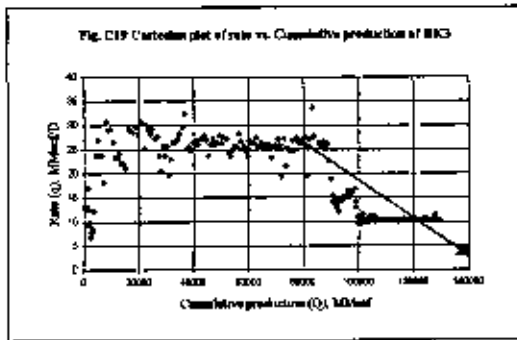
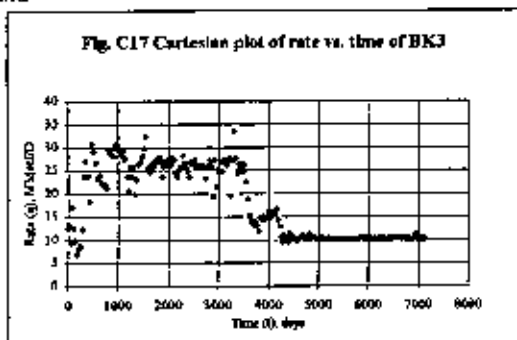
Eq. A3.8 shows that the positive slope will be exhibited when p_{wf} is graphed against q .

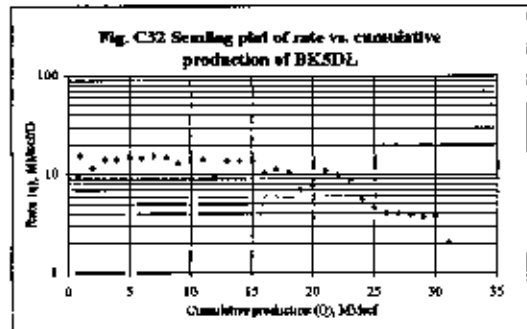
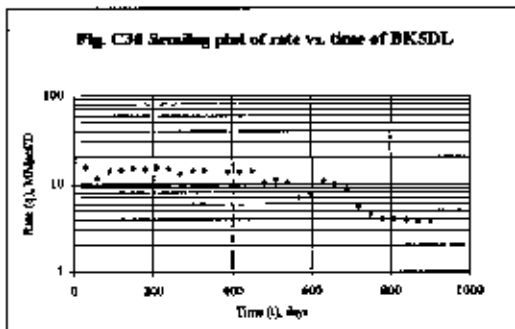
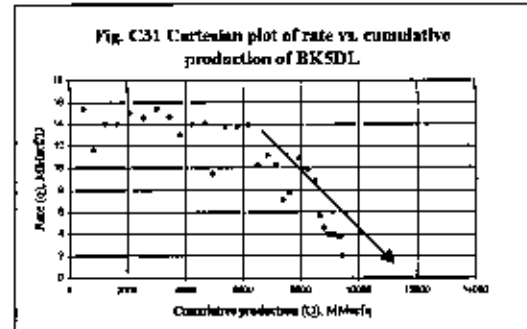
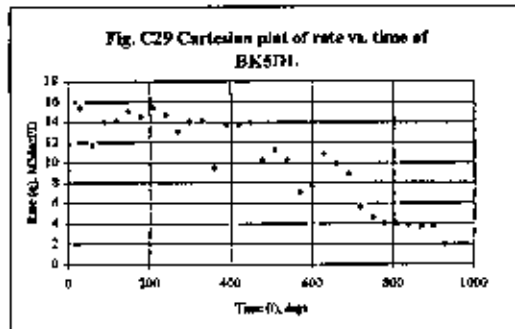
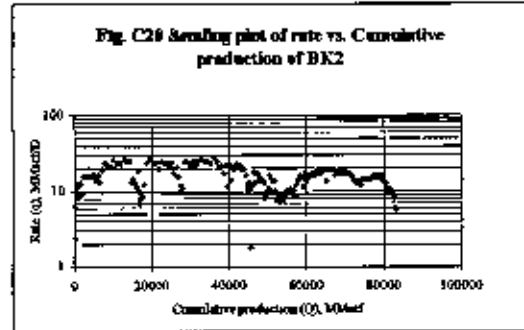
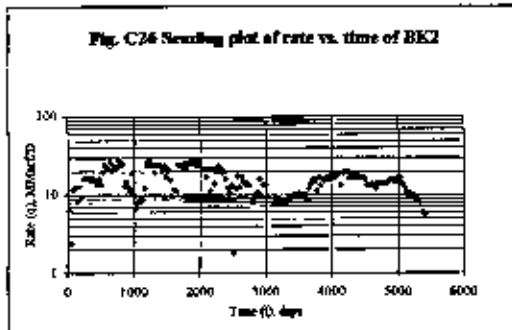
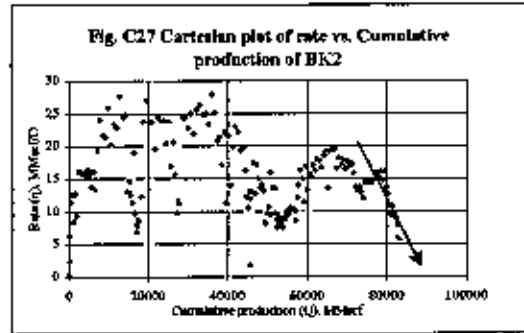
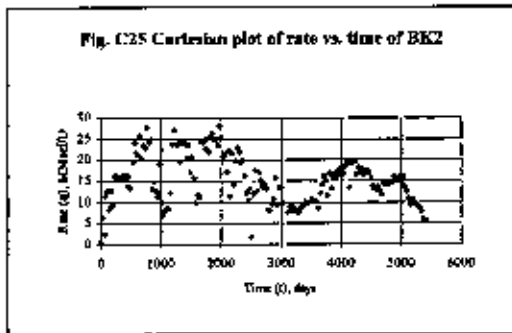
Appendix B Decline Curves of Individual Wells of Bokhrabad Gas Field

J Sand

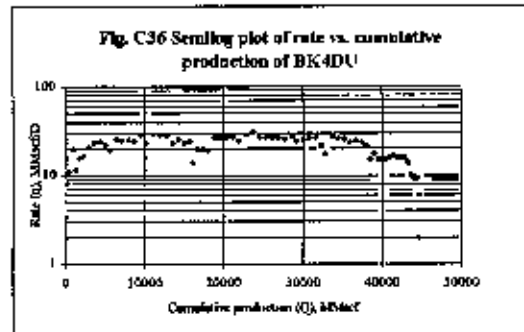
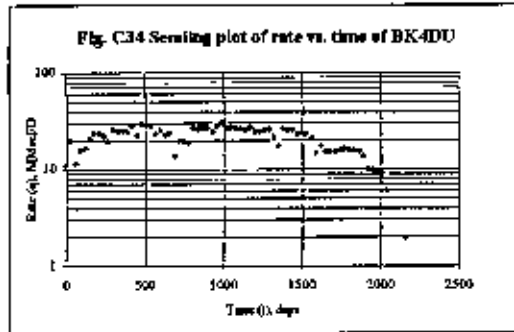
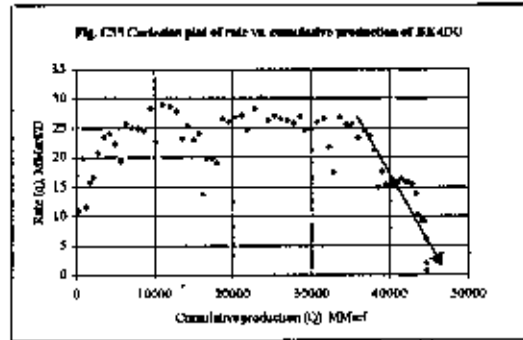
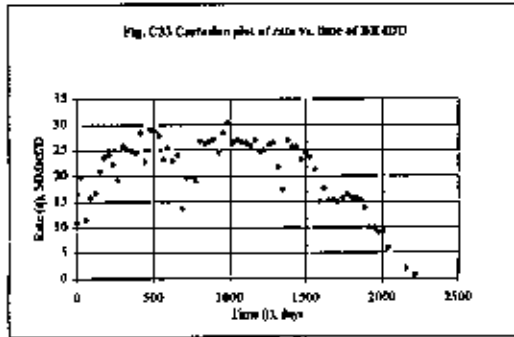




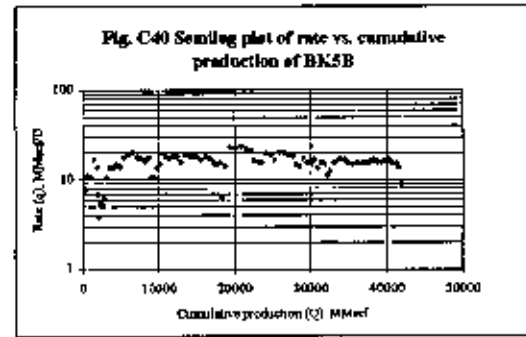
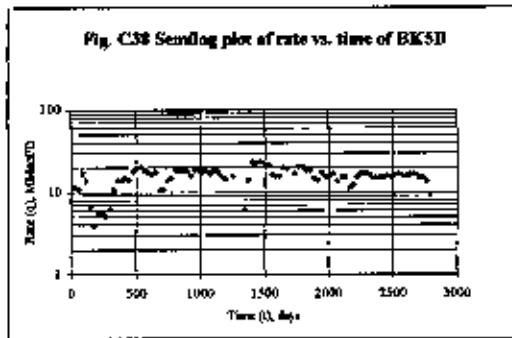
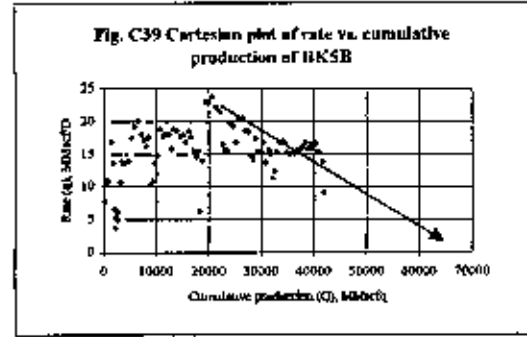
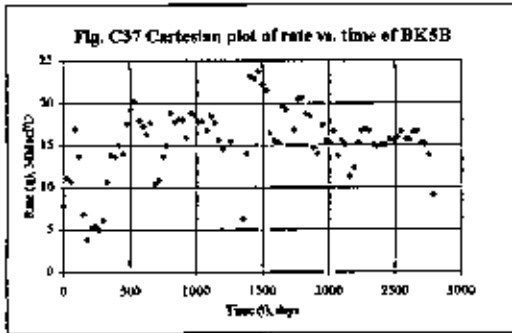




DU Sand:



B Sand



Appendix C

Input parameters for computer based PDA

Table B1: Input parameters for computer based production data analysis.

Well Information:	BK1	BK2	BK3	BK4	BK4	BK4	BK5	BK6	BK7	BK8
Name	Proven	Proven	Proven	Proven	Proven	Proven	Proven	Proven	Proven	Proven
Reserve Category	J (J Sand)	DL (DL Sand)	G (G Sand)	G (G Sand)	DU (DU Sand)	DL (DL Sand)	B (B Sand)	J (J Sand)	J (J Sand)	J (J Sand)
Pool:	BKB	BKB	BKB	BKB	BKB	BKB	BKB	BKB	BKB	BKB
Field	Gas	Gas	Gas	Gas	Gas	Gas	Gas	Gas	Gas	Gas
Fluid Type:	Producing	Suspended	Producing	Suspended	Suspended	Suspended	Suspended	Suspended	Producing	Producing
Status:										
Initial Pressure Information:										
Well Head p (psi)	2820	2540	2840	1822	2450	1717	2330	2540	2534	2374
Depth MFP (DD)(ft)	7197.5	7445	8815	7776	7155	7615	6800	8315	6297	8384
Depth MFP (TVD)(ft)	7197.5	6344	6907	7083	6546	6679	5967	7231	7140	7351.5
Struc (T ₁) (°F)	140	140	140	140	140	140	140	140	140	140
Sand Face P (psia):	3203 (Aug'86)	2952 (May'84)	3190 (Oct'85)	2194 (Oct'94)	2883 (Oct'86)	1930 (Dec'84)	2693 (Oct'88)	2985 (Dec'88)	2973 (Dec'88)	3035 (Dec'88)
Well Head Max (psia):	3180	2908	3100		2833		2540	3180	3180	3180
Sand Face Max (psia):										
Initial Reservoir Temperature:										
T _R (°F)	194.2	187	171	171	178	181	187	194.2	194.2	194.2
Wellbore Data:										
Net Pay h (ft)	238	80	122		90		63	100	280	280
Wellbore Radius R _w (ft)	0.3	0.3	0.3	0.3	0.3	0.3	0.3	0.3	0.3	0.3
MSP Depth (ft):										
Tubing Specifications:										
OD (inch)	5	5	5	5	5	5	5	5	5	5
Depth (ft):	6336.17	6426.85	7217.3		6703.08		6709.68	7443.41	7471.91	7435.18
Casing Specifications:										
ID (inch):	9.625	7	7	7	7	7	7	7	7	7
Depth (ft)	7780	6365	8990		9314		7764	8655	8485	8757
Well Head Temperature:										
Flowing (T _f) (°F):	134.6	134.6	134.6		134.6		134.6	134.6	134.6	134.6
Gas Properties:										
Gravity, G (Air)	0.59	0.59	0.59		0.59		0.59	0.59	0.59	0.59
CO ₂ (%)	0.51	0.51	0.51		0.51		0.51	0.51	0.51	0.51
H ₂ S (%)	0	0	0		0		0	0	0	0
N ₂ (%)	0.59	0.59	0.59		0.59		0.59	0.59	0.59	0.59
Porosity and Saturation:										
κ _v (%)	23	20	18		25		22	20	20	20
s _g (%)	74	69	61		76		80	74	74	74
κ _h (%):	26	31	40		24		20	28	28	26
Total Compressibility, c _t (1/psi)	0.000287	0.000328	0.000319		0.000283		0.0004	0.000287	0.000287	0.000287
PVF (Rvol/Svol):	0.0057	0.00731	0.00704		0.00663		0.00574	0.00544	0.00544	0.00544